2002

The effect of pore solutions on the elastic modulus of rocks.

Pedram. Pour Molk Ara
University of Windsor

THE EFFECT OF

PORE SOLUTIONS ON

THE ELASTIC MODULUS OF ROCKS

by

Pedram P. Molk Ara

A Thesis
submitted to the
Faculty of Graduate Studies and Research
through the department of
Earth Sciences
in partial fulfillment of the requirements for
the degree of Master of Science at the
University of Windsor

Windsor, Ontario, Canada

2002

ABSTRACT

The objective of the research was to determine the effect of saturation and ionic solutions on the elastic modulus (Young's Modulus) of rocks. It is based on the testing of 78 samples, which are considered representative of rock formations in Southern Ontario.

Initially a number of physical parameters were measured, including absorption, adsorption, porosity, unit weight and length change due to freezing. A uniaxial compressive stress frame was designed and built to facilitate the stress portion of the research program. Samples were subjected to varying levels of moisture, temperature and ionic conditions for a preset time period and immediately removed and put under stress. Stress and length change of the sample were recorded during the test. Young's Modulus was calculated from the stress and strain results.

All the results (combined with additional results extracted from the same samples in previous studies by Stephen Rigbey, 1980 and Ivan Dananaj, 2001) were subjected to multivariate statistical analysis, which included correlation tests, cluster analysis, factor analysis, regression and t tests.

The analysis of the results shows that the elastic parameters of the rock – Young's Modulus and Stress required to bring the sample to given strain (length change of 8×10^{-7}cm) – are controlled by the nature and the amount of pore water present. Rock type determines the Young's Modulus and stress required to bring the sample to a constant strain (8×10^{-7}cm), but the environmental conditions that result in increased amounts of adsorbed water in rock pores decrease the Young's Modulus and stress required to bring them to the same strain. Salt solution has the greatest negative effect in

that it produces the greatest proportion of adsorbed water in rock pores. Rock density and adsorption parameters have a significant direct and inverse correlation with Young's Modulus, respectively.

Cluster analysis effectively classifies the rocks into high, intermediate, and low strength/Young's Modulus/stress groups, which, based on their physical properties, correspond to high, intermediate, and low durability class of rocks.

DEDICATION

This thesis is dedicated to GOD who made it possible for me to have such wonderful parents; I could never thank them enough for what they have done for me.

ACKNOWLEDGEMENTS

This research was made possible through the leadership, friendship, sponsorship, fulltime support and patience of Professor P. P. Hudec, thank you Professor Hudec. The author would also like to thank the many people past and present who assisted in the construction and experimentation device as well as the computer software program, among others they include: Mr. Dieter K. Liebsch (deceased) and Mr. James Hochsreiter...

A special thank you to Dr. Saed Sayad who provided unlimited support with Visual Basic programming and data base analysis. Mr. Stephen J. Rigbey and Mr. Martin Ondrasik collected all of the samples. Also, Mr. Alireza Broujerdi assisted in some of the sample preparation.

AMEC Earth & Environmental Limited, formerly AGRA, made the required time possible for the author to finish all the requirements.

Thank you all.

TABLE OF CONTENTS

TABLE OF CONTENTS (Contd.)

TABLE OF CONTENTS (Contd.)

LIST OF TABLES

LIST OF ILLUSTRATIONS

LIST OF APPENDICES

I. INTRODUCTION

"Let the stone be taken from the quarry two years before building is to begin, and not in the winter but in the summer" (Vitruvius, the Roman architect of Emperor Augustus, from Lienhart 1994).

Despite their solid appearance, rocks contain pores within their structure, which can act as weak points (Hudec, 1991; Palchik, 1999). Higher porosity provides larger internal surface area, which creates more contact with other elements in nature such as dipolar water molecules and various chemical solutions.

When rocks are exposed to humidity such as vapor or liquid, water molecules will be adsorbed to the rock pore surface. In high room humidity and when rocks are in contact with water, water can be drawn up through the pores, by the process called capillary effect. The adsorbed water along with capillary water held in pores have different behaviors compared to free water (Dullien, 1979). The thickness of this adsorbed layer of water can increase if there are cations available in the solution. The presence of adsorbed water, capillary water and variations in temperature are the three main factors responsible for expansion and contraction in rock, which is measured as strain. Strain is caused by stress, and expansive strain can be countermanded by stress.

The first objective of this thesis is to determine the stress required to bring sample to a constant strain. The relationship between stress and strain in a rock is referred to as Young's Modulus and is proportional to the strength of the rock. This thesis examined the strain of dry and saturated rocks in water and in various ionic solutions, determined the stress required to bring the sample to constant strain, and calculated the resultant

Young's Modulus. The rock samples tested were those obtained in active quarries throughout Southern Ontario.

Many studies have shown that rocks deteriorate when they are exposed to changing moisture and temperature levels (Powers, 1975; Rogers et al., 1986; Hudec, 1991; Althaus et al., 1994; Palchik, 1999). Moreover, different rock types show different rates of deterioration when they are placed in similar conditions of moisture, temperature and ionic solutions. To understand the mechanism of deterioration it is necessary to understand the active forces involved. This research examined some of the detrimental effects of saturation and ionic solutions on the behavior of rocks.

The initial phase of this research was to determine the physical properties of rock samples collected from quarries in Southern Ontario. Absorption, adsorption, expansion, contraction and ionic concentration are the parameters governed by factors such as moisture, temperature and ionic solutions. These combined factors contribute to rock deterioration.

The purpose of the main, and second phase of this research was to determine the effect of moisture, temperature and ionic solution conditions on deformation stress and on Young's Modulus of the rock samples. The rock samples, were exposed to the various conditions mentioned above for a prescribed time, and were then immediately placed in a uniaxial compressive stress frame that was built and developed for this study. Stress was slowly applied until a predetermined, constant strain level was reached (8×10^{-7} cm). The data was then used to calculate the Young's Modulus.

The third and final step was to combine these results with those extracted from the same rock samples by Stephen Rigbey (1980) and Ivan Dananaj (2001).

II. STRESS, STRAIN, AND YOUNG'S MODULUS IN ROCKS

A. Stress, Strain and Young's Modulus

Stress is the force per unit area that exists within a specified plane in a material (Rahn, 1996).

$$\delta = F / A \tag{1}$$

δ = Stress (Pa or N/m^2)

F = Force (N)

A = Area (m^2)

The deformation measure of a material with a length of L to L∘ due to a stress is called strain (ε) (Rahn, 1996).

$$\varepsilon = \frac{L - L\circ}{L\circ} \tag{2}$$

ε = Strain L = New Length $L\circ$ = Original Length

Hooke's law represents the relationship between stress and strain. This relationship exists in a uniaxial compression or tension condition.

$$E = \delta / \varepsilon \tag{3}$$

E = Young's Modulus (N/m^2)

Young's Modulus is calculated from stress and strain measurements during the uniaxial unconfined compression test. Hookean or elastic behavior exists in a material that shows instantaneous linear relation between the stress applied and the resulting elastic strain. It is assumed that all the strains are instantaneous and completely recoverable upon removal of the stress from the loaded elastic material. One of the first

and most basic assumptions in this research is that all rock samples tested exhibit elastic behaviour. It has also been shown that most rocks and crystalline solids have Hookean behaviour in short-term laboratory tests for strains less than 1%, at low temperatures, i.e. ambient temperatures (Means, 1976).

The numerical value of the Young's Modulus depends on the maximum applied stress and loading rate. Slow loading of a sandstone may result in an E, which is 30% higher than the E value obtained from rapid loading of the same sample (Jaeger, 1972). A study by Serdengecti and Boozer (1961) performed on Berea sandstone and gabbro confirms the importance of the loading rate (Table 1). Compression tests are normally carried out at a high rate of loading from 10 to 100 psi per second. A very slow loading rate or constant high stresses can cause creep in rocks. Creep in rock material is plastic deformation or continued increase in strain for a given stress. At higher stress levels rocks behaviour is more plastic and their creep time is very short. Based on the results from Table 1 a higher stress leaves less time for creep (Serdengecti and Boozer, 1961).

Table 1. Unconfined Compressive Strength of Sandstone and Gabbro (the original numbers were in psi and converted values were rounded to the nearest integer)

Rock	Time to Failure				Strength Increase
	30 seconds		0.03 seconds		
	(psi)	(MPa)	(psi)	(MPa)	
Berea Sandstone	8000	55158	12000	82737	50%
Gabbro	31000	213738	40000	275790	30%

In addition to variability in the testing methods, the geological setting in which the rocks are found also affect Young's Modulus. Identical rock types can have different

Young's Modulus in different geological regions since the formational temperature, pressure, depth of burial and age were not exactly the same (Table 2) (Jumikis, 1983; Rahn, 1996).

Table 2. Young's Modulus of some rocks (1.Jaeger and Cook, 1976; 2.Jumikis, 1983; 3.Rahn, 1996; 4.Szechy, 1966; 5.Vutukuri, 1974)

Rock	Locality or Formation	Young's Modulus ($\times 10^9$ N/m^2)	Rock	Locality or Formation	Young's Modulus ($\times 10^9$ N/m^2)
Diabase[3]	New York	95.8	Limestone[1]	Solenhofen	53.1
Diabase[1]	Frederick	99.3	Marble[3]	New York	54.0
Dolomite[3]	Illinois	51.0	Marble[3]	Tennessee	48.3
Dolomite[2]	-	19.6	Marble[1]	Wombeyan	64.8
Dolomite[4]	-	82.4	Quartzite[3]	Minnesota	84.8
Dolomite[5]	-	93.0	Quartzite[3]	Utah	21.37
Granite[3]	Georgia	39.0	Quartzite[1]	Cheshire	78.6
Granite[3]	Maryland	25.4	Quartzite[1]	Witwatersrand	77.9
Granite[3]	Colorado	70.6	Sandstone[3]	Ohio	10.52
Granite[1]	Westerly	55.8	Sandstone[3]	Utah	21.37
Granite[1]	Charcoal	44.1	Sandstone[1]	Gosford	9.7
Granite[1]	Aplite	82.7	Shale[3]	Utah	58.19
Limestone[3]	Germany	63.8	Shale[3]	Pennsylvania	31.2
Limestone[3]	Indiana	26.96	Shale[1]	Witwatersrand	67.6

Porosity, particle size, non-homogeneity, anisotropy, direction of applied stress, sample shape and size, height to diameter ratio, and water content are some of the other factors that can effect Young's Modulus.

In unconfined situation when stress is applied a slow rate, pore water pressure build up will be minimal. It has been shown that in confined situations by increasing the confining pressure the Young's Modulus increases, but it decreases with increasing strain (Martin and Haupt, 1994).

As long as the positive internal stresses produced in rocks, due to partial or full saturation, are below the stress required for new crack creation, the rock will stiffen. This

will increase the Young's Modulus of the rock since the internal stress will cause the open cracks to close depending on the magnitude of the stress (Hilbert et al., 1994).

Price et al. (1994) showed that Young's Modulus decreases with increasing porosity in tuff samples. Although the increasing trend was distinct, there was significant scatter in the observed modulus at each porosity level, in some cases as much as a factor of two (Fig. 1).

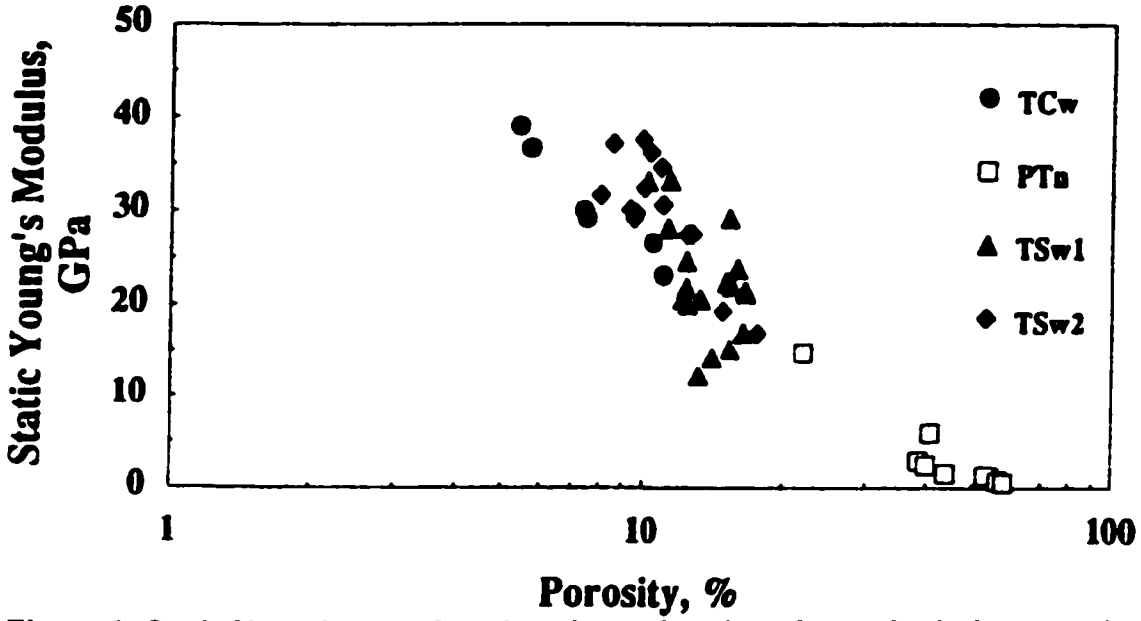

Figure 1. Static Young's modulus plotted as a function of porosity in low porosity welded tuff (TCw), non-welded porous tuff (PTn), altered welded tuff (TSw1), few lithophysal cavities vapor-phase altered welded tuff (TSw2) (Price et al., 1994).

Price et al. (1994) measured different material properties of the samples and found no distinct differences, so they suggest that the scattered pattern that is present at each porosity level might be related to the pore structure of the specimen.

Another study on carbonate rocks, revealed that the rocks that have experienced infilling of pore space by cements or significant compression, show a higher Young's

Modulus. This can be ascribed to increasing burial depth and diagenesis (Jones et al., 1994).

A similar laboratory study on shale samples in the absence of pore fluids has revealed significant higher strengths that were comparable to higher metamorphic grade rocks such as slates and schists (Kwon and Kronenberg, 1994). Fluid saturated shales have low strengths primarily due to elevated pore pressures and correspondingly low effective pressures. If the strain rate is reduced and the time available for fluid transport is increased, shales may exhibit drained response (Swan et al., 1989). Based on these studies, absolute strength of shales may depend upon pore fluid flow at micro pores and pore connectivity. Nevertheless, pores that are not drained are likely to contribute most to weakening specimens.

An experiment in triaxial compression cell at 300 °C under dry (105 °C), room humidity (as received) and water-saturated conditions has shown significant differences between dry and saturated granites (Althaus et al., 1994). Increasing porosity and pore water decreased the strength of granite. When pore water is present, the strength and angle of internal friction are reduced to low values due to the mechanical and chemical effects of pore water. Specimens with higher porosity (n=0.4%) displayed a lower strength and less sharp stress drops, as compared to the low porosity samples (n=0.3%) (Fig. 2a). The water saturation of the granite samples reduced their strength to about 35% of the dry condition (Fig. 2b) (Althaus et al., 1994).

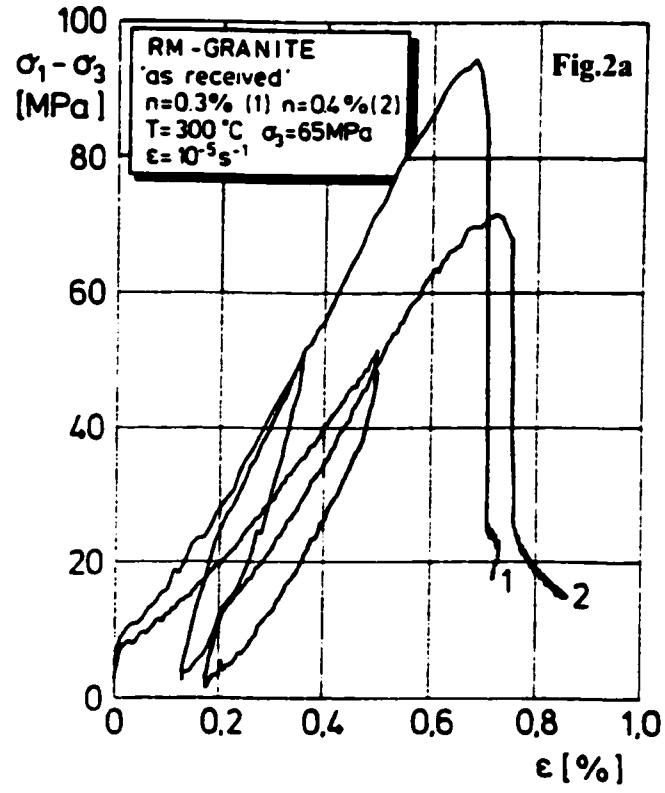

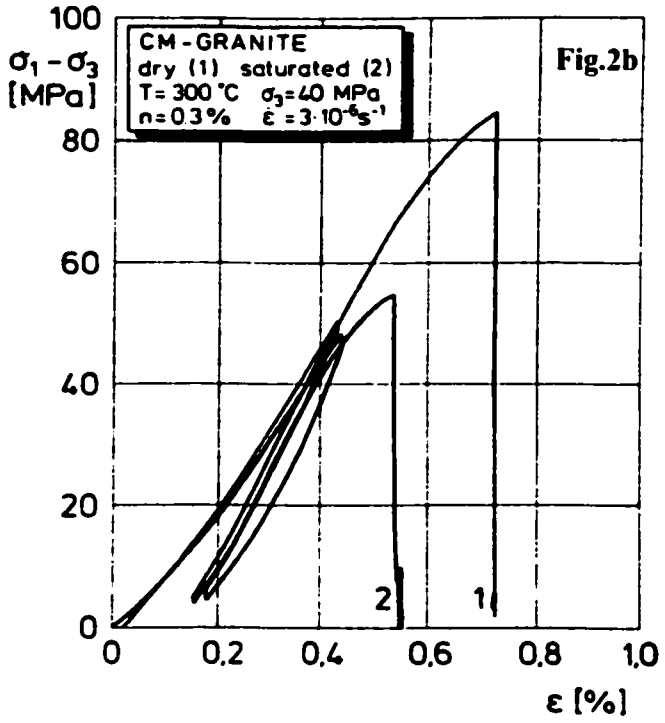

Figure 2. Axial strain versus deviatoric stress for a) granite samples with different porosities, and b) for dry and water-saturated granite (Althaus et al., 1994).

Another study has confirmed that the rocks are weaker in moist or wet conditions compared to a dry state, and generally the strength loss is higher for sedimentary rocks and lower for metamorphic and igneous rocks (Rao et al., 1987).

B. Young's Modulus, Rock Strength and Rock Properties

Porosity is one of the major rock properties known to have a direct effect on rocks' mechanical properties. A study on 85 core samples from Chase and Council Grove carbonates of Hugoton and Panoma oil and gas fields in Kansas has shown strong correlation between static Young's Modulus and porosity (Yale and Jamieson, 1994). Static Young's Modulus was measured in a triaxial cell under constant confining stress of 1500 psi without any pore fluid on six geological formations. All of them showed that porosity has a strong influence on Young's Modulus (Fig. 3).

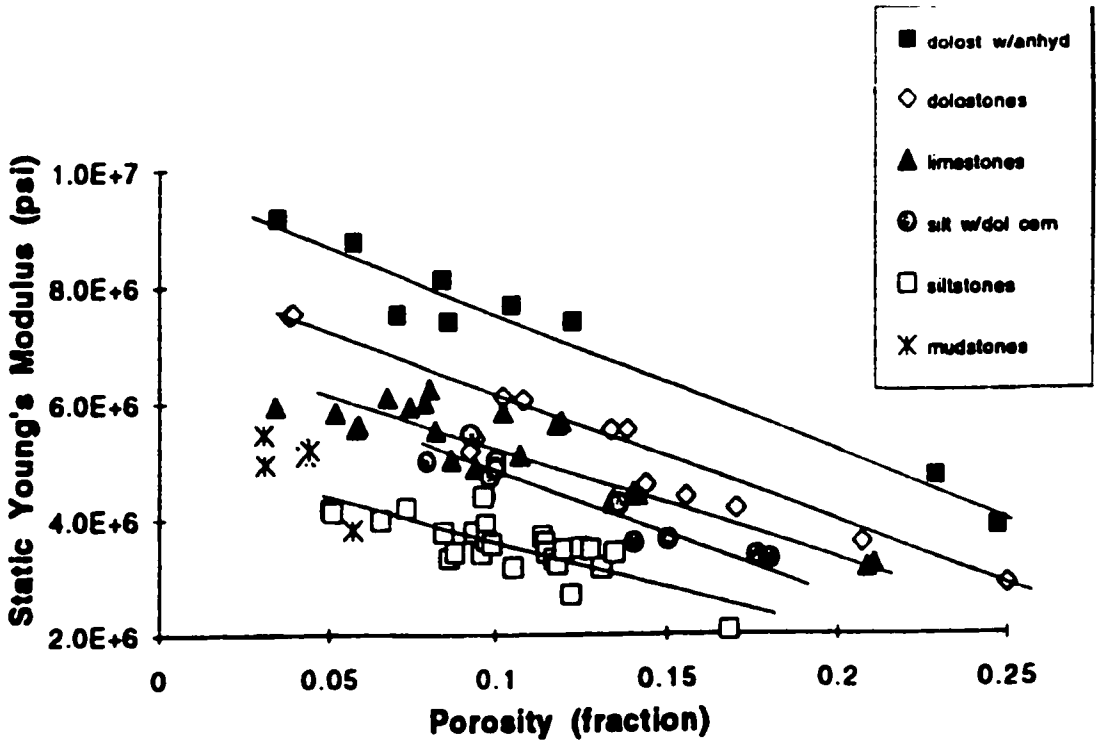

Figure 3. Young's modulus versus porosity and lithology (Yale and Jamieson, 1994).

Due to their porous nature, rocks in their natural state may contain moisture, which may weaken their strength. Surface area, surface charge, porosity and pore size are the major rock properties that determine the moisture content of the rock (Price, 1960; Colback and Wiid, 1965; Broch and Franklin, 1972; Van Eeckhout, 1976; Broch, 1979; Mandzic, 1979; Bell, 1987). The strength reduction with increasing moisture content is higher for sedimentary rocks than for metamorphic and igneous rocks. Some researchers have studied the effect of other fluids on rock strength and found that strength is inversely proportional to the surface tension of the liquid with which the rock is saturated (Boozer et al., 1962; Colback and Wiid, 1965; Vutukuri et al., 1974). There are four essential theories that are believed to be responsible for strength reduction in rocks due to moisture:

1. Surface energy reduction due to water adsorption: An increase in moisture content decreases the surface energy even though the mineralogical forces remain nearly constant. The strength drop is due to the fact that the rock specimens are covered with a layer of water (Broch, 1979) and the weakening effect is caused by a reduction of surface energy at grain boundaries and at the tip of internal flaws (Franklin and Dusseault, 1989). The surface energy of quartz and sandstone are almost equal in dry condition (640 erg/cm^2) but exposing sandstone to a humidity of 100% reduces its surface energy to 240 erg/cm^2 (Rao et al., 1987). The water molecule (H-O-H) tends to hydrolize the silicon-oxygen bonds (-Si-O-Si-) in silicates to give rise to hydroxyl groups (-Si-OH), and as a result weaken the bonds (Franklin and Dusseault, 1989). Thereby the required energy to generate

new micro cracks will be lower. An increase in moisture equilibrium affects the interparticle forces (electrical attractive and repulsive forces).

2. Pore water pressure deficiency caused by capillary tension in unsaturated rocks: If the rock is unsaturated the pore water pressure is negative due to the capillary suction. Based on Karl Terzaghi's 1925 effective stress Formula (4) (Franklin and Dusseault, 1989), total stress in rock specimens is carried in part by solid contacts, and in part by the water pressure in the pore.

$$\delta n = \delta' n + u \qquad (4)$$

δn = Total Stress $\qquad$ $\delta' n$ = Effective Stress $\qquad$ u = Pore Water Pressure

Suppose the pore water pressure (u) within the rock specimens is decreased. Since the effective stress has not changed, the total stress will decrease due to pore water pressure deficiency.

3. Increase of pore pressure due to confining pressure: In saturated rocks under external applied stresses pore water is subjected to a hydrostatic pressure due to its inability to drain out and its incompressible nature. Based on Formula (4), the effective stress between the solid contacts has to be decreased by a corresponding amount to the pore pressure increase, which consequently causes a reduction in shear strength (Franklin and Dusseault, 1989).

4. Friction coefficient reduction with increase of moisture: Due to an increase in moisture content, surface energy decreases resulting in a reduction in friction. A study on mica containing gneisses has revealed a significant difference in the coefficient of friction from dry to water saturated condition (Broch, 1979). Thus there can be no doubt that water reduces the internal friction of rocks.

Strength changes of four different Indian sandstones were measured under various moisture content (Rao et al. 1987). In all cases, peak compressive strengths decreased with an increase in moisture content. Stress-strain curves for one of the sandstones (Kota sandstone) is presented in Figure 4.

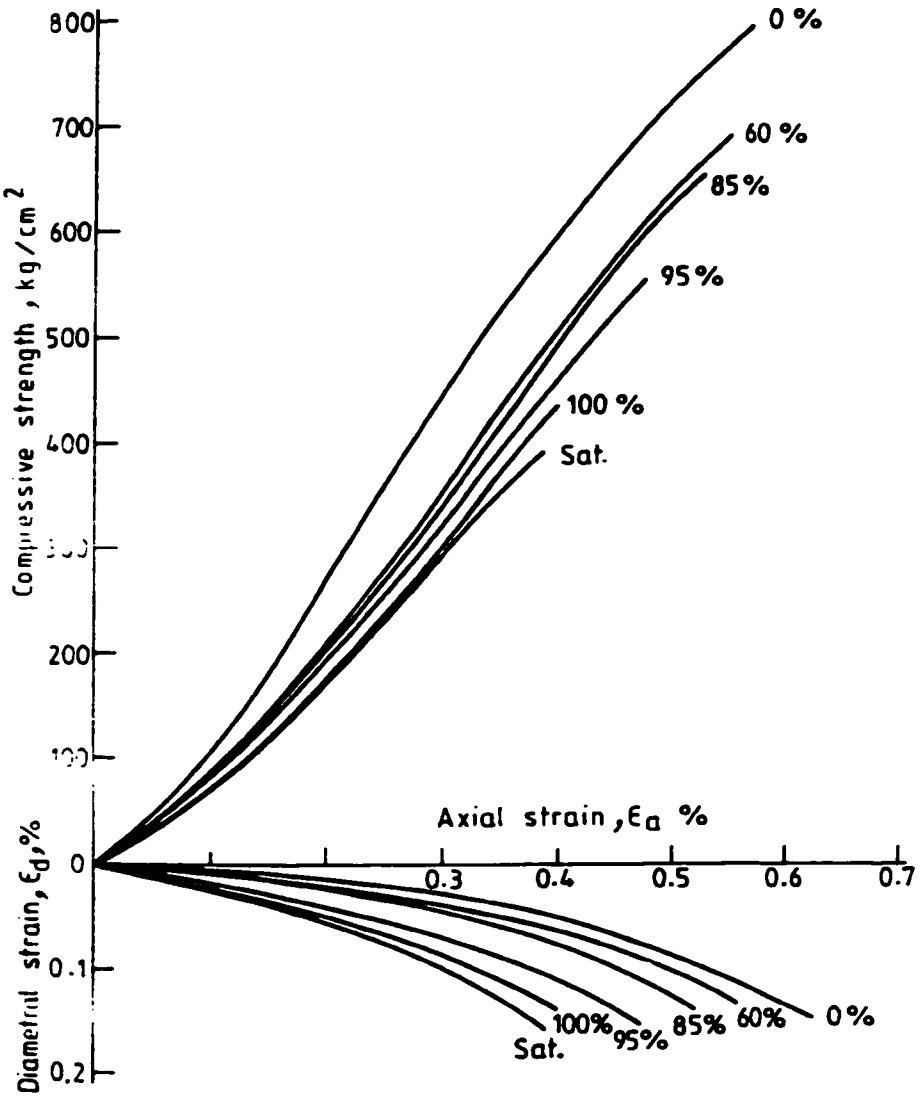

Figure 4. Stress-Strain curves at different humidities (Rao et al., 1987).

A comparison between dry and saturated values of uniaxial compressive strength for the same samples displayed a strength reduction of 33% to 52% (Fig. 5). Similar variations in Brazialian strength and point load strength were observed for all four types of sandstones.

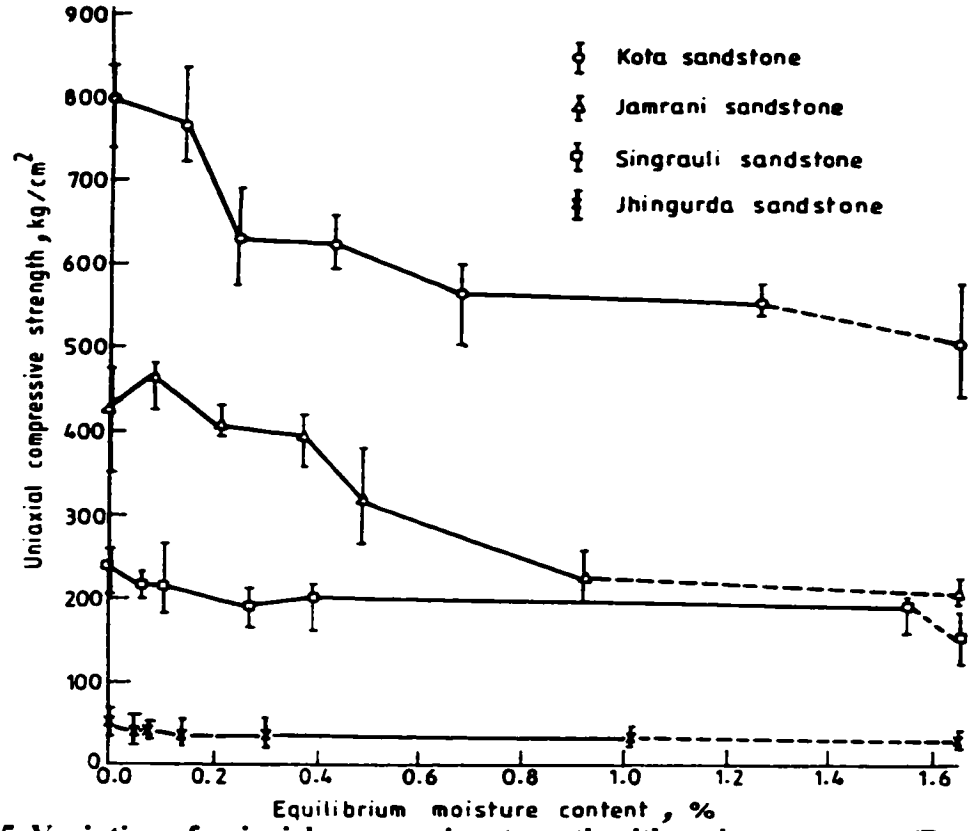

Figure 5. Variation of uniaxial compressive strength with moisture content (Rao et al., 1987).

Tensional Young's Modulus of rocks is a mechanical factor that controls rock durability in frost weathering. There are three natural processes known to be responsible for freezing expansion, including volumetric expansion, adsorptive suction, and expansion of non-freezable or adsorbed water. Due to volumetric expansion of water of 9%, subzero temperatures in a closed system of porosity under fully saturated conditions can develop pressures (up to 200 MPa) higher than tensional Young's Modulus (Lienhart, 1994). This can result in rock failure. Also, cyclic freezing and thawing causes fatigue in rock, and as the force exceeds the tensile strength, failure may occur. Pore water migration towards the boundary between the frozen and unfrozen portions of rock by capillary action and by suction due to negative pore pressure is the second natural process held accountable for expansion. Adsorbed water (non-freezable water) has shown an

expansion of 0.6% as the temperature decreases from +4°C to -10°C (Winkler, 1992 from Lienhart, 1994). Adsorbed water has different physical properties than normal water. Low temperatures cause hydration or reordering of the adsorbed water that eventually result in disruption of the rock. All these processes need sufficient amount of water. Rocks with a total porosity of 25% or less require a saturation of 75% or more to reach their critical saturation (Dunn and Hudec, 1965).

Many researchers have studied the relationship between mean grain size and uniaxial compressive strength of rocks. Previous studies have reported that the uniaxial strength of marbles and limestones increases linearly with the inverse square root of mean grain size (Fredrich et al., 1990; Wong et al., 1996). A recent study on sandstone samples has shown a weak linear correlation between uniaxial compressive strength and mean grain size (Fig. 6) (Palchik, 1999). Hatzor and Palchik (1998) have reported that a good correlation between these two parameters can only be achieved if the tested samples are extremely homogenous in which the only textural variable is the mean grain size.

The elastic modulus of rocks increases linearly with their uniaxial compressive strength (Fig. 7) (Palchik, 1999). The same study has shown the negative impact of porosity on uniaxial compressive strength. Based on these results, Palchik (1999) developed a linear function, which describes the relationship between uniaxial compressive strength and the elastic modulus and porosity as:

$$\sigma_c = a\,(E / n) \qquad (5)$$

σ_c = Uniaxial compressive strength (MPa) $\qquad$ a = Empirical coefficient

E = Elastic modulus (MPa) $\qquad$ n = Porosity (%)

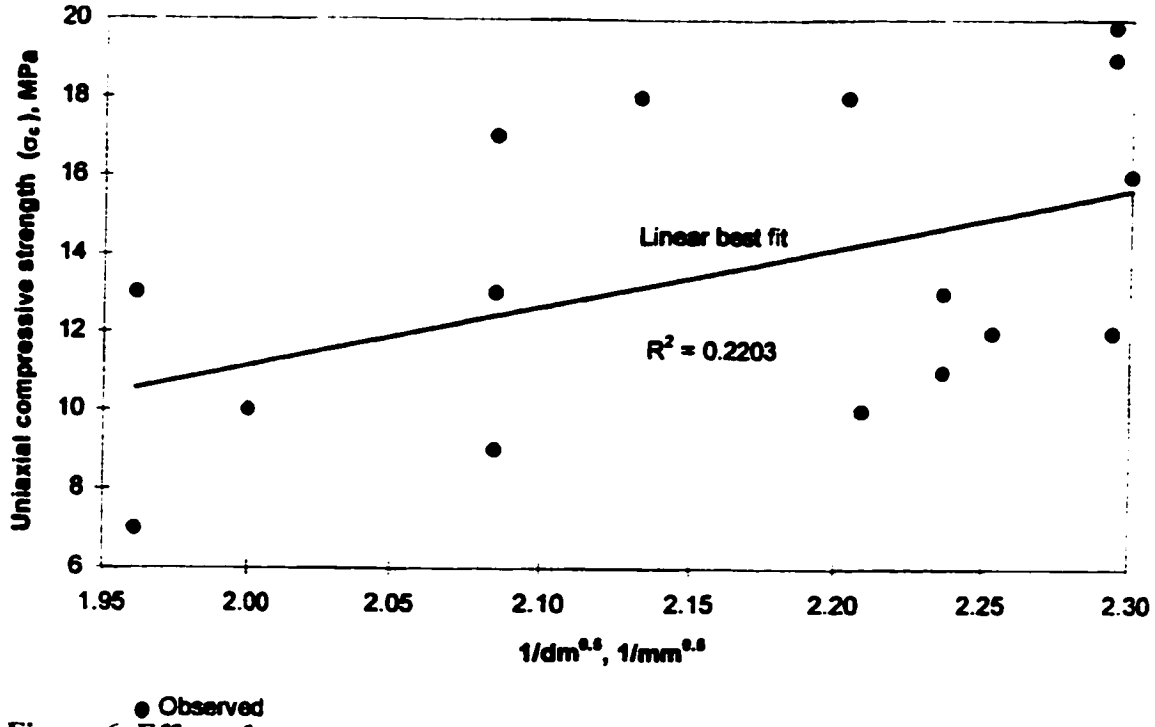

Figure 6. Effect of mean grain size (dm) on uniaxial compressive strength (δ c) (Palchik, 1999).

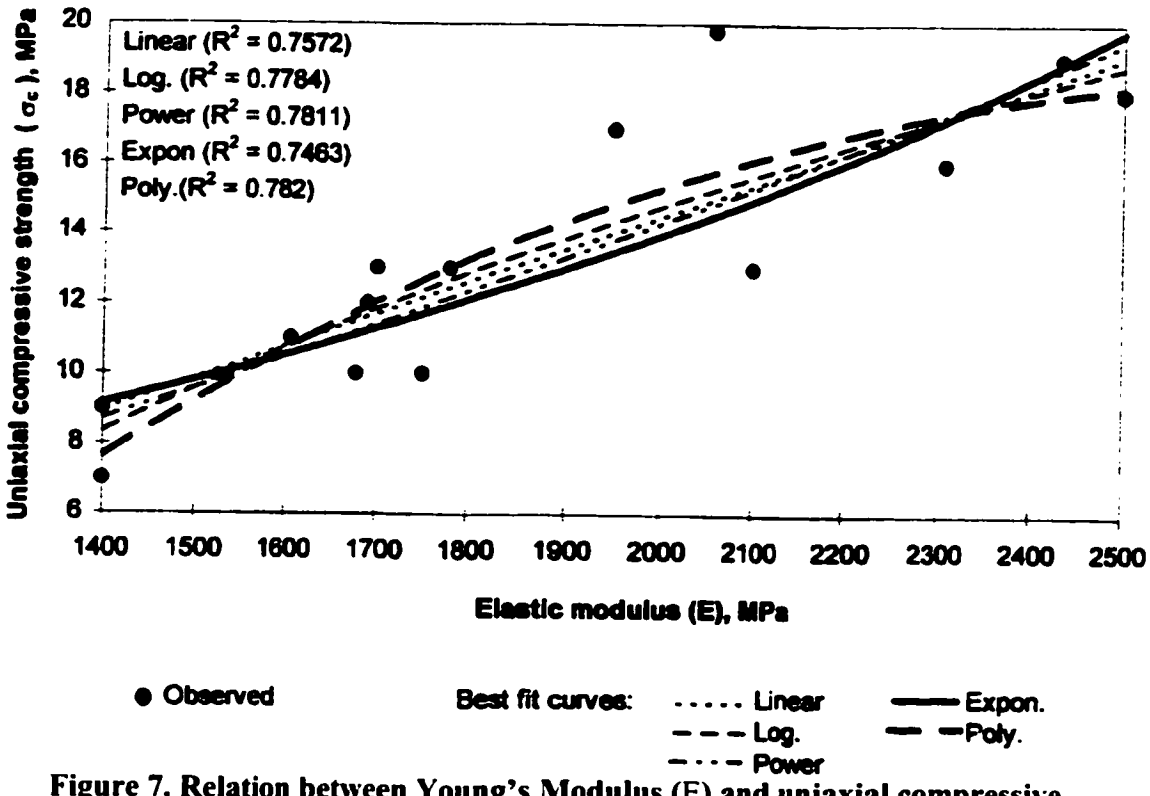

Figure 7. Relation between Young's Modulus (E) and uniaxial compressive strength (δ c) (Palchik, 1999).

Palchik (1999) plotted the reported test data against his model predictions (Eq. 4) (Fig. 8). This empirical model explains the influence of microstructural parameters on uniaxial compressive strength in soft porous Donetsk sandstones (Ukraine).

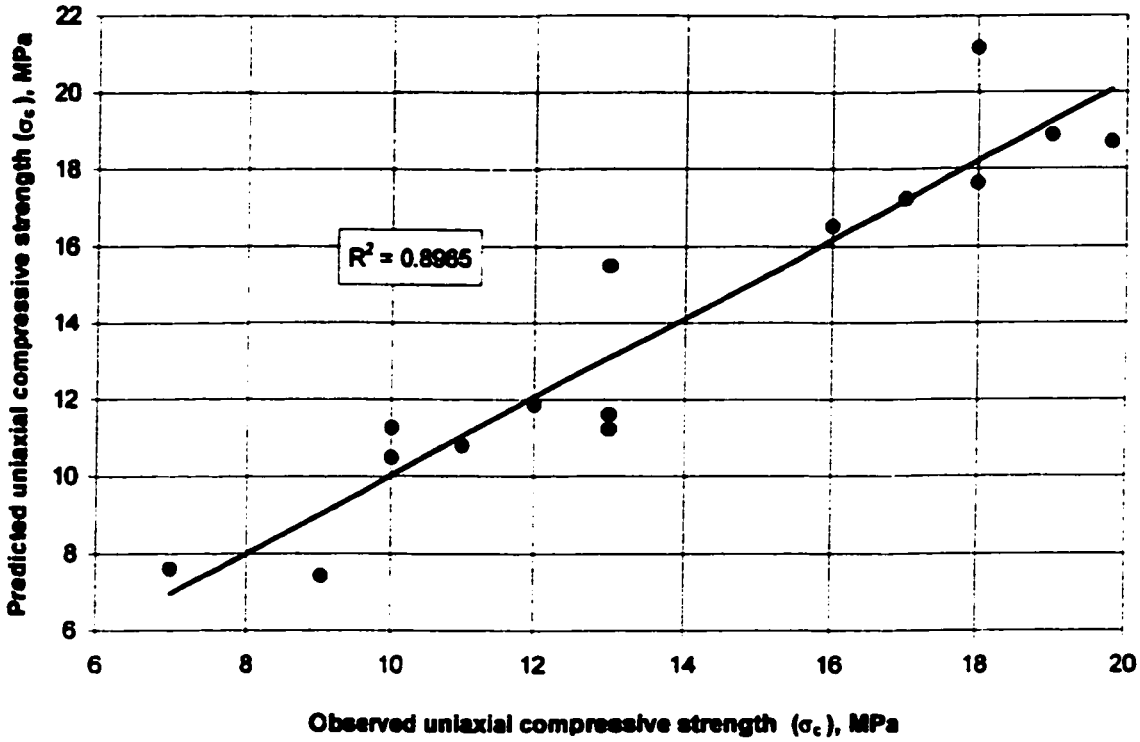

Figure 8. Comparison of predicted and observed uniaxial compressive strength (Palchik, 1999).

III. ROCK TYPES AND THEIR POROSITY

A. Rock Types

Igneous rocks can be divided into two main groups based on their origin and grain size: intrusive rocks and extrusive rocks. There is a wide difference in porosity between these two groups and as a result the igneous samples that have been used in this study are all from the intrusive rock group. Porosity in igneous rocks depends on the rate of cooling of the magma. Quick cooling produces fine crystals with porous texture; whereas

large crystals that are formed upon slow cooling show less porosity. The highest amount of porosity among igneous rocks can be seen among volcanic rocks (Jumikis, 1983). The intrusive rocks usually have a very low porosity because they are formed by crystallization of liquid magma and intergrowth of crystals, which leaves almost no voids.

The microstructure of the sedimentary rocks is different. Sedimentary rocks have typically the highest porosities. They can be divided into two major groups, clastic and chemical precipitates. Chemically precipitated sedimentary rocks show low porosities that are quite similar to intrusive igneous rocks. The reason for the low porosity in these rocks is the crystal growth from solution. Clastic sedimentary rocks usually have a high porosity since they are composed of transported grains that are deposited due to gravitational forces. These grains form a three-dimensional pore network after being deposited, referred to as initial porosity. Limestone is a result of biological and biochemical processes that take place in seawater. It can be found in every geological period from the Cambrian onwards. It can also be found in the Precambrian Era but there it is commonly dolomitic. As the sediments are deposited the stress due to weight of upper layers will increase the pressure and temperature. This will trigger different chemical, physical and biological processes, which in turn reduce the porosity. This series of complex events is called diagenetic processes. Dissolution, precipitation, recrystallization, compaction and consolidation are some of the major diagenetic processes. There is still debate over the origin of dolomite; some consider it as a result of a diagenetic process called dolomitization, but there is also evidence for direct precipitation of authogenic dolomite (Tucker, 1991).

Sandstones are another member of sedimentary rock group that usually consists of mineral grains or rock fragments that are the result of weathering of crystalline rocks. The source rocks can be igneous or metamorphic rocks or preexisting sandstones. Quartz makes up to about 60% of all the sandstones and is accompanied with feldspars (Garrels and MacKenzie, 1971).

Metamorphic rocks are the result of transformation (metamorphism) of igneous, sedimentary and other metamorphic rocks. Generally high pressure and temperature (over 200-300 °C) cause this metamorphism. Due to this transformation almost all of the metamorphic rocks have a lower porosity than the source rocks.

B. Rock Pores, and the Direct Effect of Grain Size on Pore Size, and Internal Surface Area

One of the most important causes of non-uniformity in rocks are pores. Pore microstructure influences most of the physical properties of rocks. Based on the rock type and the mode of formation, the porosity can vary from almost zero in igneous rocks to greater than 0.5 in some clastic sedimentary rocks. Pores have a negative impact on the mechanical behavior of rocks, such as strength (Fig. 9), as confirmed by researchers (Palchik, 1999).

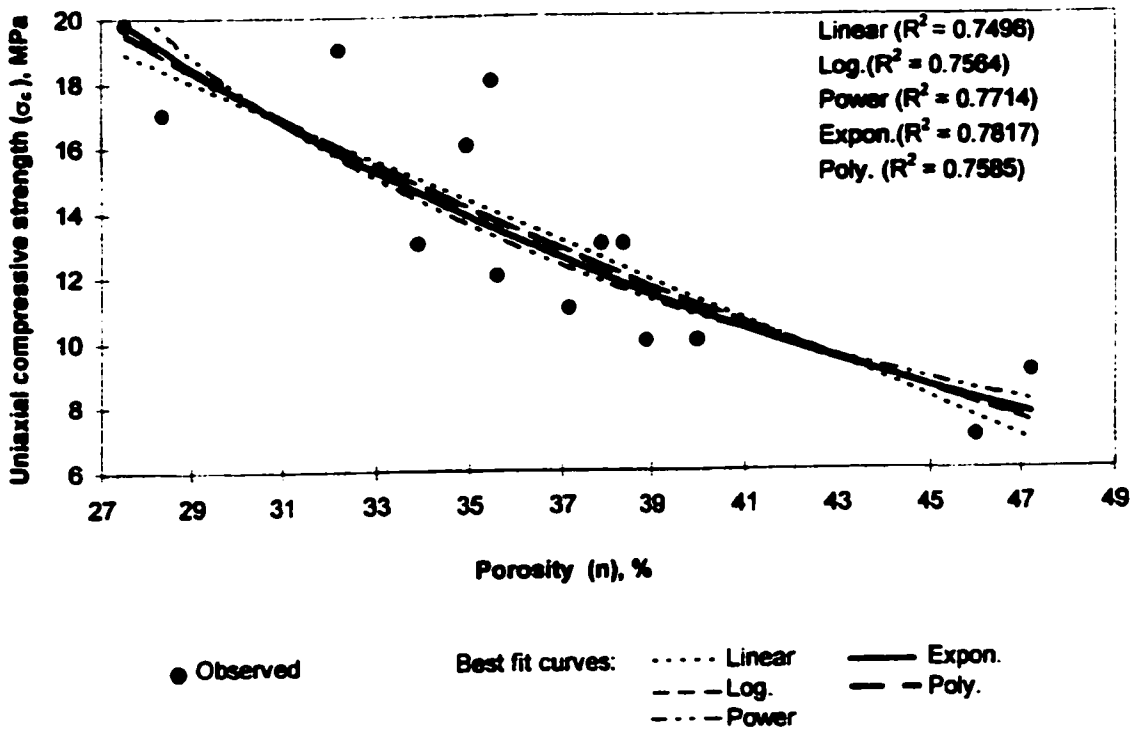

Figure 9. Effect of porosity (n) on uniaxial compressive strength (δc) of soft brittle porous sandstones (Palchik, 1999).

Porosity can be defined in many different ways. The amount of pores in a rock is expressed as porosity. Porosity is the amount of voids in a rock relative to the total volume of that rock:

$$n = Vv / V \qquad (6)$$

n = Porosity

Vv = Volume of the Voids

V = Total Volume

It should be noted that porosity determination by itself does not provide any information regarding the pore size, their distribution, or the degree of connectivity.

In sedimentary rocks the cementing material binding the particles, the particle size, and their distribution determine the total porosity.

A study performed by Hudec (1989a) has revealed the significance of the relationship between grain size and pore size. Based on this study the total pore volume among limestone samples with fine grain minerals was 33% less than the medium grain samples (Table 3).

Table 3. Relationship Between Internal Area, Total Pore Volume (vacuum absorption), and Grain Size Among Limestone and Dolostone Samples (Hudec, 1989a).

Internal area (mm^2/g)	Specific gravity	Absorption (%)	Vacuum absorption (%)	Intrusion volume (cc/g)	65% relative humidity (%)	Grain size
<0.25	2.62	1.07	1.36	1.60	3.70	Medium
>0.25	2.75	0.33	0.39	0.50	24.50	Fine

Pore size and pore surface area also have major effects on the water absorption rate and the amount of water being absorbed. Smaller pore size diameter causes faster rate of capillary absorption and larger pore size diameter provides more room for absorption. The long-term durability of rocks is directly related to their grain size and pore size. The relationship between grain size, pore size and internal surface area is revealed through this example. Imagine a 1000 cm^3 filled with a total of eight, 5 cm diameter spheres in a cubic packing pattern (Fig. 10). The pore size and internal surface area for such a sample is presented in Table 4. Replacing the 5 cm spheres with 2.5 cm spheres while maintaining the same cubic packing pattern requires 64 spheres to fill the same cube. This change effects both pore size and internal surface area. The difference between the two systems can be seen in the same chart.

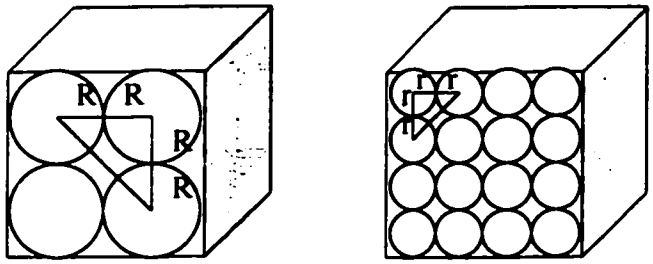

Figure 10. Imaginary cubic packing pattern of grains with two different sizes.

Table 4. Relationship between pore radius (pore size) and internal surface area

Scenario	Sphere Diameter (cm)	Sphere Volume (cm^3)	Total Number of Spheres	Minimum Pore Radius (cm)	Surface Area/Sphere (cm^3)	Total Surface Area (internal) (cm^3)
1	5	523.6	8	4.1	314.2	314.2
2	2.5	65.5	64	2.1	78.5	2904.5
Ratio	×1/2	×1/8	×8	×1/2	×1/4	×9.2

As can be seen from the table above, a proportional relationship exists between grain size and pore size. If grain size is reduced by half then half also reduces pore size and surface area decreases to a quarter of its original size ($S_{sphere} = 4\pi r^2$). On the other hand, total surface area (internal) increased nine times by decreasing the grain size to half the original size in the second scenario.

There are two factors that determine pore characteristics. The first being pore surface activity, which is a function of the surface charge, as determined by the number of unsatisfied bonds along the pore surface. Pore size is the second factor. Hudec (1987) has classified pores into three groups based on their size. Force pores are the smallest size pores with a size of less than one micrometer, and contain only adsorbed water that can be filled under high humidity conditions. Capillary pores, the second type, can be further subdivided into Micro capillary pores which contain both capillary and adsorbed water and range from one to five micrometers and Macro capillary pores with a size greater than five micrometers and less than one millimeter can only be filled after a very long submersion or through vacuum saturation. Bulk pores are the largest pores and mostly contain bulk water and can easily filled and drained. These pores are usually interconnected and are greater than one millimeter in size.

The accepted method of determining pore size distribution is by mercury injection. In this method all the pore water is removed from the rock and then it is immersed in a mercury bath in a pressure vessel at atmospheric pressure. Pressure is gradually applied to the vessel. The displaced mercury volume at each step after increasing the pressure is a representative of the pore size and also pore volume.

IV. EFFECT OF MOISTURE, TEMPERATURE AND IONIC SOLUTIONS ON ROCKS

A. Absorbed Water

Absorbed water is the water held in the rock pores after immersion in water. When a rock is immersed in water, most of the pores are filled, but some air remains trapped. To achieve complete saturation, the water is introduced to the rock under vacuum, or the rock is boiled in water. At boiling, all air in the pores is displaced by vapor, which condenses upon cooling, creating vacuum, drawing in water, and completely saturating the rock.

Pore water in completely saturated rock samples can alter the response for the rock to applied stress in a confined situation. Pore water pressure (or in general pore fluid pressure) reduces the effective value of the mean normal compressive stress (Rudnicki, 1985). Pore fluid pressure can increase or decrease if the pore volume decreases or increases which eventually will cause the effective stress to decrease or increase. In unconfined compression condition, the effect of pore fluid is minimal. The fact that pore fluid can support part of the elastic load in dynamic cases was confirmed by other researches (Yale and Jamieson, 1994). Pore fluid pressure drawdown in oil field production, can cause pore collapse in weak, porous rocks, which will result into a large decrease in permeability and production (Mowar et al., 1994).

B. Adsorbed Water

Due to the di-polar nature of water molecules and the polarity of the pore surface, water molecules are attracted to the pore surface and may form up to several layers of adsorbed water (Fig. 11) (Hudec, 1993).

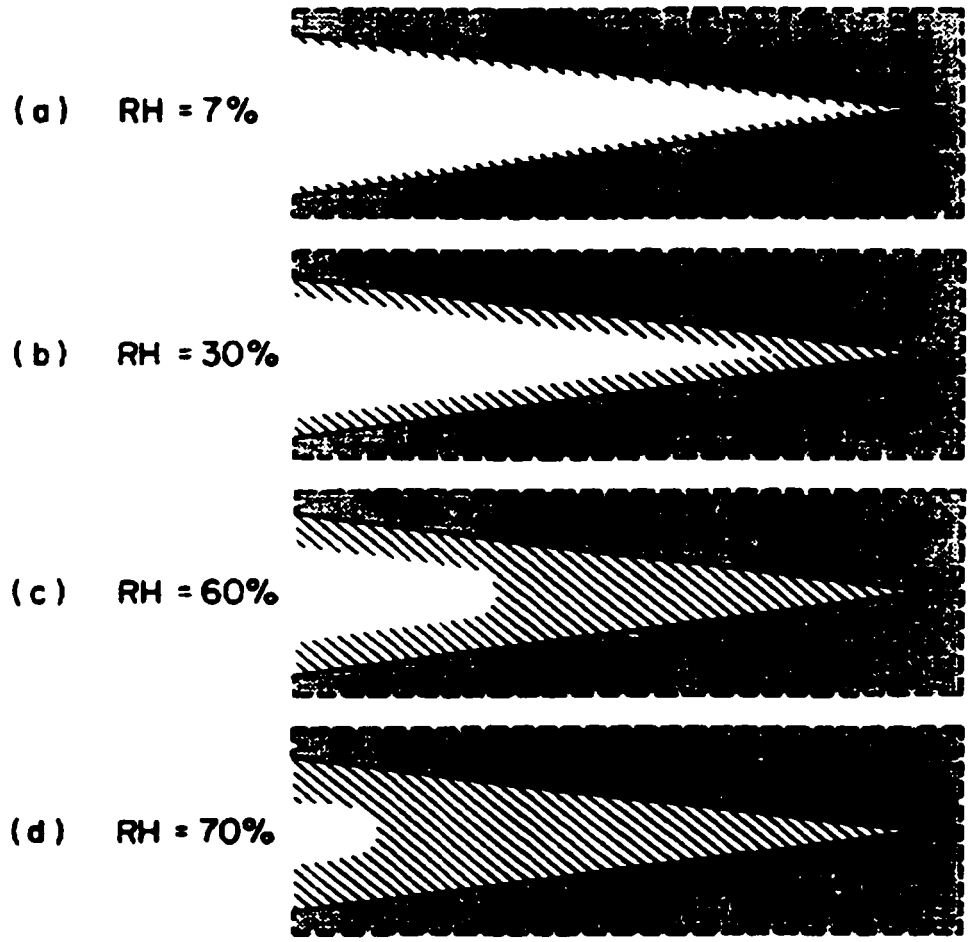

Figure 11. Gradual filling of micropore due to adsorption and capillary condensation (Horrigmoe, 1985; from Bazant, 1972).

Rock pores in nature always contain a certain amount of water, depending on the environment and temperature. Under some conditions the water can be bound (adsorbed)

to the mineral crystal faces as a film (Fig. 12.a), which exhibits different behavior than free water. This type of water cannot be drained mechanically or gravitationally, and it does not freeze. In some other environments rock pores can be fully saturated with adsorbed water. Fully saturated rocks transmit the P and S waves much easier than the partially saturated rocks. As a result, over-breakage can be seen in rock blasting more among fully saturated rocks (Lienhart, 1994). Based on these findings it can be stated that most of the interactions between rock, water and ions create a stress that may result in a rapid contraction or expansion of the rock. Rocks when initially wetted undergo contraction by capillary tension (Hudec and Sitar, 1975). When all the capillaries are filled, the rock enters a relaxation period and may cause an expansion in some instances. As a result, normal alternate wetting and drying may cause the rocks to expand and contract, which can then result in a rock's deterioration.

Water molecules interact with the pore walls through Van der Waals forces. The physical adsorption releases 4 Kcal/mole heat per gram (Jumikis, 1983). This interaction reduces the surface energy of the pores until the molecular chemical potential (μ s) of the adsorbed layer is equal to the chemical potential (μ v) in the bulk solution. Adsorbed water has different physical characteristics than regular water. It is physically rigid and it exerts pressure against the pore walls (Hudec, 1974).

Adsorption capacity of a sample plays a major role in its specific surface area.

$$\text{Specific Surface Area} = \text{Surface Area} / \text{Unit Volume of the Solid} \qquad (7)$$

The nature of the pore surface is another factor that determines the adsorption potential. Different types of surfaces possess different amounts of surface charge; the higher the charge, the thicker the adsorbed layer of water. There are four different types

of surfaces in nature. The highest surface charge belongs to a fractured surface. Amorphous minerals have the next highest polarity on their surface since they are not crystallized and as a result the bonds are not satisfied. Cleavage surface is a plane of relative weakness in the mineral, and presents an intermediate sorptive surface. Crystal surface has least charge compared to cleavage surface, since the atoms are bound to each other and the charges are satisfied, and has the least charge (Hudec, 1993).

By increasing the relative humidity (RH), the thickness (diameter) of adsorbed layer of water increases (Fig. 11). The adsorbed layer's thickness can increase to up to five molecules provided that the pore size allows it. The minimum pore diameter required to have such a layer on both sides of the pore wall was calculated to be 26 angstroms or 10 molecules. A capillary meniscus will develop in sufficiently high relative humidity, if the diameter of the pore allows it (Horrigmoe, 1985).

C. Ion Adsorption

Since cations possess a stronger charge than the water dipole, they are adsorbed more easily to the negatively charged pore wall. Due to the same strong charge they attract more water dipoles and therefore increase the thickness of the adsorbed water and also accelerate capillary pore filling (Fig. 12.a and 12.c) (Hudec, 1980 and 1993). As a result, in their presence a larger portion of the pore will be filled with adsorbed water. Ion behavior is based on their charge/ionic ratio. This explains more aggressive behavior of Na^+ compared to K^+ ions (Hudec, 1989). Based on Kelvin's equation, the vapor pressure is a function of the surface tension of the solution, the pore radius and the temperature:

$$\text{Ln}\,(p/p_\circ) = -2\,\delta\,M / \rho\,R\,T\,r \qquad (8)$$

p = pressure over concave surface

$p_\circ$ = pressure over plane surface

$p / p_\circ$ = relative vapour pressure

δ = surface tension of the solution

M = molecular weight of the solution

ρ = density of the solution

R = the gas content

T = absolute temperature

r = radius of the pore

As can be inferred from Kelvin's formula, a decrease in the pore radius, and in the temperature can increase the relative vapor pressure. On the other hand, an increase of dissolved ion content in the water increases the molality of the water and therefore decreases the relative vapor pressure. At the same time, since the cations are adsorbed to the pore wall, they adsorb more water dipoles and increase the thickness of the adsorbed layer. This may cause the larger pores to fill and increase the osmotic differential in the smaller pores. When two bodies of water with different relative vapor pressure and osmotic potential are in contact, the resulting difference causes the flow of water from the high vapor pressure area towards the low vapor pressure area. Due to the concentration of the ions in small pores, this flow is usually from large pores to small pores, which can cause an expansion in the rock.

D. Osmotic Pressure

Adding more salt to a liquid, liquid evaporation or solution freezing will increase the ionic concentration in a liquid. Adding fresh water to a liquid, by any means such as melting the existing ice crystals in the pores will decrease the ionic concentration in that liquid. For all these reasons, the ionic concentration in a liquid may change and create an unbalanced ionic concentration. Based on the definition of equilibrium state in thermodynamics, a system at equilibrium is disturbed when one or more of its parameters are changed. The disturbed system will always tend to move towards equilibrium state; this causes an osmotic potential in the pore system (Anderson, 1996). The flow of water molecules in an unbalanced ionic liquid is always from the more dilute or low ionic concentration area to the high ionic concentration area and this flow creates a hydraulic pressure in the system (Fig. 12.e).

The osmotic pressure developed between two bodies of water can be calculated by the formula (Hudec, 1993 from Glasstone, 1946):

$$P_o V_l = R\ T\ Ln\ (p/p_o) \qquad (9)$$

P_o = Osmotic pressure (dynes cm^3)

V_l = Volume occupied by 1 mole of solvent (ml)

R = Gas constant

T =Absolute temperature (K)

p/p_o = relative vapour pressure

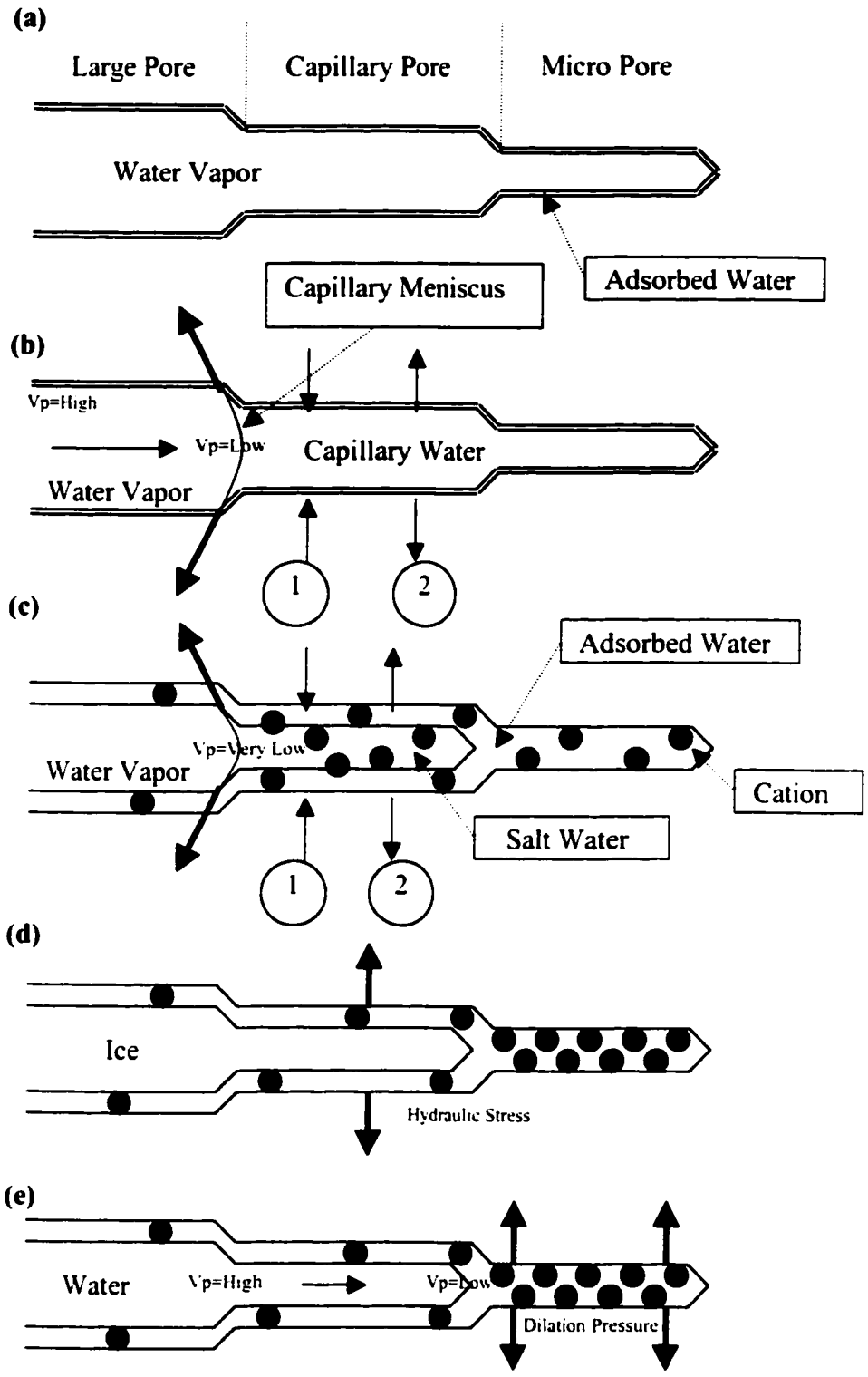

Figure 12. Various states of water and direction of forces in rock pores. (a) Adsorbed water. (b) Capillary water. (c) Salt water solution in room temperature. (d) Salt water solution in subzero temperature. (e) Exposure of rock pore containing salt water solution and ice to room temperature ((1) Contraction, (2) Expansion).

The presence of salts like NaCl in pore water accompanied with cycles of freeze and thaw creates an osmotic pressure between adjacent pores with different sizes (Hudec, 1991) (Fig. 12.d and 12.e). Pore water in micro pores consists of non-freezable adsorbed water however pore water in macro pores freezes in subzero temperatures. Since the water in large pores freezes in sub zero temperatures, Na^+ ions will be expelled and capillary water migrates towards the micro pores. This results in a higher concentration of Na^+ ions in the non-freezable adsorbed water in micro pores, while the large pores become depleted of Na^+. As a result, micro pores will have a greater ion to pore volume ratio than the macro pores after ice is formed in macro pores. The osmotic potential is reversed during thawing. The water regenerated due to the ice melting in large pores has low ion concentration and flows into the micro pores under osmotic potential; the flow causes dilation pressure in micro pores that cause expansion of the system.

Three potentially different behaviors can be recorded based on the relationship of tensile strength of the rock to osmotic pressure of pore fluid. If the tensile strength of the rock is higher than the pore fluid osmotic pressure, nothing will happen, but if the osmotic pressure is higher than the pore wall's tensile strength, then the system will expand and possibly generate a tension crack. The new crack will cause further hydraulic pressure in the system since it is a narrow, new pore. It will adsorb water and ions and causes more hydraulic pressure on the pore wall. The process of crack development and pressure generation continues and may result in expansion or deterioration in the whole rock system.

E. Capillarity Effect on Rocks

One of the factors affecting rock behavior in presence of water is the capillary flow and tension. The capillary theory predicts that the pressure difference at the curved meniscus (capillary meniscus) of the air-water interface determines the suction force, which causes the water migration inside the pores (Matsuka, 1989). Water presence in a rock is either the result of capillarity sorption or imbibition, caused by high humidity or immersion, respectively. Rock permeability controls the water transport properties. When a porous media and a liquid are in contact, the liquid will be "sucked up" by capillary pores at a rate which is a function of the pore radius (r), the surface tension of the liquid and contact angle (θ) between liquid and the pore wall (Fig. 13) (Hudec, 1989). Capillary surface moves inside the pore until it reaches a point, where the gravitational weight of the liquid column balances the capillary tension (Bellanger et al., 1993). The maximum height of liquid in a pore is called capillary rise. Capillary rise has a direct relationship with surface tension of the liquid and an inverse relationship with the capillary radius:

$$h \propto p / r \tag{10}$$

h = Capillary Rise

p = Surface Tension

r = Capillary Radius

As the water is introduced to a rock or any porous system, the capillary suction draws the water into the capillary pores. The rock experiences tension, which causes contraction. The tension can be calculated from this formula:

$$Pc = 2 \times \gamma \times \cos\theta / r \qquad (11)$$

Where: r = Pore (capillary or meniscus) Radius

γ = Surface tension of the liquid

θ = Contact angle between the pore liquid and the pore wall

Pc = Capillary Tension

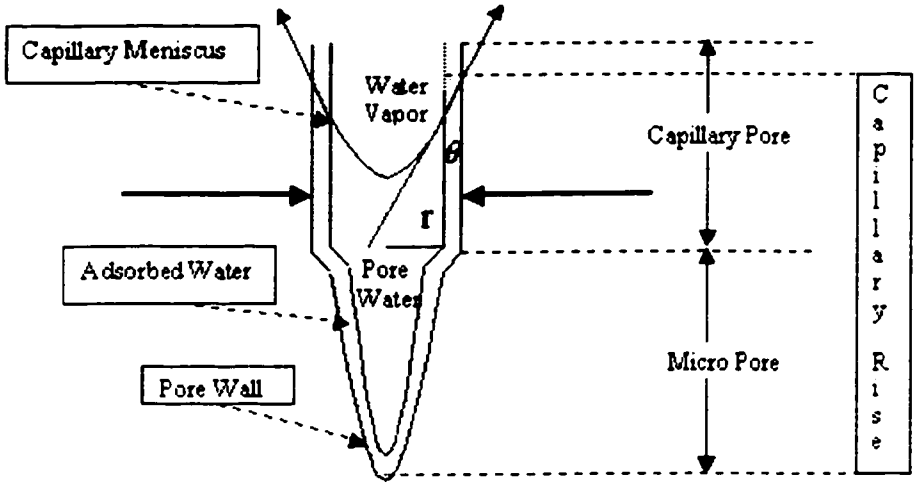

Figure 13. Diagram illustrating a capillary system.

As can be seen from the formula (10), any increase in surface tension of the liquid or reduction in the diameter of the pore wall will result in a higher capillary rise. The contact angle between the pore wall and the liquid depends on their characteristics and varies among different materials. Water molecules are always available in the air in the form of vapor and form a layer over pore walls. For exact determination of the capillary tension, the thickness of the adsorbed layer should be subtracted from the pore radius.

Hudec (1987) has shown the effect of grain size on capillary absorption in rocks. The coarse grain rocks show a logarithmic rate of saturation trend, which starts rapidly but slows over time. In the same test, fine grained rocks achieved 80% saturation within

the same time that the coarse grain pores reached only 40% saturation. As soon as capillary suction begins, a rapid rock mass contraction takes place. By the time larger capillaries are filled, the contraction has stopped and the rock goes into a relaxation state and when all the macro capillaries are filled with water the rock returns to its original dry volume (Hudec and Sitar, 1975). Rocks that consist mostly of force (micro) pores expand beyond their original volume due to the adsorbed water held in the pores. The adsorbed water creates an osmotic pressure difference and continues to adsorb more water (Fig. 12.b)

When rocks are subjected to sub zero temperatures, capillary pore water starts to freeze. However, due to the presence of surface interaction forces and normal super cooling, the freezing point of pore water is lower than 0°C. The freezing process starts with larger pores and is directly related to the pore geometry (Marchand et al., 1994). Once the ice crystals are formed, there will be a 9% expansion due to the water – ice phase change. If all the pores are fully saturated, a hydraulic pressure will cause expansion in the system.

The presence of cations in the water reduces the vapor pressure in capillary water and causes more contraction. When fresh water is introduced to the system by rain or melting snow, more water molecules will be attracted, eventually causing expansion. Under certain climatic conditions the contraction and expansion will be cyclical, causing a break down and eventually failure of the rock.

F. The Effect of Temperature on Rocks

Temperature fluctuations can cause rocks to expand or contract. The expansion or contraction is due to the internal stresses that are produced within rock crystals.

$$\Delta L = \alpha_t (T_2 - T_1) \tag{12}$$

ΔL = Length Change

α_t = Coefficient of linear thermal expansion

T_1 = Initial Temperature

T_2 = Final Temperature

The coefficient of linear thermal expansion varies for different rock types. It should be noted that the rock composition, density, moisture content and the other factors all affect the thermal expansion of rock (Zimmerman, 2000).

V. SAMPLE COLLECTION AND PREPARATION

A. Sample Collection and Description

Originally 129 bulk samples in the form of large rock blocks from a total of 44 locations were collected on two separate occasions from active quarries in Ontario. Stephen J. Rigbey (1980) and Martin Ondrasik (1996) obtained all of the samples used in this study. The samples included a variety of sedimentary, igneous and metamorphic rocks. Sedimentary rocks, especially limestone and dolomite are the main rock aggregate source in Ontario, therefore comprised the two major rock types used in this research.

Stephen J. Rigbey gathered the first set of bulk samples (ID #1 to 118) in the spring of 1977; Martin Ondrasik gathered the second set (ID#120 to 131) in 1995. With the exception of two bulk samples (ID#114 and 118) gathered along road cuts, the remainder of the bulk samples were collected from freshly worked faces of active quarries in Eastern and Southern Ontario. Quarry name, number, location, sample identification and lithological description of all the samples can be found in Appendix A.1. The sample location map is provided in Appendix G.1. For convenience and comparison, the sample identification nomenclature used by Rigbey and Ondrasik has been maintained.

From a possible pool of 129 bulk samples collected, 88 were available for this study. Among those available samples, 10 could not be used due to either cracks, or inadequate core lengths. Sample population table including rock types, number of samples and their percentage from the whole population can be seen in Table 5.

Table 5. Rock type distribution and their percentage

	Rock Type	Number of Samples	Percentage
Paleozoic	Dolomite	43	56
	Limestone	24	31
	Sandstone	4	5
	Shale	1	1
Precambrian	Granite	1	1
	Hornblende	1	1
	Nepheline	1	1
	Marble	3	4

B. Geological Description of the Rock Samples

Samples were collected from 17 geologic formations of Eastern and Southern Ontario. A brief description of depositional environment, lithology and distribution of each formational unit follows. Sample location and lithology can be seen in Appendices A.1 and G.1.

Potsdam Formation, with an undetermined depositional environment, is distributed in the subsurface of southwestern Ontario and consists of arkosic conglomerate and orthoquartzitic sandstone (Winder and Sanford, 1972; Sanford and Quillian, 1959 in Geology of Ontario, 1992).

March Formation, formed in a supratidal to subtidal depositional environment, and consists of interbedded sandstones and dolostones. It is distributed in eastern Ontario (Bond and Greggs, 1973; Williams, 1991 in Geology of Ontario, 1992).

A supratidal to intertidal, hypersaline depositional environment has been suggested for Oxford Formation. The Oxford Formation dolostone outcrops in Eastern Ontario (Williams, 1991 in Geology of Ontario, 1992).

Gull River and Bobcayegon Formations comprise the Simcoe Group in south-central Ontario (Liberty, 1969 in Geology of Ontario, 1992), and can also be found in the subsurface of eastern and southwestern Ontario. They represent a continuous deposition on a generally deepening shelf (Brookfield and Brett, 1988; Coniglio et al., 1990 in Geology of Ontario, 1992). The Gull River Formation is typically a limestone, which is locally argillaceous, silty or dolomitic (Okulitch, 1939; Liberty, 1969; Williams, 1991 in Geology of Ontario, 1992). The Gull River Formation represents deposition within a hypersaline supratidal to intertidal flat environment with coarser grained beds representing storm deposition (Barnes, 1967; Mukherji, 1969; Coniglio et al., 1990 in Geology of Ontario, 1992).

The Bobcaygeon Formation consists mainly of fossiliferous limestone, with variable argillaceous content (Williams, 1991 in Geology of Ontario, 1992). The grain size, sedimentary features and fauna suggest a shallow subtidal, well-agitated depositional environment (Barnes, 1967; Coniglio et al., 1990 in Geology of Ontario, 1992).

Billings Formation is distributed in eastern Ontario and its depositional environment is below the storm wave base. It appears in dark brown to black color and is a calcareous to noncalcareous shale with thin interbeds of limestone (Wilson, 1946; Williams, 1946 in Geology of Ontario, 1992).

Some of the sandstone samples that were tested in this research belong to the Medina Group. The Medina Group or Cataract Group is distributed in southern Ontario, and formed in lower Silurian and is part of the Whirlpool Formation, Manitoulin Formation, Cabot Head Formation and Grimsby Formation. All of these Formations

belong to a shallow marine and turbulent environment. The lithology in these Formations includes shale, sandstone, dolostone and limestone (Geology of Ontario, 1992).

The argillaceous dolostones and dolomitic limestones of the Reynales Formation occur in the subsurface of southwestern Ontario and Niagara Peninsula area, representing a subtidal to basinal depositional environment (Bolton, 1957; Sanford, 1969; Brett et al., 1990 in Geology of Ontario, 1992).

Amabel dolostones are exposed in Manitoulin Island and Bruce Peninsula to Burlington and also can be found in subsurface of southwestern Ontario. This Formation represents a shallow high-energy basinal environment (Bolton, 1957; Armstrong and Goodman, 1990 in Geology of Ontario, 1992).

The Decew Formation, a thin argillaceous dolostone, deposited in shallow restricted environment, is geographically restricted to the northern rim of the Appalachian Basin (Bolton, 1957 and 1964; Crowley, 1973 in Geology of Ontario, 1992).

The only Formation in this research that has samples of two different rock types (limestone and dolomite) is the Lockport Formation. Lockport Formation forms parts of the Niagara Peninsula and extends in the subsurface under much of southwestern Ontario (Bolton, 1957; Hewitt, 1971; Sanford, 1969 in Geology of Ontario, 1992). Lockport Formation's depositional environments range from shallow, high energy to partly restricted subtidal environments (Crowley, 1973; Brett et al., 1990 in Geology of Ontario, 1992).

The Guelph Formation dolostone is exposed in southwestern and northwest Ontario. It was deposited in reef and inter-reef environments (Liberty et al., 1976 in Geology of Ontario, 1992).

The resistant dolostones of Bertie Formation are exposed in Niagara Peninsula area. An intertidal to supratidal environment has been suggested as the depositional environment for Bertie Formation (Chapman and Putnam, 1984 in Geology of Ontario, 1992).

The Oriskany Formation, distributed in Niagara Peninsula area, is a coarse-grained calcareous quartz sandstone. This relatively thin formation represents a shallow marine depositional environment (Kobluk et al., 1977; Sanford, 1968; Uyeno et al., 1982 in Geology of Ontario, 1992).

The Bois Blanc Formation is characterized by cherty limestone in Appalachian Basin, and then grades westward into dolostones in Michigan basin. It is distributed in southwestern Ontario and represents a shallow marine depositional environment (Sanford, 1968; Uyeno et al., 1982 in Geology of Ontario, 1992).

The Lucas Formation (Detroit River Group), a gray to brown thin to medium bedded limestone and dolostone, deposited in very shallow marine to evaporitic environment, is found in southwestern Ontario (Sanford, 1968; Uyeno et al., 1982; Johnson et al., 1985 in Geology of Ontario, 1992). It thins toward the margins of the Michigan Basin and pinches out in the Port Dover area on the Niagara Peninsula (Telford and Hamblin, 1980).

The Dundee Formation was deposited in lagoonal, open shelf, and deep-water environments, with a rich fossiliferous, micritic limestone beneath Quaternary sediments in a broad, northwest-trending belt in southwestern Ontario. It extends from central Lake Erie to Lake Huron, and also underlies parts of the Windsor-Essex area and Pelee Island in Lake Erie (Uyeno et al., 1982; Birchard, 1990 in Geology of Ontario, 1992).

C. Samples Preparation

EX-size rock cores were obtained from the block samples by Rigbey and Ondrasik. Rock core length ranged from 40 mm to 56 mm with a constant diameter of 19 mm (Fig. 14).

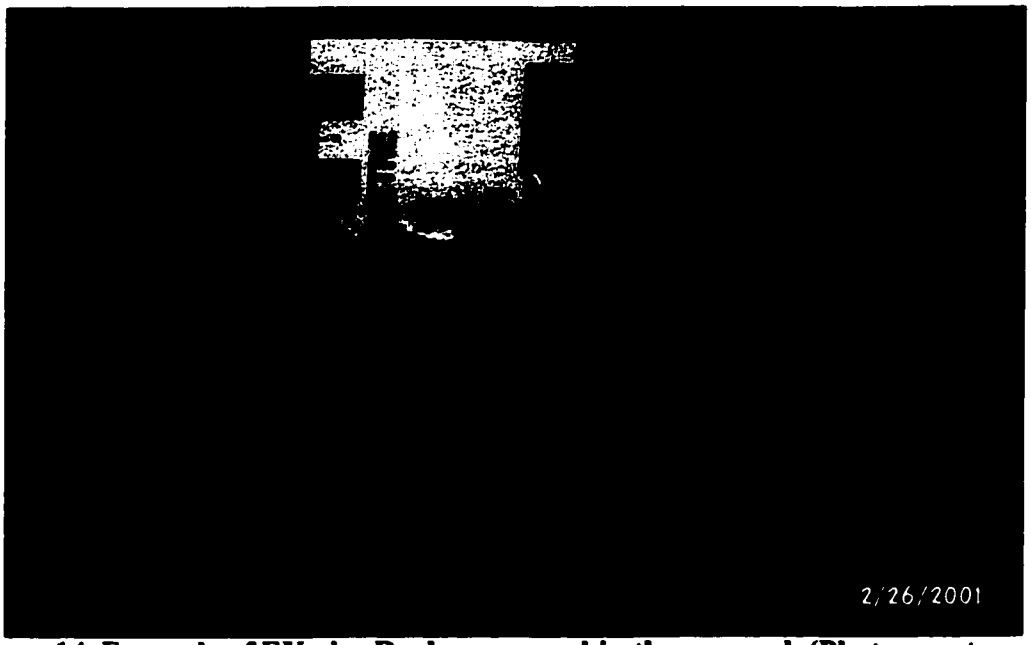

Figure 14. Example of EX-size Rock cores used in the research (Photo courtesy of Dr. P.P. Hudec).

All samples were cored at right angles to their foliation or bedding plane. The samples underwent additional preparation to make them suitable for this research. The first step was cleaning the cores of any deleterious material such as oil, salt and dirt. The cleaning program consisted of immersing samples in fresh water for a period of three months. Within the three-month period, the water was replaced with fresh water on a biweekly basis. To ensure that the ends of samples were at right angles to their length, a grinding machine was used to square off the ends. The samples were then immersed in water again to leach any remaining salts for a final four-week period.

VI. EXPERIMENTAL METHODS

A. Outline

The prepared samples, three cores per sample, were subjected to two sets or phases of experiments. The first phase consisted of determining the basic rock properties. The properties measured included: unit weight, adsorption, absorption, porosity, and expansion/contraction due to freezing. The second phase of the research consisted of modulus of elasticity measurements of the core samples under seven different combinations of temperature and humidity.

B. Basic Rock Property Tests

1. Dry Unit Weight

The dry unit weight of rock is expressed as the ratio of the weight of the dry rock to the volume of the rock, including all the voids (Jumikis, 1983):

$$\gamma_d = \frac{Wd}{V} \tag{13}$$

γ_d = Dry Unit weight Wd = Dry Weight V = Volume of the Rock

Accordingly, rocks containing more voids in their structure will have a lower unit weight. In this research, core samples were divided into random groups of 20, placed in an aluminum foil container and put in an air-circulating oven together with containers of phosphorous pentoxide. The oven temperature was set at 105°C and the samples were left for a period of 24 hours. They were then transferred into groups of 20, to a desiccator containing phosphorous pentoxide, and left there for an hour to cool. From there, they were weighted using a very sensitive digital single pan balance with a minimum accuracy of 0.00001 gram. Length and diameter of each core were measured to an accuracy of

0.001 millimeter. The volume of each sample was calculated from the measured dimensions and then dry unit weight was determined.

2. Moisture Content

Weight of the water present in rock divided by oven-dried weight of the rock, which is expressed, as a percentage is the moisture content or degree of saturation of rock:

$$M = \frac{Ww - Ws}{Ws} * 100 \qquad (14)$$

M = Moisture Content Ww = Weight of the water Ws = Oven-dried weight

3. Adsorption

Adsorption of each sample was measured first at 50% and then at 98% relative humidity (RH) at room temperature. Prior to entering an air tight humidity chamber, all the samples went through an oven-drying period of 24 hours at a temperature of 105°C, then were allowed to cool, and weighed. The desired humidities were achieved by using a super-saturated solution of salts for a period of 72 hours (Lide and Frederikse, 1998). The 50% RH was maintained by a super-saturated solution of Calcium Nitrate Tetra Hydrate ($Ca(NO_3)_2.4H_2O$) . Samples were then transferred to a desiccator in groups of 10, and then immediately weighed. The same procedure was followed for adsorption in 98% humidity except that a super-saturated solution of Copper Sulfate Penta Hydrate ($CuSO_4.5H_2O$) was used to achieve the desired humidity. In both 50% and 98% humidity conditions the temperature of the chamber was maintained at 20°C. Adsorption was then calculated based on the following equation:

$$\text{Adsorption} = \frac{W\text{ads.}}{W\text{dry}} * 100 \qquad (15)$$

*W*ads. = Weight of adsorbed water= Weight of sample - Weight of dry sample

Wdry = Weight of dry rock

4. Absorption

All samples were immersed in fresh water for a 24-hour period. The mass difference between the saturated sample and the oven-dried sample was calculated as:

$$\text{Absorption} = \frac{W\text{abs.}}{W\text{dry}} * 100 \qquad (16)$$

Wabs. =Weight of absorbed water=Surface dried weight - Weight of dry sample

Wdry =Weight of dry rock

5. Total Effective Porosity (Vacuum Absorption)

All samples were first immersed in water and then boiled for a period of four hours. Boiling displaces the air that occupies the voids by vapor, and upon cooling, the vapor condenses and fills the void with water (Hudec, 1989). After cooling, the samples were surface towel dried and weighed. The mass difference between the fully saturated sample and the oven-dried sample was calculated, and used in equation (6) to obtain the effective porosity of the sample. This value is also known as 'vacuum' absorption, since evacuating all the air prior to immersing the sample will achieve the same result.

6. Length Change

Samples were taken from room humidity and temperature condition, and placed in a freezer where temperature was set at -18°C and humidity at 65% for a period of 48 hours. They were individually removed from the freezer and their lengths were immediately measured to an accuracy of 0.001 millimeter, using an electronic vernier device. To determine the length change, samples length in freezer was subtracted from their length in room temperature.

C. Construction and Operation of the Stress Frame

The apparatus used in this research consisted of one solid rigid frame that held a hydraulic jack and a base. The hydraulic jack was connected to a hand operated hydraulic pump and also to a hydraulic wheel (Figs. 15 and 16). Pumping the hydraulic pump caused the hydraulic fluid to flow into the hydraulic jack and exert the stress via a piston mounted on the base. The hydraulic wheel was used to finely regulate the pressure. A hydraulic stress gauge measured the approximate stress applied on the sample while a Viatran pressure transducer, mounted on the hydraulic wheel, measured the exact pressure. The transducer was connected to a digital display showing the stress in psi. A digital LVDT strain gage (Mitoyoto IDF125E) was placed on the frame to measure the length change (strain) of the sample due to the applied stress.

The digital pressure gage and LVDT strain gage were both connected to a data acquisition card, which linked the data to a personal computer. Labview software was used to program the computer to receive and record the incoming data at a programmed rate. The data was then transferred into Excel spreadsheet for reduction, and to Systat software for statistical evaluation.

D. Unconfined Uniaxial Elastic Modulus Compression Test

In this test a rock core specimen is placed under increasing stress and the resultant deformation or strain is measured. The Young's Modulus of the rock sample can be calculated from the stress and strain data. If the applied stress is sufficiently high, the sample may fail, and the ultimate strength can be determined. The stress/strain results usually show some dispersion due to microfissures, and also due to the absence of a

lateral stress. For this reason the standard deviation for uniaxial test results is always greater than standard deviation for confined triaxial tests. The ratio of height to diameter in this research usually ranged between 2.5 to 3, with an average of 2.7 (ASTM, 1965). Compressive strength of rocks is also dependent on factors discussed in section II.B (geological region, porosity, particle size, non-homogeneity, anisotropy, loading rate, direction of applied stress, sample shape and size, height to diameter ratio, and water content).

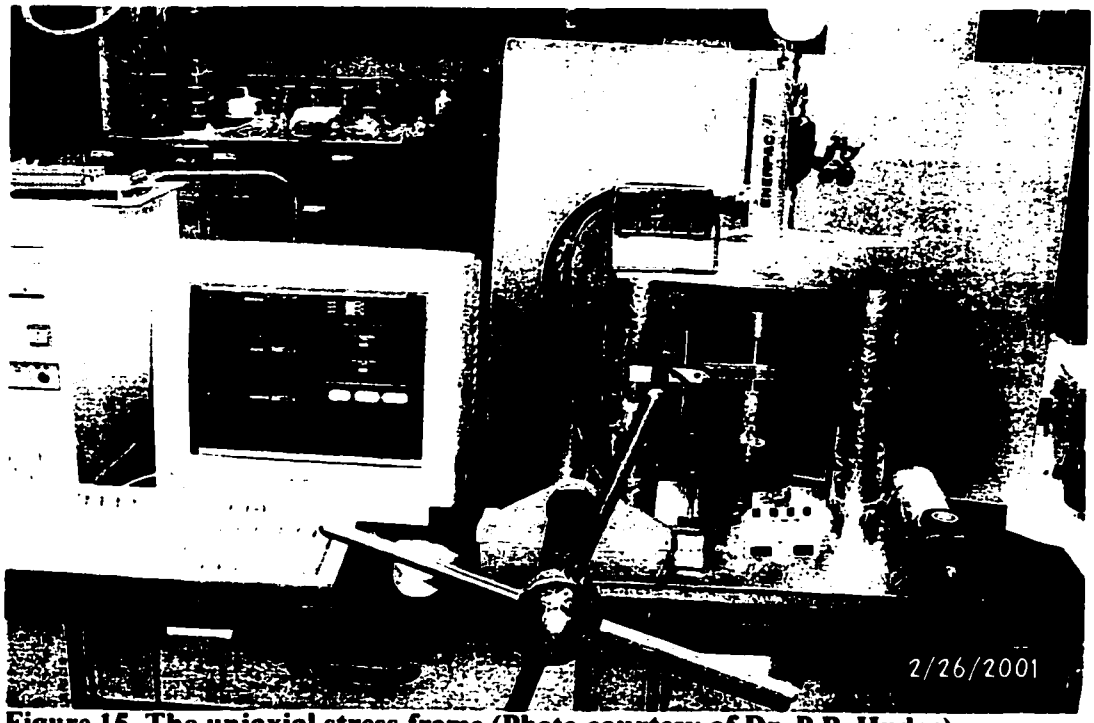

Figure 15. The uniaxial stress frame (Photo courtesy of Dr. P.P. Hudec).

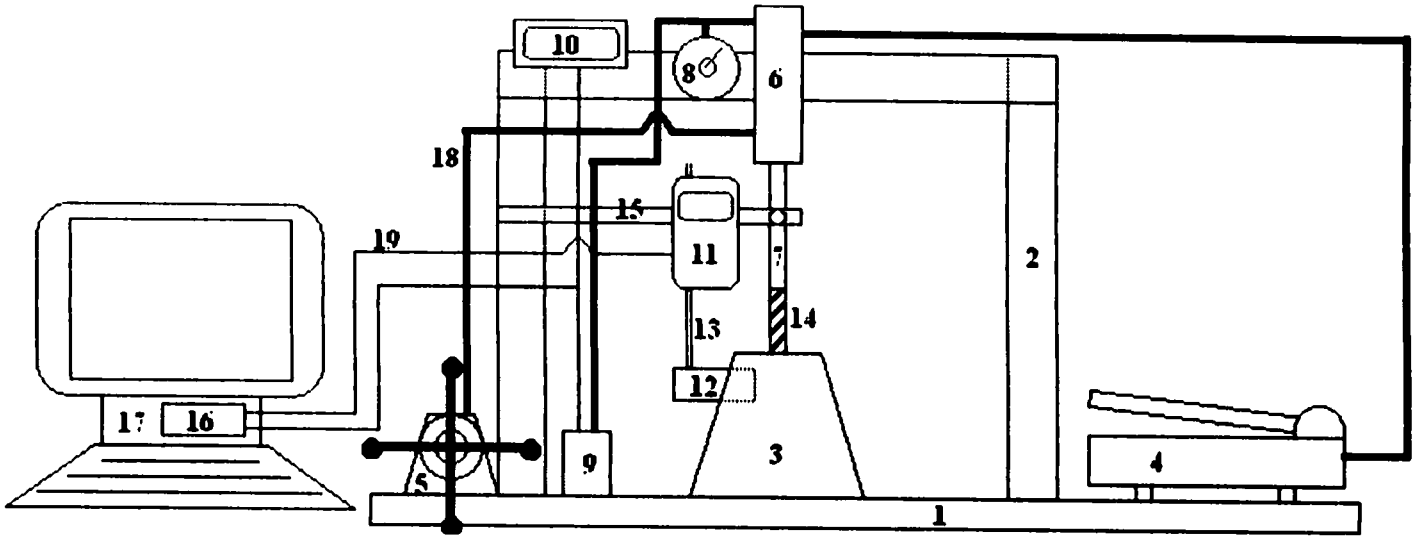

Legend:

1. Base
2. Frame
3. Sample base and sample holder
4. Hydraulic Pump
5. Hydraulic Wheel
6. Hydraulic Jack
7. Piston
8. Hydraulic stress gauge
9. Viatran pressure transducer
10. Digital stress gauge
11. Digital LVDT strain gage
12. LVDT sensor base
13. LVDT sensor
14. Sample
15. LVDT frame
16. Data acquisition card
17. Personal computer
18. Hydraulic line
19. Wire

Figure 16. Schematic diagram illustrating the uniaxial stress frame.

E. Stress-Strain Measurement under Different Exposure Conditions

Seven different environmental conditions were created in the laboratory. Samples were first oven dried and then left in the specific environmental condition for a period of time. They were then removed from the specific environment and immediately subjected to stress, which was applied manually at a constant, approximate rate of 175 Kilopascal per second on samples. Length change and stress readings were taken each second by an interfaced computer. The stress versus strain curve of a shale sample (B108) is plotted in Figure 17. As soon as stress is applied to the sample, longitudinal strain can be detected. Each dot in the curve presents one reading of stress and strain. The time lapse between each dot is one second. The slope of the stress-strain curve for none of the samples was a straight line, so none of them can be classified as a true elastic material. The stress-strain curve of entire sample population follows the same pattern as presented in Figure 17, under all different exposure conditions.

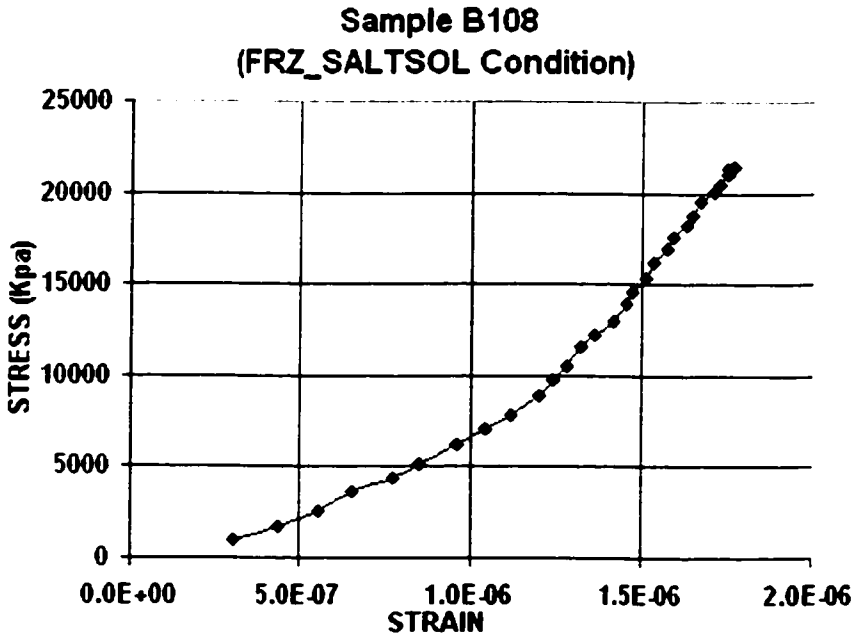

Figure 17. Relationship between axial load and longitudinal strain.

1. Room Humidity – Room Temperature (Initial)

All samples were left in room humidity and temperature condition (temperature of 22°C and humidity of 22%) to equilibrate for at least seven days, and then each specimen was placed under stress in the uniaxial compressive stress frame. The ultimate amount of stress applied depended on the rock type and varied from sample to sample.

2. 98% Humidity – Room Temperature

An airtight humidity chamber with humidity of 98% and temperature of 22°C was prepared by using a super saturated solution of hydrated copper sulphate ($CuSO_4.5H_2O$) (Lide and Frederikse, 1998). All samples were left in the humidity chamber for a minimum period of three days to ensure the equilibrium has been achieved (Hudec, 1983). Samples were then individually removed from the chamber and immediately subjected to stress/strain testing.

3. 65% Humidity – 48 hrs Freezing

All samples were oven dried at 105°C and left in room condition (temperature of 22°C and humidity of 50%) for seven days, then they were all placed in freezer (temperature of -18°C and humidity of 65%) for a period of 48 hours. Samples were then individually removed from the freezer, placed in a cooled PVC jacket and immediately subjected to stress/strain testing. The PVC jacket was cooled to -18C temperature prior to each test to help to maintain the cold temperature of the core during testing.

4. 24 hrs Saturation – Room Temperature

Samples were immersed in tap water at room temperature of 23°C for 24 hours. They were then individually removed from the water, surface dried by a towel and immediately subjected to stress/strain testing.

5. 24 hrs Saturation – 48 hrs Freezing (A) (freezer-exposed samples)

The samples were immersed in tap water at a room temperature of 23°C. After a 24 hour period of immersion, they were individually removed from the water, surface dried by a towel and placed in freezer in aluminum containers for a period of 48 hours. They were then individually removed from the freezer, placed in a cold PVC jacket, and immediately subjected to stress/strain testing.

6. 24 hrs Saturation – 48 hrs Freezing (B) (samples in sealed containers)

The freezer used normally contained exposed ice adhering to its freezing coils. In the previous test, the exposed samples would equilibrate with that ice. To isolate the samples from the ice, a second freezing experiment was conducted. All samples were submerged in tap water at room temperature of 23°C. After a 24 hour period of immersion, they were individually removed from the water, surface dried by a towel and placed in airtight plastic bags in groups of 20. Plastic bags containing the samples were left in a freezer for a period of 48 hours (temperature of -18°C). They were then individually removed from the bag, placed in a frozen PVC jacket, and immediately subjected to stress/strain testing.

7. 48 hrs Saturation in 20% Salt-Water – Room Temperature

Previous research has shown that the presence of deicing cations can be destructive, depending on their concentration. It has been found that maximum destruction in the rocks happens when the concentration falls between 3% to 5%. In the same study it was found that a freeze-thaw test in 20% solution causes damage to the samples similar to that found in freeze-thaw test in water (Hudec, 1991). Since it was intended to use the samples for other studies and to minimize rock deterioration, a 20% solution was used.

A 20% by weight salt solution was prepared and all the samples were immersed for a period of 48 hours. After a two-day period, samples were individually removed from the salt solution and immersed in fresh water for 4 hours. They were then individually removed from the fresh water, and immediately subjected to stress/strain testing.

The placement in fresh water prior to testing was to intended to allow the sample to imbibe more water by osmosis.

8. 48 hrs Saturation in 20% Salt-Water – 48 hrs Freezing (sample in sealed containers)

All samples were immersed in a 20% salt solution for a period of 12 days. They were then individually removed from the salt solution, and placed in airtight plastic bags in groups of 20. A small amount of fresh water was added to each bag. Plastic bags containing the samples were left in freezer for a period of 48 hours (temperature of 18°C). They were then individually removed from the freezer, placed in a frozen PVC jacket, and immediately subjected to stress/strain testing.

9. Room Humidity – Room Temperature (Final)

To test the repeatability and accuracy within the testing program results, the initial room humidity-room temperature environment testing was repeated. Since in some of the previous test the samples were exposed to salt-water solution, all samples were left in fresh water for two weeks to flush out the salt prior to performing the test. During the two-week period, water was changed on a daily basis. Samples were then oven dried at 105°C and left under room condition (temperature of 22°C and humidity of 70%). The final condition test was performed after samples were left to equilibrate under room conditions for seven days.

10. Ultimate Strength

The equivalent of a tensile strength of the samples was determined by Dananaj (2001) by conducting the Brazilian (indirect, diametrical tensile) strength test. Oven dried specimens were placed horizontally under stress. The load was then applied until a diametrical failure occurred. The ultimate tensile strength was then calculated based on equation (17) (Coates, 1975 from Dananaj, 2001).

$$\delta_T = \frac{2F}{\pi dl} \qquad (17)$$

δ_T = Ultimate tensile strength F = Stress (kg)

d = Diameter of specimen (mm) l = Length of specimen (mm)

F. Data Extraction

As the stress was applied to each sample, stress (psi) and length change (mm) data were recorded every second by the Lab View software through the data acquisition card. Stress and strain data were then converted from lab view software format to Corel Quattro Pro 8, and then to Microsoft Excel format. The recorded stress in psi was converted to KPa. Also strain was calculated from the length change data (equation 2). To find out the amount of stress required to reach the constant strain of 8×10^{-7} cm, the two nearest stress-strain results of higher and lower than 8×10^{-7} cm strain were used (Fig. 18):

$$\text{Strain at } S_2 > 8\times10^{-7} \text{ cm} > \text{Strain at } S_1$$

$$\text{Stress at } S_2 > \text{Required Stress} > \text{Stress at } S_1$$

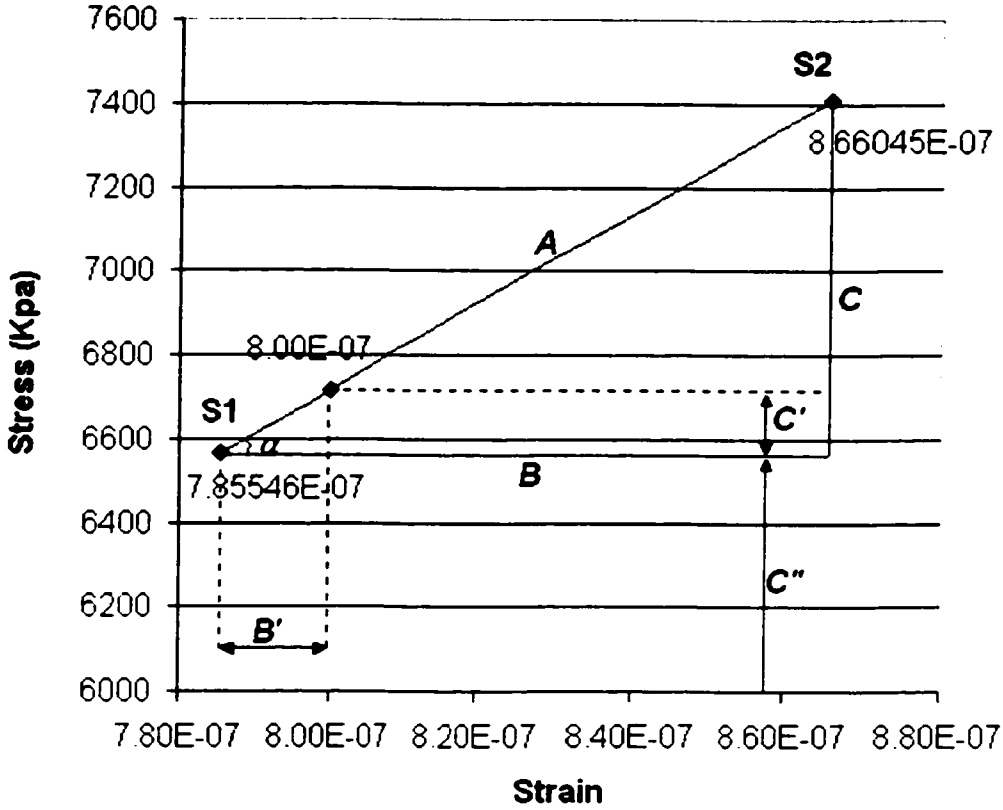

Figure 18. Calculation of required stress at 8.00E-07 cm strain (sample 23B, at Room Temperature – Room Humidity (Final Test) condition (RT_RH_FIN)).

Stress-strain curve between the two points of S_1 and S_2 is a straight line (*A*), their strain difference is marked as *B* and their stress difference is *C*. The required stress can be calculated as follows:

$$tg\alpha = \frac{C}{B} \qquad C' = tg\alpha \times B'$$

$$\text{Required Stress at } 8\times10^{-7} \text{ cm strain} = C' + C''$$

The Young's Modulus was calculated based on the upper portion of the stress-strain curve (Fig. 22, part C of the curve) (equation 3.). Data base was produced based on the Stress, Young's Modulus, Physical properties, and other related parameters of the samples measured by previous graduate students. The produced data base was then used for the statistical analysis.

G. Sources of Error

Errors can be divided into three groups, instrument error, sample inhomogeneity, and human errors. The following instrument errors are suggested: Due to the high pressure that existed within the hydraulic system during each test, there was always a possibility of a very minor hydraulic fluid leakage from the joints. There also existed the possibility of air entering into the hydraulic system, which was dealt with by de-airing the system after every 20 tests.

In lieu of a mechanical pump to apply stress at a steady rate, stress was applied manually. Although care was taken to apply the stress with a constant rate, the stress rate may not have been constant. Human errors could also affect the results in measuring other physical properties of the samples.

Although the difference in length produces an error to bring the samples to a constant strain of 8×10^{-5} cm, but since samples behaviour are being compared to each other, it will not effect the results.

Microscopic discontinuities that can not be identified with the unaided eye exist in almost all rock samples, thus affecting the mechanical properties of the samples. It was assumed that all samples exhibit a true elastic behavior to facilitate the calculations. Some rock sample may have been permanently deformed during one or more tests, affecting the results of subsequent tests.

The results of physical properties tests performed in this research were compared to the previous research conducted on the same samples. They generally showed a good correlation. The results for 98% humidity condition for dolomite and limestone samples (Figs. 19 and 20) indicate a good linear relationship between the two sets of results.

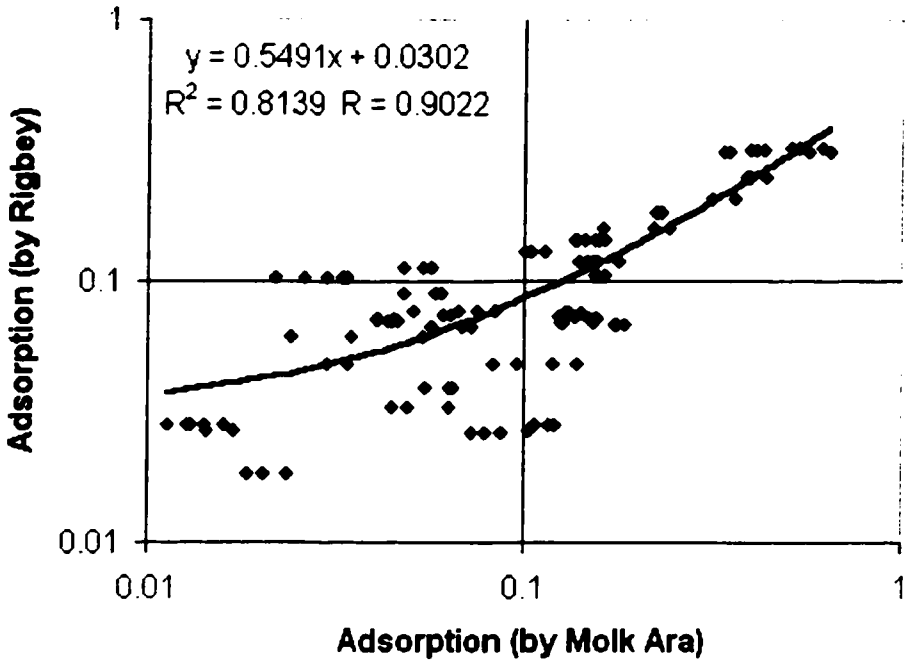

Figure 19. Correlation of adsorption results on Dolomite samples.

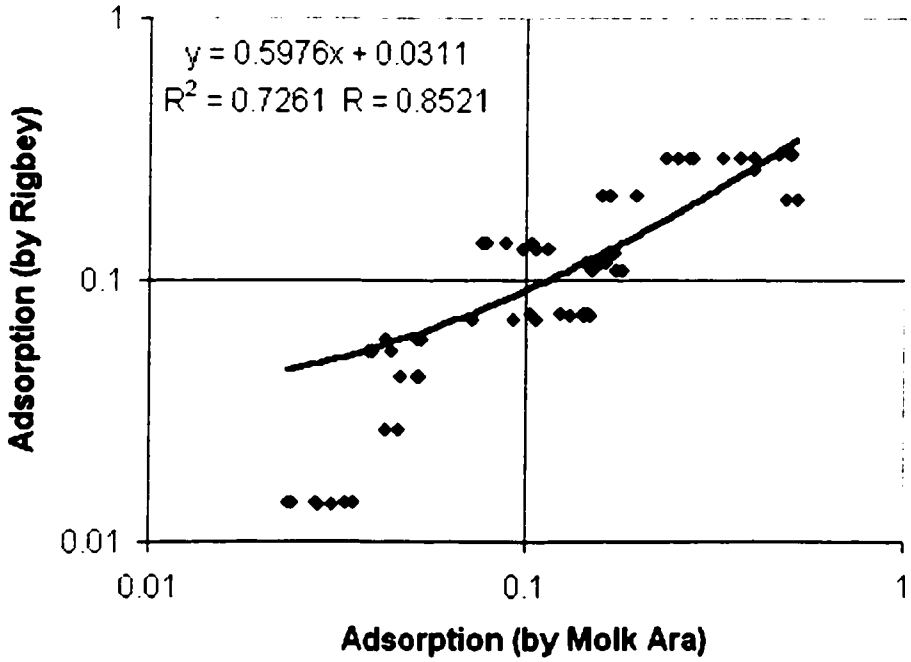

Figure 20. Correlation of adsorption results on Limestone samples.

VII. STATISTICAL ANALYSIS AND DISCUSSION

In order to study the relationship among all variables obtained in this study as well as previous studies on the same samples, a sophisticated statistical program was used (Systat 7.0). The program made it easier to apply the various statistical analyses such as correlation analysis, cluster analysis, group mean test, stepwise regression and also factor analysis to the laboratory study results. The analyses helped to classify the samples into three groups, and helped to discover the factors governing their relationships.

In addition to the results obtained in this study (Appendices B.1, B.2, and B.3), two more sets of data were used for statistical analysis. The first part included the data on void and surface area obtained by Rigbey (1980) and Ondrasik (1996). The second set consisted of strength data from Dananaj (2001).

Statistical analysis was performed on the three groups of data. First group consisted of the results obtained in this study. A combination of the first group and previous data on void and surface area parameters formed the second group. The third group consisted of the second group plus the strength data obtained by Dananaj (2001). Since the third group consists of all the data available on these rocks, it is called the Group Sigma. Tables 6 and 7 include list of variables used in the statistical analysis.

Table 6. List of variables included into the statistical analysis (group one)

Acronym	Description	Unit
RT_RH_INI	Stress to fixed strain at Room Temp. – Room Humidity (Initial Test)	Kpa
RT_RH_FINAL	Stress to fixed strain at Room Temp. – Room Humidity (Final Test)	Kpa
RT_98RH	Stress to fixed strain at Room Temperature – 98% Humidity	Kpa
FRZ_65RH	Stress to fixed strain at 48hrs Freezing – 65% Humidity	Kpa
RT_SATURATED	Stress to fixed strain at Room Temperature – 24hrs Saturation	Kpa
FRZ_SAT_A	Stress to fixed strain at 48hrs Freezing – 24hrs Saturation (A)	Kpa
FRZ_SAT_B	Stress to fixed strain at 48hrs Freezing – 24hrs Saturation (B)	Kpa
FRZ_SALTSOL	Stress to fixed strain at 48hrs Freez. – 48hrs Sat. in 20% Salt-Water	Kpa
RT_SALTSOL	Stress to fixed strain at Room Temp. – 48hrs Sat. in 20% Salt-Water	Kpa
ADSORPTION50	Room Temperature – Adsorption at 50% Humidity	% of dry w
ADSORPTION98	Room Temperature – Adsorption at 98% Humidity	% of dry w
ABSORPTION	Room Temperature – Absorption	% of dry w
FULL_ABSORP	Room Temperature – Vacuum Absorption	% of dry w
UNIT_WEIGHT	Unit Weight	g/cm³
DELTA_L	Length Change due to Freezing	% of Length
Y_RT_RH_FINL	Young's Modulus at Room Temp. – Room Hum. (Initial Test)	N/m²
Y_RT_RH_INI	Young's Modulus at Room Temp. – Room Hum. (Final Test)	N/m²
Y_RT_98RH	Young's Modulus at Room Temperature – 98% Humidity	N/m²
Y_FRZ_65RH	Young's Modulus after 48hrs Freezing – 65% Humidity	N/m²
Y_RT_SATURTD	Young's Modulus at Room Temperature – 24hrs Saturation	N/m²
Y_FRZ_SAT_A	Young's Modulus after 48hrs Freezing – 24hrs Saturation (A)	N/m²
Y_FRZ_SAT_B	Young's Modulus after 48hrs Freezing – 24hrs Saturation (B)	N/m²
Y_FRZ_SALTSO	Young's Mod. after 48hrs Freez.–48hrs Sat.(20% Salt-Water)	N/m²
Y_RT_SALTSOL	Young's Mod. at Room Temp.–48hrs Sat.(20%Salt-Water)	N/m²

Table 7. List of variables included into the statistical analysis (Rigbey, 1980; Ondrasik, 1996; and Dananaj, 2001)

Acronym	Description	Unit
ADS_98_RIGBY	Adsorption at 98% Humidity	[% of dry r]
SUSPENSION	Suspension test	min.
RDEN	Density	[g cm³]
RADS	Adsorbed water	[% of dry r]
RPORO	Porosity (vacuum absorbed water)	[% of dry r]
RCAP32S	Rate of water absorption (after 32 min.)	[% of dry r]
RADSB	Adsorbed water fraction	[% of ABS w]
DRYLOSS	Loss of dry weight (after one drying cycle)	[% of dry r]
RVABGNV	Gain of vacuum absorbed water pore fraction	[% of Vac w]
RCAP32B	Rate of water fraction absorption (after 32 min.) (capillary rise)	[% of ABS w]
RSATBIF	Degree of saturation before testing	[% of Vac w]
RBUV	Bulk water pore fraction	[% of Vac w]
RABS	Absorbed water fraction	[% of dry r]
RBUS	Bulk water	[% of dry r]
RBUB	Bulk water fraction	[% of ABS w]
Strength	Tensile strength (brazilian test)	MPa

Appendix C.1 contains a basic statistical summary of the test results of the samples obtained during this study. It includes number of cases, minimum, maximum, mean, standard deviation and units for each variable.

A. F Test

Prior to performing any statistical analysis, normal distribution of the data had to be determined. F test determines equality of variances among variables. F test is the theoretical distribution of values that would be expected by randomly sampling from a normal population and calculating, for all possible pairs of sample variances, the ratios:

$$F = \frac{S_1^2}{S_2^2} \tag{18}$$

$F = F\ Test$

S_1 = Sample Variance of Variable one

S_2 = Sample Variance of Variable two

The F-test is used to test if the standard deviations of two populations are equal and to test the null hypothesis that the variances of the two samples are equal, i.e., that the sample belong to the same population. In this case, the F-test was used to determine if statistical differences exist among the Stress and Young's Modulus results obtained when tested under different environmental conditions. The probability P determined the significance of the difference, if any, between the tests. The P of less than 0.05 signified the probability of more than 95% that the groups tested were different.

Based on their lithology, the samples were divided in to three groups of: dolomite, limestone and both limestone and dolomite samples. Other lithologies were not included in the test due to their small population. Tables 8 to 10 show only the results for F test that were significant. In all three sets of data, F test was run for Stress and Young's Modulus variables.

F test on stress variables on all three groups showed significant difference among some of the variables indicating that the environmental conditions had a significant effect on stress required to bring the sample to constant strain, and on the modulus of elasticity. Out of 28 cases that confirmed the stress results originated from different populations, 26 of them belonged to salt solution conditions under room and freezing temperature (RT_SALTSOL and FRZ_SALTSOL). As was mentioned in section C of Chapter IV, the presence of ions in the pore system increases the thickness of the adsorbed layer, adding elasticity to the system (Dananaj, 2001), reducing the required stress to reach a strain level of rock. The resultant greater deformation results in strength reduction. The results of this research have shown that salt water solution has the most influence on strength and elasticity properties of rocks.

F test among Young's Modulus variables of dolomite samples revealed a significant difference among Young's Modulus after 48hrs Freezing – 65% Humidity (Y_FRZ_65RH) and other variables. As mentioned in section F of Chapter IV, freezing temperatures contract the rock samples, i.e., introduce a measure of strain not found under other conditions. Thus Young's Modulus under frozen conditions can be considered as that of a pre-stressed sample, and therefore yields results quite different from those obtained under room temperature conditions.

Table 8. F test among dolomite samples

	Rock Type	Compared Variables		Pf
Stress	Dolomite	FRZ_65RH	RT_SALTSOL	0.000
	Dolomite	FRZ_65RH	FRZ_SALTSOL	0.005
	Dolomite	FRZ_SAT_A	RT_SALTSOL	0.003
	Dolomite	FRZ_SAT_B	RT_SALTSOL	0.010
	Dolomite	RT_98RH	RT_SALTSOL	0.021
	Dolomite	RT_98RH	FRZ_65RH	0.030
	Dolomite	RT_RH_FINAL	RT_SALTSOL	0.005
	Dolomite	RT_RH_INI	RT_SALTSOL	0.004
	Dolomite	RT_SATURATED	RT_SALTSOL	0.002
Young's Modulus	Dolomite	Y-FRZ_65RH	Y-FRZ_SAT_B	0.006
	Dolomite	Y-FRZ_65RH	Y-RT_SATURATED	0.020
	Dolomite	Y-FRZ_SAT_B	Y-RT_SALTSOL	0.023
	Dolomite	Y-FRZ_SAT_B	Y-FRZ_SALTSOL	0.053
	Dolomite	Y-RT_98RH	Y-FRZ_65RH	0.018
	Dolomite	Y-RT_RH_FINAL	Y-FRZ_65RH	0.023
	Dolomite	Y-RT_RH_INI	Y-FRZ_SAT_B	0.024

Table 9. F test among dolomite and limestone samples as one group

	Rock Type	Compared Variables		Pf
Stress	Limestone & Dolomite	FRZ_65RH	RT_SALTSOL	0.001
	Limestone & Dolomite	FRZ_65RH	FRZ_SALTSOL	0.008
	Limestone & Dolomite	FRZ_SAT_A	RT_SALTSOL	0.011
	Limestone & Dolomite	FRZ_SAT_A	FRZ_SALTSOL	0.043
	Limestone & Dolomite	FRZ_SAT_B	RT_SALTSOL	0.004
	Limestone & Dolomite	FRZ_SAT_B	FRZ_SALTSOL	0.019
	Limestone & Dolomite	RT_98RH	RT_SALTSOL	0.050
	Limestone & Dolomite	RT_RH_FINAL	RT_SALTSOL	0.003
	Limestone & Dolomite	RT_RH_FINAL	FRZ_SALTSOL	0.014
	Limestone & Dolomite	RT_RH_INI	RT_SALTSOL	0.004
	Limestone & Dolomite	RT_RH_INI	FRZ_SALTSOL	0.019
	Limestone & Dolomite	RT_SATURATED	RT_SALTSOL	0.001
	Limestone & Dolomite	RT_SATURATED	FRZ_SALTSOL	0.008
Young's Modulus	Limestone & Dolomite	Y-FRZ_65RH	Y-FRZ_SAT_B	0.001
	Limestone & Dolomite	Y-FRZ_65RH	Y-RT_SATURATED	0.005
	Limestone & Dolomite	Y-FRZ_65RH	Y-FRZ_SAT_A	0.025
	Limestone & Dolomite	Y-FRZ_SAT_B	Y-FRZ_SALTSOL	0.027
	Limestone & Dolomite	Y-FRZ_SAT_B	Y-RT_SALTSOL	0.041
	Limestone & Dolomite	Y-RT_98RH	Y-FRZ_65RH	0.005
	Limestone & Dolomite	Y-RT_RH_FINAL	Y-FRZ_65RH	0.026
	Limestone & Dolomite	Y-RT_RH_INI	Y-FRZ_SAT_B	0.023

Table 10. F test among limestone samples

	Rock Type	Compared Variables		Pf
Stress	Limestone	FRZ_SAT_A	FRZ_SAT_B	0.050
	Limestone	FRZ_SAT_B	FRZ_SALTSOL	0.009
	Limestone	RT_RH_FINAL	FRZ_SALTSOL	0.025
	Limestone	RT_RH_INI	FRZ_SALTSOL	0.035
	Limestone	RT_SATURATED	FRZ_SALTSOL	0.008
	Limestone	RT_SATURATED	FRZ_SAT_A	0.048
Y M	Limestone	Y-RT_RH_FINAL	Y-RT_SALTSOL	0.049

B. Wilcoxon Test

Sometimes a population may be distinctly non-normal (i.e., not normally distributed). In such circumstances, non-parametric statistical tests is used. The Wilcoxon test compares the rank values of the selected variables, pair by pair, and displays the count of positive and negative differences. For ties, the average rank is assigned. It then computes the sum of ranks associated with positive differences and the sum of ranks associated with negative differences. Two-sided probabilities are computed from an approximate normal variate constructed from the lesser of the sum of the positive ranks and the sum of the negative ranks. So, it can be said that the test statistic is the lesser of the two sums of ranks (Davis, 1986).

For this test, the samples were divided into four groups of stress, adsorption, absorption and Young's Modulus variables and then each group was subjected to Wilcoxon test. The results are shown on Table 11 Based on the results, both stress and Young's Modulus results at Room Temperature – Room Humidity (Initial Test) (RT_RH_INI) compared to Room Temperature – Room Humidity (Final Test) (RT_RH_FINAL) did not show a significant difference. This confirms that the procedure gives repeatable results, and also that the character of the samples was not markedly

affected by the testing. Also no significant difference exists among Room Temperature – Room Humidity (Initial Test) (RT_RH_INI) and Room Temperature – Room Humidity (Final Test) (RT_RH_FINAL) variables and 48hrs Freezing – 65% Humidity (FRZ_65RH) variable, due to the fact that samples under 48hrs Freezing – 65% Humidity (FRZ_65RH) condition went through contraction against all the other conditions since the provided moisture was not enough to initiate any expansion. Since in all the other conditions the provided moisture was almost the same and the rock samples behaved very similarly, therefore in most cases there is not a significant difference among variables of Young's Modulus or stress. Wilcoxon test among adsorption in 50% and 98% relative humidity revealed a highly significant difference. This is due to the fact that in 50% humidity all the available moisture in rock is adsorbed water; however by increasing the humidity to 98% capillary meniscus can develop in those pores that their diameter allows it (Horrigmore, 1985). Absorption and vacuum absorption results did not show any significant difference. This can be attributed to the heterogeneity of the samples and their pore systems: some samples with open porosity can fully be saturated, while others do not.

Wilcoxon Test among stress, physical properties and Young's Modulus

	RT_RH_INI	RT_RH_FINAL	RT_98RH	FRZ_65RH	RT_SATURATED	FRZ_SAT_A	FRZ_SAT_B	FRZ_SALTSOL
RT_RH_INI	1.000							
RT_RH_FINAL	0.291*	1.000						
RT_98RH	0.000	0.000	1.000					
FRZ_65RH	0.037	0.461*	0.000	1.000				
RT_SATURATED	0.000	0.000	0.484*	0.000	1.000			
FRZ_SAT_A	0.089*	0.002	0.002	0.002	0.000	1.000		
FRZ_SAT_B	0.000	0.000	0.812*	0.000	0.218*	0.000	1.000	
FRZ_SALTSOL	0.000	0.000	0.000	0.000	0.000	0.000	0.000	1.000
RT_SALTSOL	0.000	0.000	0.034	0.000	0.531*	0.000	0.077*	0.008

	ADSORPTION50	ADSORPTION98
ADSORPTION50	1.000	
ADSORPTION98	0.000	1.000

	ABSORPTION	FULL_ABSORP
ABSORPTION	1.000	
FULL_ABSORP	0.077*	1.000

	Y_RT_RH_FIN	Y_RT_RH_INI	Y_RT_98RH	Y_FRZ_65RH	Y_RT_SAT	Y_FRZ_SAT_A	Y_FRZ_SAT_B	Y_FRZ_SLTSOL
Y_RT_RH_FINL	1.000							
Y_RT_RH_INI	0.243*	1.000						
Y_RT_98RH	0.000	0.000	1.000					
Y_FRZ_65RH	0.891*	0.133*	0.000	1.000				
Y_RT_SAT	0.000	0.000	0.103*	0.000	1.000			
Y_FRZ_SAT_A	0.001	0.005	0.377*	0.000	0.002	1.000		
Y_FRZ_SAT_B	0.000	0.000	0.017	0.000	0.330*	0.001	1.000	
Y_FRZ_SALTSO	0.012	0.142*	0.162*	0.029	0.001	0.903*	0.001	1.000
Y_RT_SALTSOL	0.000	0.001	0.196*	0.000	0.767*	0.016	0.478*	0.007

Note: * Members of the compared groups can belong to one group.

Table 11. Wilcoxon test results on stress, adsorption, absorption and Young's Modulus variables

C. Correlation Test

Existence of a relationship between two variables and the degree of this relationship can be determined by a correlation analysis. The degree of relationship between two variables is expressed by a correlation coefficient (R) without providing any reasons of the relationship. Correlation coefficient reveals the magnitude and also the direction of a relationship whether it is direct or inverse. Correlation coefficient ranges from +1 to −1 and indicates the degree of relationship (Williams, 1986). An interpretation can be made based on (R) value (Motulsky, 1999):

$R = 0$	The two variables do not vary together at all.
$0 > R > 1$	The two variables tend to increase or decrease together.
$R = 1.0$	Perfect correlation.
$-1 < R < 0$	One variable increases as the other decreases.
$R = -1.0$	Perfect negative or inverse correlation.

There always exists the chance that random sampling would result in a correlation coefficient as far from zero (or further). P value helps to find out if there really is a correlation between the two variables. A (P) value of 0.01 means that the correlation coefficient is highly significant to 99%. A (P) value of 0.05 means that the correlation coefficient is significant to 95%. A (P) value of higher than 0.05 means that the variables don't really correlate to each other.

Appendix D.1 shows correlation coefficients between the stress and Young's Modulus data, and the entire data set. Ultimate strength data was not included in the correlation test since the number of observations was very limited. Rows or columns, which did not contain any significant coefficients, were excluded from the table. The table in Appendix D.2 presents the number of cases included into each correlation test.

The number of cases varies among correlation tests since some results were missing or the erratic results were rejected. In this table, correlations significant to 0.01 level are indicated by **, and those significant to 0.05 level are indicated by * next to the R coefficient. Appendix D.3 contains only the significant correlations with an indication of the relationship being positive or negative.

There exists a highly significant to significant direct moderate correlation with an R ranging from 0.46 to 0.667 between the stress data and the Young's Modulus data. This relationship was expected since the stress data and the Young's Modulus data are calculated in part from the stress data. It was found that the increase of moisture and ionic concentration lower the required stress to reach a preset strain in rocks. Young's Modulus is the ratio of stress to strain. Given that the required stress to reach a constant strain is decreased and since the strain was constant, a lower Young's Modulus was obtained. Due to the varied amount of moisture, ionic concentration, temperature and required stress from one condition to another, the degree of relationship and its significance is different from one variable to another. A highly significant relationship was found between stresses under Room Temperature – Room Humidity (Initial Test) (RT_RH_INI) and (Final Test) (RT_RH_FINAL) and Young's Modulus under both conditions. This confirms the repeatibility of the testing procedure since both tests were performed under same conditions. The stress under Room Temperature – Room Humidity (Initial Test) (RT_RH_INI) condition also showed a highly significant direct relationship with Young's Modulus at Room Temperature – 98% Humidity (Y_RT_98RH), 48hrs Freezing – 65% Humidity (Y_FRZ_65RH), and 48hrs Freezing – 24hrs Saturation (B) (Y_FRZ_SAT_B), and a significant direct relationship at Room

Temperature – 48hrs Saturation (20% Salt-Water) (Y_RT_SALTSOL). Also, the stress under Room Temperature – Room Humidity (Final Test) (RT_RH_FINAL) showed a highly significant direct relationship with Young's Modulus at all conditions except 48hrs Freezing – 24hrs Saturation (A) (Y_FRZ_SAT_A). Since both of the mentioned stress tests (Room Temperature – Room Humidity (Initial Test) (RT_RH_INI) and Room Temperature – Room Humidity (Final Test) (RT_RH_FINAL)) represent the same condition and they also originate from same population, their results can be combined together. The reason for lower significant relationship between the first test and the rest of Young's Modulus data can be attributed to changes in the sample every time it is stressed, resulting in minor, permanent changes. Another cause of lower significant relationship between variables is due to changing shape of the stress-strain curve. A typical stress-strain curve (Fig. 21) can be divided into three regions.

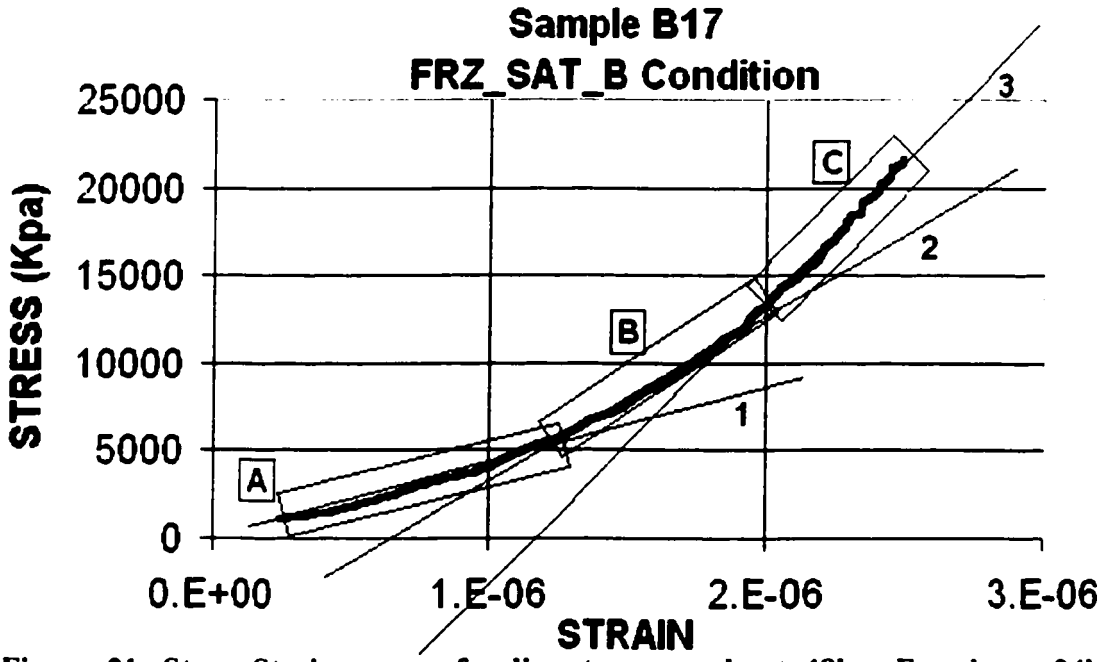

Figure 21. Stress-Strain curve of a limestone sample at 48hrs Freezing – 24hrs saturation (B) (FRZ_SAT_B) condition.

The stress-strain curve starts with a slightly convex upward section and then turns into very nearly linear portion in which it concaves downward, reaching the maximum point. In Figure 21 lines 1, 2, and 3 are drawn tangential to those three sections of the stress-strain curve. The stress results were recorded when the samples reached strain of 8×10^{-7} cm. However, the test continued, and the Young's Modulus was calculated from the final portion of the curve (Section C). Since the stress results are usually taken from the early stage of the curve and the Young's Modulus is calculated from the final stage of the curve, correlation between the two is not always possible. Overall, stress at Room Temperature - Room Humidity (Final Test) (RT_RH_FINAL), Room Temperature - 98% Humidity (RT_98RH), 48hrs Freezing - 48hrs Saturation (20% Salt-Water) (FRZ_SALTSOL) showed a highly significant direct relationship with all the Young's Modulus results.

Table 12. Highly significant to significant correlations between Young's Modulus results and physical properties

Variables		Positive (+) or Negative (-) Relationship	Significance of R
Y-RT_RH_FINAL	vs Unit Weight gr/cm³	+	1%
Y-RT_RH_FINAL	vs RDEN	+	1%
Y-RT_RH_INI	vs Unit Weight gr/cm³	+	1%
Y-RT_RH_INI	vs RDEN	+	1%
Y-RT_98RH	vs Unit Weight gr/cm³	+	5%
Y-RT_98RH	vs RDEN	+	5%
Y-FRZ_65RH	vs Unit Weight gr/cm³	+	1%
Y-FRZ_65RH	vs RDEN	+	1%
Y-RT_SATURATED	vs Unit Weight gr/cm³	+	1%
Y-RT_SATURATED	vs RDEN	+	5%
Y-FRZ_SAT_A	vs Unit Weight gr/cm³	+	5%
Y-FRZ_SAT_B	vs Unit Weight gr/cm³	+	5%
Y-FRZ_SAT_B	vs RDEN	+	5%
Y-RT_SALTSOL	vs 50% Adsorption	-	5%
Y-RT_SALTSOL	vs 98% Adsorption	-	5%
Y-RT_SALTSOL	vs Unit Weight gr/cm³	+	5%
Y-RT_SALTSOL	vs RADS	-	5%

From the results presented in Table 12, all Young's Modulus data show a direct significant moderate relationship with unit weight (UNIT_WEIGHT) except 48hrs Freezing - 48hrs Saturation (20% Salt-Water) (Y_FRZ_SALTSO). There exists a reverse relationship between porosity and unit weight. When a rock sample is placed under stress, pores will start to close by increasing the stress. At intermediate stress levels (Figure 21, Section B), the behavior of most rocks becomes linear elastic. At this point all of the macro pores have been closed; however the micro pores are still open, so the strain increments become proportional to applied stress (Franklin and Dusseault, 1989). Porosity of the samples (as obtained by water absorption) was not determined with the same accuracy as their unit weight, since the samples had to be towel dried manually, which is an in-exact art. As a result, an error can be introduced into the measurement of the absorbed and fully absorbed water. This can be considered as one of the reasons that no significant relationship is seen between Young's Modulus and all the absorption data. On the other hand, a very sensitive balance was used to measure the dry weight of samples and an extreme care was taken to measure the volume of samples, to achieve an accurate unit weight. A higher unit weight means less porosity in the sample (Section VII.B.1) and as a result there will be less room for contraction under stress. Thus a higher stress is required to achieve a certain amount of stress resulting in a higher Young's Modulus. Therefore a highly significant relationship is seen between Young's Modulus and unit weight. Under 48hrs Freezing – 65% Humidity (Y_FRZ_65RH) condition the samples went through contraction and as a result the porosity has been decreased to its minimum prior to testing compared to the other conditions. Thus the highest significant relationship can be seen between 48hrs Freezing – 65% Humidity (Y_FRZ_65RH) and

unit weight. Among all of the Young's Modulus variables only Room Temperature – 48hrs Saturation (20% Salt-Water) (Y_RT_SALTSOL) has shown a significant inveverse relationship with adsorption in 50% and 98% relative humidity.

The amount of adsorbed water in each sample has a direct relationship with its surface area (Section B, Chapter III). The higher the surface area, the larger the amount of adsorbed water. The presence of ions will add to the thickness of adsorbed water and increase the amount of adsorbed water (Section C, Chapter III), which eventually increases the amount of moisture in the sample. Based on the findings by previous researchers, (Section B, Chapter II), increase of moisture decreases the compressive strength of rocks. As stated in (Section B, Chapter II), Young's Modulus increases with increasing compressive strength. Therefore it can be concluded that increase of adsorption and ionic concentration can have an inverse impact on Young's Modulus and on compressive strength. Selected highest correlations among the variables are shown in the following figures (Figs. 22 to 26) (outliers are excluded).

Figure 22 shows plot of stress applied on samples in room temperature-room humidity condition (RT_RH_INI) at the start of the uniaxial experiments versus the stress applied to the samples under almost the same temperature and humidity conditions at the end of the uniaxial experiments. The correlation has a correlation coefficient R=0.851 at 100% significance level. The slope of 0.85 suggests that the final moduli obtained were proportionately lower, most likely due to weakening of the samples as the result of prior modulus testing.

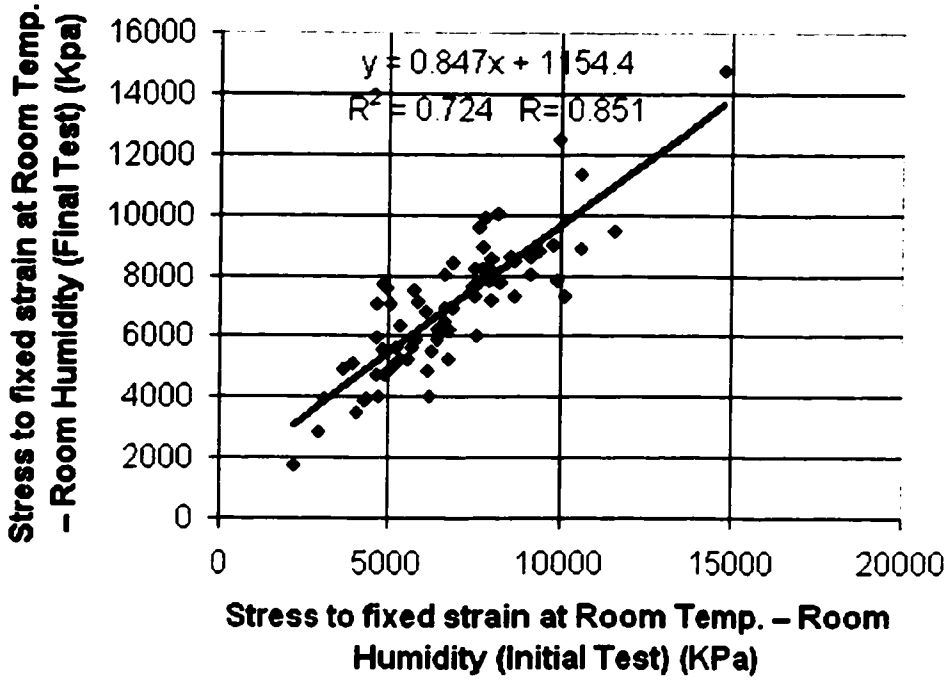

Figure 22. Graph of Stress to fixed strain at Room Temp. – Room Humidity (Initial Test) versus (RT_RH_INI) Stress to fixed strain at Room Temp. – Room Humidity (Final Test) (RT_RH_FINAL).

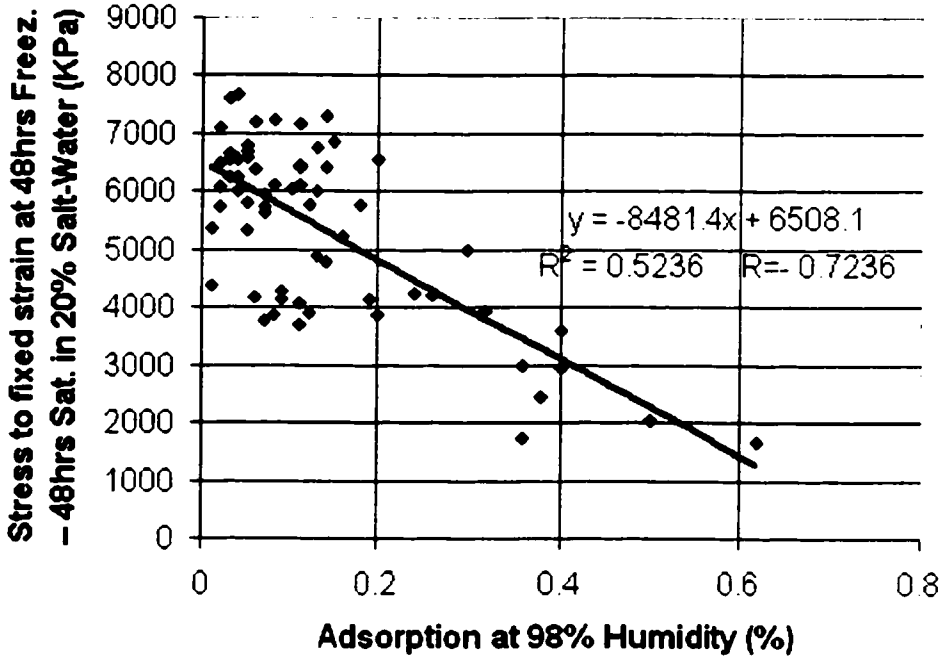

Figure 23. Graph of stress required for given constant strain of samples frozen after immersion in salt solution (FRZ_SALTSOL) versus water adsorption (from Rigbey data).

Figure 23 shows plot of stress applied on samples after immersion in a 20% salt solution followed by freezing at -18°C, versus adsorption at 98% relative humidity. The variables have an inverse correlation coefficient R=-0.7236 with 95% significance level. The plot reveals that the amount of stress required to reach a constant, predetermined strain level decreases with increasing the amount of adsorption. Since it has been shown by Hudec (1989) that adsorption increases with increase in surface area, it can be concluded that rocks with higher internal surface area achieve greater deformation under lower level of stress. It has also been shown by Ondrasik (1996) that the amount of water frozen is inversely proportional to the internal surface area. This would suggest that the solution in the rocks with a large surface area is unfrozen. The presence of ions will add to the thickness of adsorbed water and increase the amount of adsorbed water. Dananaj (2001) has shown that adsorbed water has elastic properties. Thus rocks with adsorbed water in their pores are more easily deformed, which explains the inverse relationship between adsorption and required stress to deform the rock.

Figure 24 is a plot of Young's Modulus at Room Temperature – 48hrs Saturation in 20% Salt-Water (RT_SALTSOL) condition versus adsorption in 98% humidity. The inverse correlation of the variables has correlation coefficient R=-0.6887 with 99% significance level. This plot suggests that increase of surface area decreases the Young's Modulus and shows that a lesser amount of stress is needed to deform the rock with high adsorption and therefore high internal surface area. This supports the observations in the previous paragraph, and is explained in similar way as above.

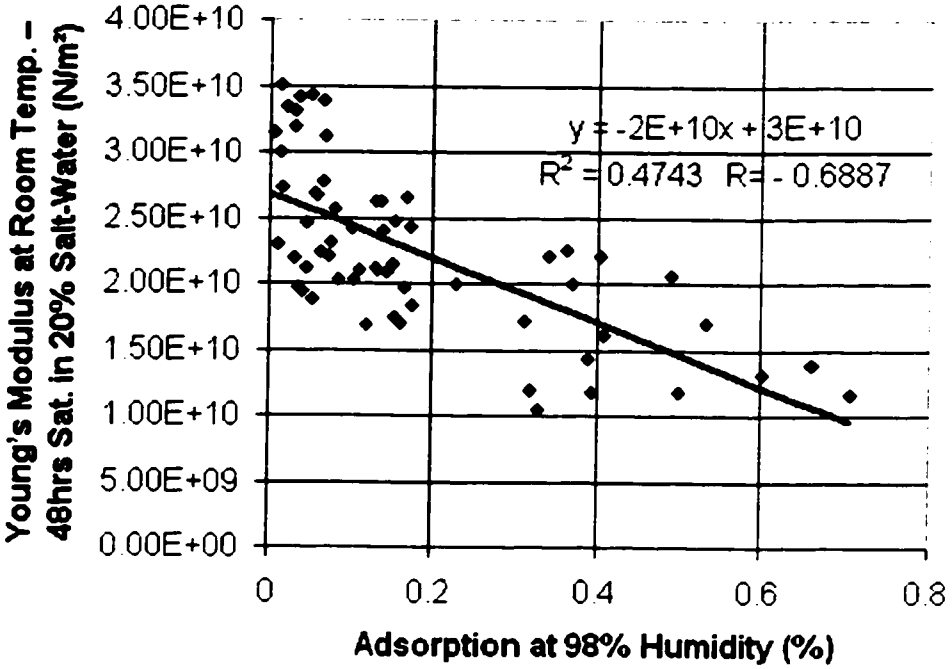

Figure 24. Graph of Young's Modulus at Room Temperature – 48hrs Saturation in 20% Salt-Water (RT_SALTSOL) condition versus adsorption in 98% humidity.

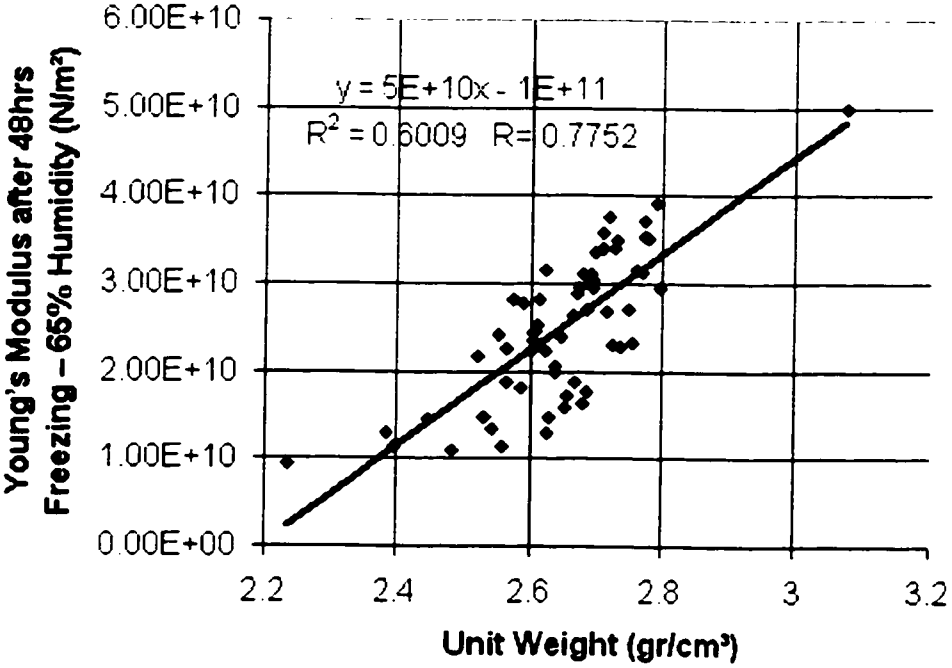

Figure 25. Graph of Young's Modulus after 48hrs Freezing – 65% Humidity condition versus unit weight.

Figure 25 shows plot between Young's Modulus after 48hrs Freezing – 65% Humidity condition (FRZ_65RH) and unit weight. The direct correlation of the variables has a correlation coefficient R=0.7752 with 99% significance level. Since majority of samples are carbonates, i.e., composed of minerals of similar density, the bulk density of these samples is determined largely by their porosity. The less dense, the more porous the sample, the less stress is required to deform it to a given strain (i.e., lower modulus), as shown by the inverse relationship. Frozen, low humidity samples have minimum of adsorbed water in the pores, and no ice present, thus pore water pressure does not play a factor in the relationship.

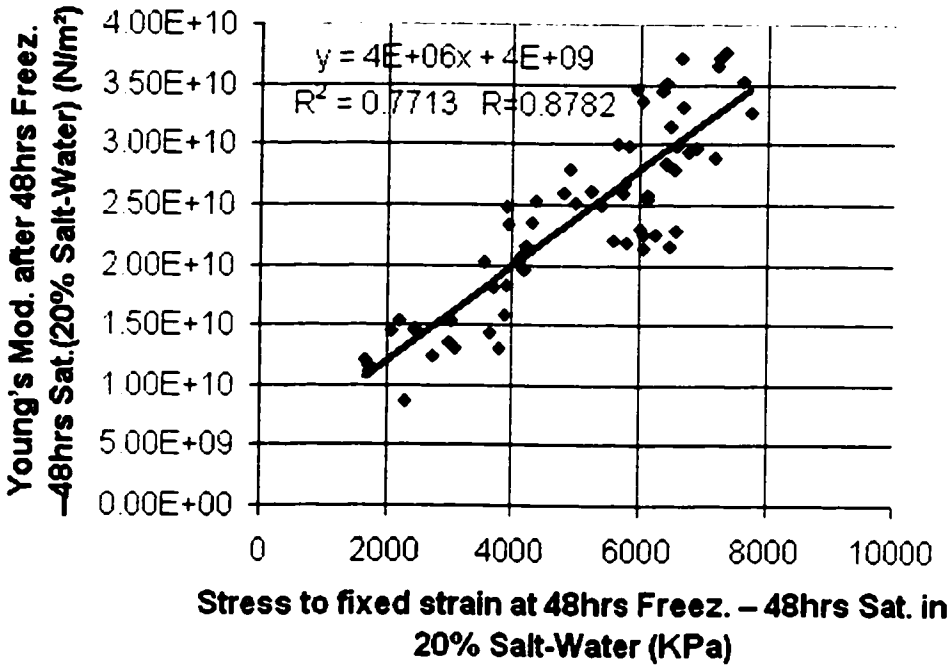

Figure 26. Graph of Young's Modulus after 48hrs Freezing–48hrs Saturation (20% Salt-Water) in (Y_FRZ_SALTSO) condition versus Stress to reach constant strain at 48hrs Freezing – 48hrs Saturation in 20% Salt-Water (FRZ_SALTSOL) condition

Figure 26 shows plot of the correlation between stress to fixed strain at 48hrs Freezing – 48hrs Saturation in 20% Salt-Water and Young's Modulus after 48hrs

Freezing – 48hrs Saturation (20% Salt-Water) (FRZ_SALTSOL) condition. The direct correlation has a correlation coefficient R=0.8782 with 99% significance. This plot shows a high correlation, since both parameters are similar in nature. Same level of correlation was observed among all Young's Modulus and stress parameters.

D. Two-Group Student t-Test

A method that measures the significance of the difference between the means of two populations, based on the means and distributions of the two populations, is called t-test (Williams, 1986).

The t-test was run in three steps. In the first step, samples were divided into four groups: dolomite, limestone, siliciclastic, and crystalline silicate rocks. All sandstone and shale samples were grouped as detrital, and crystalline rocks group consisted of igneous and metamorphic rocks. The t-test was also run among variables within the two major groups of dolomite and limestone samples. The final run consisted of running t-test among stress and Young's Modulus variables within all samples.

The two group student t-test was used for all the three sets and only the t-tests with a probability of being the same population of less than 0.05 (95%) were selected to appear on the t-test tables, since they represent a statistically significant difference among the tests. Appendix E.1 shows the results of the two-group t-test between dolomite and limestone samples. When stress results were compared dolomite samples had significantly higher means in four of the conditions that include: Stress to fixed strain at Room Temperature – Room Humidity (Initial Test) (RT_RH_INI), Stress to fixed strain at Room Temperature – Room Humidity (Final Test) (RT_RH_FIN), Stress to fixed strain at 48hrs Freezing – 24hrs Saturation (A) (FRZ_SAT_A), Stress to fixed strain at

48hrs Freezing – 48hrs Saturation in 20% Salt-Water (FRZ_SALTSOL). Based on the comparison of the means, dolomite samples also show significantly higher values of Young's Modulus under all of the conditions. The difference in the amount of total adsorbed water as a function of rock type as shown in Appendix E.1, as well as other properties shown in that table can be used to explain the differences in behavior. Increase in the proportion of adsorbed water relative to bulk water will decrease the elastic modulus of rocks where such conditions exist – i.e., whenever the rock is saturated, whether at room temperature or frozen.

Dolomite samples also have the highest means for unit weight, and ultimate strength values. The same table shows significantly higher adsorption values for limestone samples. It can be inferred from these results that rocks with a higher unit weight have higher strength and are more durable compared to rocks with higher adsorption.

Appendix E.2 shows the results of the two group t-test between crystalline and detrital samples. Since the number of samples was low, the degree of freedom is also low (df = N-2). The table shows significantly higher absorption values for detrital rocks. Crystalline rocks group show significantly higher values for unit weight and Young's Modulus in three of the conditions: Young's Modulus at Room Temperature – 24hrs Saturation (Y_RT_SATURTD), Young's Modulus after 48hrs Freezing – 24hrs Saturation (A) (Y_FRZ_SAT_A), and Young's Modulus at Room Temperature – 48hrs Saturation (20% Salt-Water) (Y_RT_SALTSOL). This suggests a higher porosity for detrital samples and the inverse relationship between Young's Modulus and porosity.

Table 13. Summary of the t-tests (The terms in the body of the table indicate the rock type with significantly higher value in the given test)

Test	Dolomite Limestone	Crystalline Siliciclastic	Limestone Crystalline	Limestone Siliciclastic	Dolomite Crystalline	Dolomite Siliciclastic
Stress to fixed strain at Room Temp. – Room Humidity (Initial Test)	Dolomite					
Stress to fixed strain at Room Temp. – Room Humidity (Final Test)	Dolomite				Dolomite	
Stress to fixed strain at Room Temperature – 98% Humidity						
Stress to fixed strain at 48hrs Freezing – 65% Humidity		Siliciclastic			Dolomite	
Stress to fixed strain at Room Temperature – 24hrs Saturation						
Stress to fixed strain at 48hrs Freezing – 24hrs Saturation (A)	Dolomite				Dolomite	
Stress to fixed strain at 48hrs Freezing – 24hrs Saturation (B)						
Stress to fixed strain at 48hrs Freez. – 48hrs Sat. in 20% Salt-Water	Dolomite			Siliciclastic		
Stress to fixed strain at Room Temp. – 48hrs Sat. in 20% Salt-Water						
ADSORPTION50			Limestone			
ADSORPTION98			Limestone			
ABSORPTION		Siliciclastic	Limestone	Siliciclastic	Dolomite	Siliciclastic
FULL_ABSORPTION		Siliciclastic	Limestone	Siliciclastic	Dolomite	Siliciclastic
UNIT_WEIGHT	Dolomite	Crystalline		Limestone		Dolomite
DELTA_L						
Young's Modulus at Room Temp. – Room Hum. (Initial Test)	Dolomite			Limestone		Dolomite
Young's Modulus at Room Temp. – Room Hum. (Final Test)	Dolomite					Dolomite
Young's Modulus at Room Temperature – 98% Humidity	Dolomite			Limestone		Dolomite
Young's Modulus after 48hrs Freezing – 65% Humidity	Dolomite			Limestone		Dolomite
Young's Modulus at Room Temperature – 24hrs Saturation	Dolomite	Crystalline	Crystalline			Dolomite
Young's Modulus after 48hrs Freezing – 24hrs Saturation (A)	Dolomite	Crystalline	Crystalline	Limestone		Dolomite
Young's Modulus after 48hrs Freezing – 24hrs Saturation (B)	Dolomite					Dolomite
Young's Mod. after 48hrs Freez.–48hrs Sat.(20% Salt-Water)	Dolomite					Dolomite
Young's Mod. at Room Temp.–48hrs Sat.(20%Salt-Water)	Dolomite	Crystalline	Crystalline			Dolomite

Appendices E.3 to E.6 show the results of the two group t-test between limestone and crystalline rocks, limestone and detrital rocks, dolomite and crystalline rocks, and dolomite and detrital rocks respectively. The summary of Appendices E.1 to E.6 is shown in Table 13.

This table shows that rocks with higher unit weight have a significantly higher Young's Modulus than rocks, which have a higher adsorption or absorption.

E. Paired Student t-Test

Paired t-test was performed on a database containing all different rock samples named group sigma (this group includes all the rock types and variables) and was also run on stress and Young's Modulus data separately. Appendices F.1 and F.2 present the t-test results and Tables 14 and 15 show a summary of the t-test results.

Table 14. Summary of paired t-test on Group Sigma (all samples) stress results

Test	RT_RH_INI	RT_RH_FIN	RT_98RH	FRZ_65RH	RT_SATURTD	FRZ_SAT_A	FRZ_SAT_B	FRZ_SALTSOL	RT_SALTSOL
Room Temp. – Room Humidity (Initial Test)									
Room Temp. – Room Humidity (Final Test)									
Room Temperature – 98% Humidity	+	+							
48hrs Freezing – 65% Humidity			-						
Room Temperature – 24hrs Saturation	+	+		+					
48hrs Freezing – 24hrs Saturation (A)		+	-	+	-				
48hrs Freezing – 24hrs Saturation (B)	+	+		+		+			
48hrs Freez. – 48hrs Sat. in 20% Salt-Water	+	+	+	+	+	+	+		
Room Temp. – 48hrs Sat. in 20% Salt-Water	+	+	+	+		+	+	-	

(+) Column variable is significantly higher than row variable
(-) Column variable is significantly lower than row variable

Paired t-test of stress results between Stress to fixed strain at Room Temperature – Room Humidity (Initial Test) (RT_RH_INI) and Stress to fixed strain at Room Temperature – Room Humidity (Final Test) (RT_RH_FIN) has shown no significant difference. Since both tests represent same condition and were performed at the start and end of experiment, it shows again that the stress-strain experiments have a good

repeatability. Among all conditions Room Temperature – Room Humidity (Final Test) (RT_RH_FIN) requires the highest stress to reach a constant strain of 8×10^{-7} cm. Each time that samples are stressed, a small irreversible strain remained in the samples. Also final test was performed in Room Temperature – Room Humidity condition under lower humidity than the Room Temperature – Room Humidity (Final Test) (RT_RH_FIN), and as a result required somewhat higher average stress.

As the moisture level in the samples increases the amount of stress required to reach a constant 8×10^{-7} cm strain decreases. When samples are exposed to humidity and ionic solutions in sub zero temperature, the required stress is at its minimum. The ionic solutions decrease the amount of water freezing, and the low temperature contracts the rock pores, as well as decreasing the amount of adsorbed water. The rock can be considered to be in super-saturated conditions with unfrozen, un-attached water that can be easily expelled under applied stress. On the other hand, the required stress to reach the constant strain of 8×10^{-7} cm is at its maximum at 48hrs Freezing – 65% Humidity condition (FRZ_65RH). Under this subzero temperature and low humidity the samples have contracted, and the low humidity assures that the pores remained unfilled, and the adsorbed water is at its minimum. Therefore the required stress is even higher than the stress at room temperature – room humidity condition (Initial Test) (RT_RH_INI).

The environmental conditions can be ranked based on the required stress to reach a strain of 8×10^{-7} cm starting with the maximum stress required condition (Fig. 27):

1. Room Temperature – Room Humidity (Final Test) (RT_RH_FIN)
2. 48hrs Freezing – 65% Humidity (FRZ_65RH)
3. Room Temperature – Room Humidity (Initial Test) (RT_RH_INI)

4. 48hrs Freezing – 24hrs Saturation (A) (FRZ_SAT_A)
5. Room Temperature – 98% Humidity (RT_98RH)
6. Room Temperature – 24hrs Saturation (RT_SATURATED)
7. 48hrs Freezing – 24hrs Saturation (B) (FRZ_SAT_B)
8. Room Temperature – 48hrs Saturation in 20% Salt-Water (RT_SALTSOL)
9. 48hrs Saturation in 20% Salt-Water after 48hrs Freezing (FRZ_SALTSOL)

Based on the ranking presented in Figure 27, the required stress decreases with increase of moisture content, decrease of temperature to subzero temperatures in sealed saturated condition, and presence of ionic solutions. However the required stress increases with decrease of moisture, and decrease of temperature to subzero temperatures accompanied with moisture loss. Presence of moisture in Room Temperature – 98% Humidity condition (RT_98RH) develops a layer of adsorbed water on rock pore surfaces. The thickness of adsorbed water increases with increase of humidity and also presence of ionic solutions (Section II.B). Presence of adsorbed water decreases the surface energy at grain boundaries, which results in rock strength weakening. In Room Temperature – 24hrs Saturation condition (RT_SATURATED) the amount of moisture is increased to a level that capillary surfaces are formed. Capillary suction fills the rock pores with water that is accompanied with contraction and when the pores are full, the rock relaxes, which reduces its strength . When saturated sample is subjected to sub zero temperatures in 48hrs Freezing – 24hrs Saturation (B) condition (FRZ_SAT_B), capillary pore water freezes causing expansion in the rock that weakens the rock. Presence of

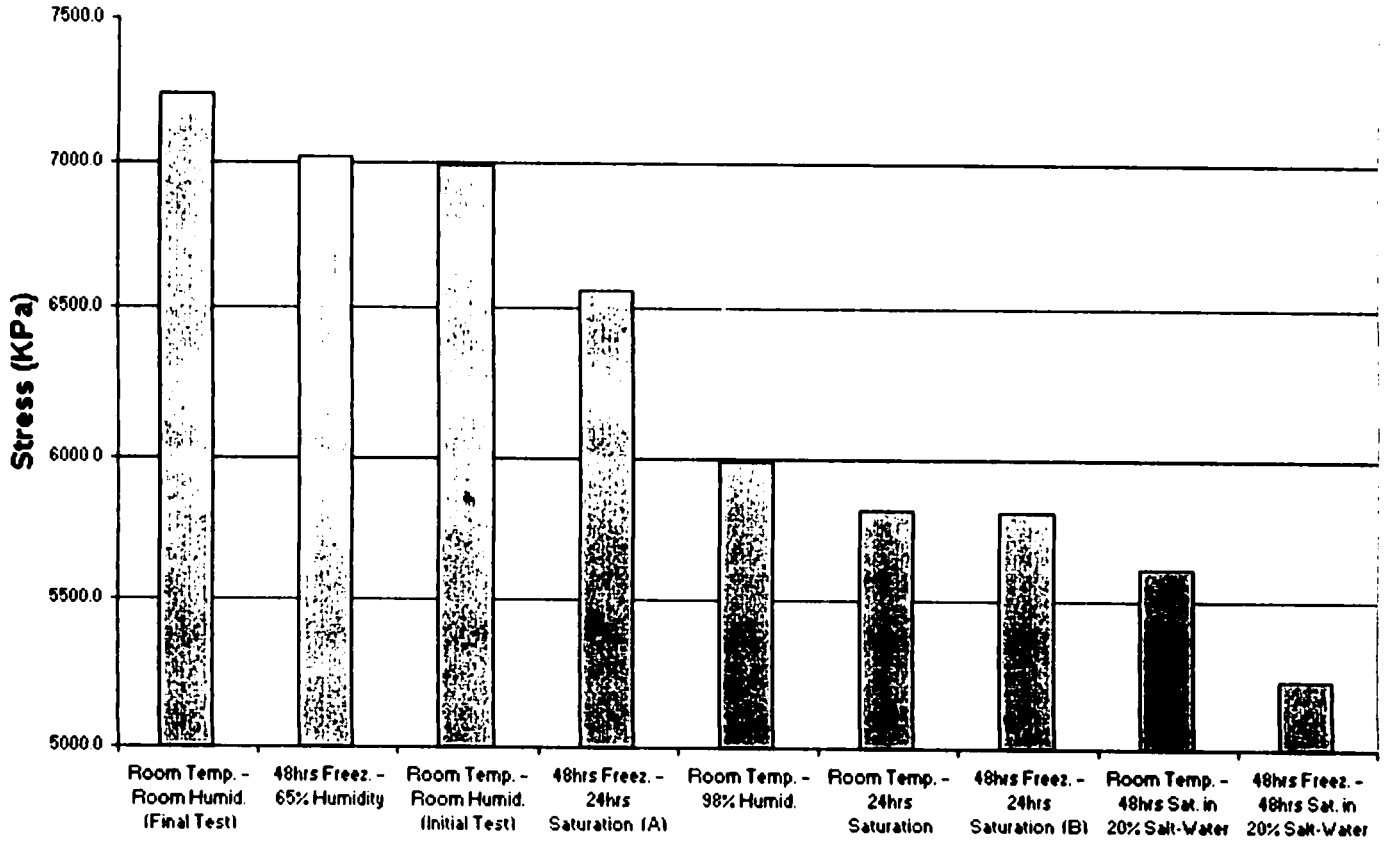

Figure 27. Paired t-test on Group Sigma (all samples) stress for a given constant stress results.

cations in Room Temperature – 48hrs Saturation in 20% Salt-Water (RT_SALTSOL) reduces the strength to a lower level by increasing the thickness of adsorbed layer. The adsorbed layer of water reaches its maximum in 48hrs Saturation in 20% Salt-Water after 48hrs Freezing condition (FRZ_SALTSOL) since some of the macro pore water freezes expelling more cations to micro pores producing thicker adsorbed layer of water.

Table 15. Summary of paired t-test on Group Sigma Young's Modulus results (all samples)

Test	Y_RT_RH_INI	Y_RT_RH_FIN	Y_RT_98RH	Y_FRZ_65RH	Y_RT_SATURTD	Y_FRZ_SAT_A	Y_FRZ_SAT_B	Y_FRZ_SALTSOL	Y_RT_SALTSOL
Room Temp. – Room Humidity (Initial Test)									
Room Temp. – Room Humidity (Final Test)									
Room Temperature – 98% Humidity	+	+							
48hrs Freezing – 65% Humidity	-		-						
Room Temperature – 24hrs Saturation	+	+		+					
48hrs Freezing – 24hrs Saturation (A)	+	+		+	-				
48hrs Freezing – 24hrs Saturation (B)	+	+	+	+		+			
48hrs Freez. – 48hrs Sat. in 20% Salt-Water		+		+	-		-		
Room Temp. – 48hrs Sat. in 20% Salt-Water	+	+		+					

(+) Column variable is significantly higher than row variable
(-) Column variable is significantly lower than row variable

Paired t-test of Young's Modulus data showed almost similar results to paired t-test of stress data, as may be expected; however some differences exist. The Young's Modulus obtained at both Room Temperature – Room Humidity (Initial Test) (Y_RT_RH_INI) and (Final Test) (Y_RT_RH_FIN) are significantly higher than at all the other conditions except 48hrs Freezing – 65% Humidity condition (Y_FRZ_65RH).

Paired t-test revealed that maximum Young's Modulus is achieved at 48hrs Freezing – 65% Humidity (Y_FRZ_65RH) condition. Under this subzero temperature and low humidity the samples have contracted, and the low humidity assures that the pores remained unfilled, and the adsorbed water is at its minimum. Therefore the strain is minimal and Young's Modulus is even higher than the Young's Modulus at room temperature – room humidity (Initial Test) (Y_RT_RH_INI) and (Final Test) (Y_RT_RH_FIN) condition.

The paired t-test of Young's Modulus results shows the lowest values at Room Temperature – 48hrs Saturation in 20% Salt-Water (Y_RT_SALTSOL), Room Temperature – 24hrs Saturation (Y_RT_SATURATED) and 48hrs Freezing – 24hrs Saturation (B) (Y_FRZ_SAT_B) condition. Under such conditions, the water in the pores is mostly in adsorbed state and acts as an elastic solid (Dananaj, 2001) and facilitates compression. On the other hand, pure water in saturated pores acts as a hydraulic fluid, i.e., is incompressible, and resists compression. Since the adsorbed layer of water acts as an elastic solid it decreases the effective pore diameter. Therefore a bottleneck effect is produced making it even harder for pore fluid to flow. When a sample is saturated in 20% Salt-Water for 48hrs, and then frozen for 48hrs, very little of the water freezes, and it adds up to the bottleneck effect. This leaves even less space for the unfrozen water, which acts as a hydraulic fluid resisting stress. As a result more stress is required to produce a given strain and the Young's Modulus value will be higher.

All conditions can be ranked based on the Young's Modulus value stating with the condition that highest value was obtained from it (Fig. 28):

1. 48hrs Freezing – 65% Humidity (Y_FRZ_65RH)

2. Room Temperature – Room Humidity (Final Test) (Y_RT_RH_FIN)
3. Room Temperature – Room Humidity (Initial Test) (Y_RT_RH_INI)
4. 48hrs Saturation in 20% Salt-Water after 48hrs Freezing (Y_FRZ_SALTSOL)
5. 48hrs Freezing – 24hrs Saturation (A) (Y_FRZ_SAT_A)
6. Room Temperature – 98% Humidity (Y_RT_98RH)
7. Room Temperature – 48hrs Saturation in 20% Salt-Water (Y_RT_SALTSOL)
8. Room Temperature – 24hrs Saturation (Y_RT_SATURATED)
9. 48hrs Freezing – 24hrs Saturation (B) (Y_FRZ_SAT_B)

To re-iterate, the thickness of adsorbed water increases with increase of humidity and also presence of ionic solutions (Section II.B). Adsorbed layer of water acts as an elastic solid facilitating compression. It can be concluded that Young's Modulus decreases with increase of adsorbed layer of water, decrease of temperature to subzero temperatures in sealed saturated conditions, and presence of ionic solutions.

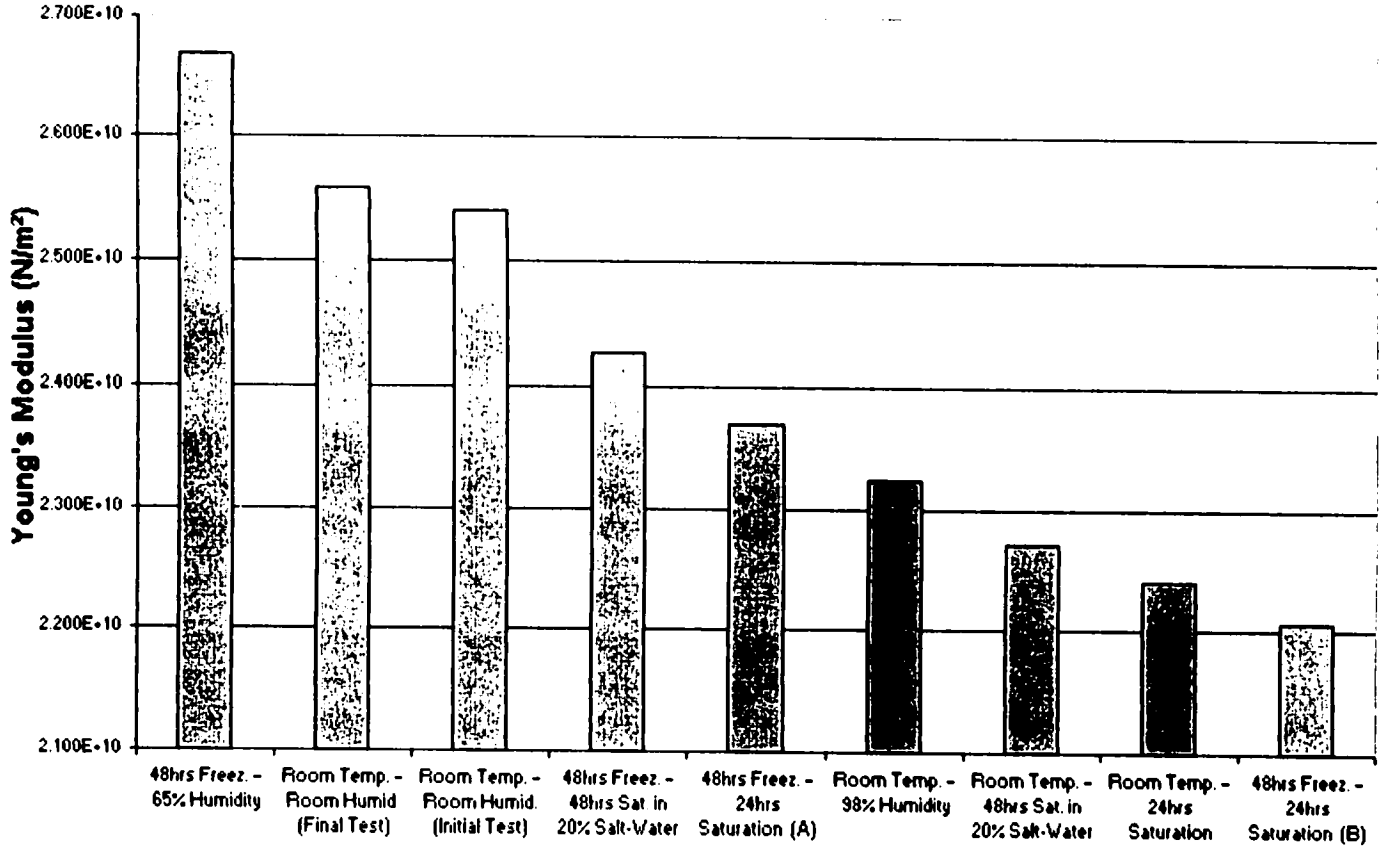

Figure 28. Paired t-test on Group Sigma (all samples) Young's Modulus results.

F. Cluster Analysis

Cluster analysis is a multivariate statistical method that groups relatively similar, homogeneous data into a selected number of clusters. The analysis clusters the data by the squared Euclidean distance between two cases. There are different clustering methods available such as hierarchical clustering, K-means, and additive clustering. K-means clustering method was used to cluster the data in this study. K-means starts with one cluster and splits it into two clusters by picking the case farthest from the center as a seed for a second cluster and assigning each case to the nearest center. It continues splitting one of the clusters into two (and reassigning cases) until specified number of clusters are formed. In this analysis three clusters were specified. K-means reassigns cases until the within-groups sum of squares can no longer be reduced. K-means clustering splits a set of objects into a selected number of groups by maximizing between-cluster variation relative to within-cluster variation (Systat, 1997).

Group Sigma (containing all samples and variables) data set was chosen for K-means clustering into three clusters. The identifying variable chosen was the rock type. The summary statistics for each cluster include mean, standard deviation, and minimum and maximum values. Only the means are presented in the tables below.

Sample distribution by K-mean clustering is presented in Table 16 and Figure 29. Cluster 1 with 21 samples contains 50% of all limestone, 80% of all siliciclastic, 17% of all crystalline, and only 9% of all dolomite samples. This cluster consists of 57% limestone, 19% dolomite, 19% siliciclastic and 5% crystalline rocks. Samples in this cluster have low mean Young's Modulus and strength, high adsorption and absorption,

and low unit weight. Based on the characteristics of its members, cluster 1 contains fairly weak and not very durable rocks.

Cluster 2 contains 49% of all dolomite, 42% of all limestone, 33% of all crystalline and only 20% of all siliciclastic samples. Within the cluster, it consists of 62% dolomite, 29% limestone, 6% crystalline and 3% siliciclastic rocks. The rocks in Cluster 2 have median values of adsorption, absorption, unit weight, and also Young's Modulus compared to the other two clusters. These rocks are more durable than rocks in cluster 1.

About 78% of Cluster 3 consists of dolomite samples 13% of crystalline rocks, followed by the least amount of limestone at 9%, and no siliciclastic samples. Cluster 3 is characterized by high values of Young's Modulus and unit weight and low values of adsorption and absorption. The rocks in this cluster have higher strength than the other rocks and are also more durable. Mean values of each cluster are presented in Table 17.

Table 16. Sample distribution by K-mean clustering based on rock type

	Dolomite			Limestone			Siliciclastic Sandstone&Shale			Crystalline Igneous & Metamorphic		
	N	% of All Dol.	% of Cluster	N	% of All Lim.	% of Cluster	N	% of All Sil.	% of Cluster	N	% of All Crys.	% of Cluster
Cluster 1	4	9	19	12	50	57	4	80	19	1	17	5
Cluster 2	21	49	62	10	42	29	1	20	3	2	33	6
Cluster 3	18	42	78	2	8	9	0	0	0	3	50	13

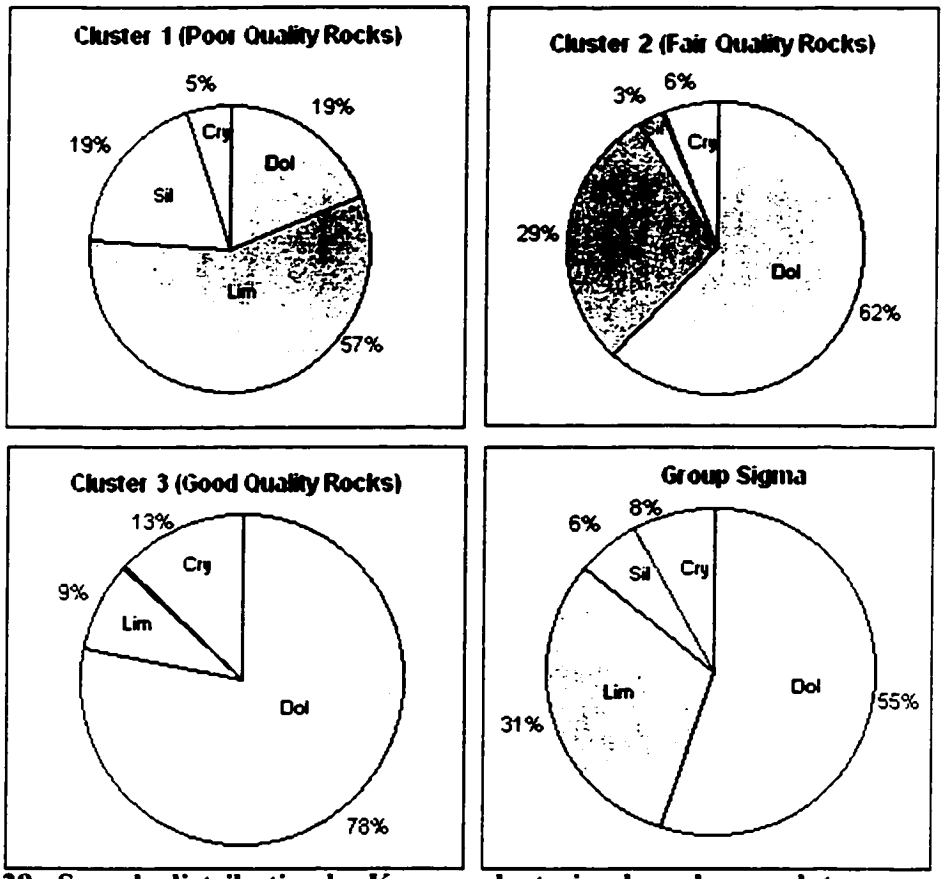

Figure 29. Sample distribution by K-mean clustering based on rock type.

Table 17 shows that members of Cluster 3, possess higher strength, Young's Modulus, and they also require higher stress to reach a constant strain. Their adsorption is less than 50% of cluster 2, and about 25% of cluster 1. They also have the lowest absorption compare to the other two clusters. It is also shown that they have the highest unit weight. Based on the previous study by Hudec (1989) (Table 3), cluster 1 consists of fine grained, cluster 2 of medium grained, and cluster 3 consists of coarse grained material.

Table 17. Mean values of clusters 1, 2, and 3 based on K-mean clustering

	Variable	Cluster means		
		Cluster 1	Cluster 2	Cluster 3
Stress Data	Room Temp. – Room Humidity (Initial Test)	5233.08	7037.77	8547.22
	Room Temp. – Room Humidity (Final Test)	5312.26	7414.58	8910.87
	Room Temperature – 98% Humidity	4239.87	6234.03	7220.31
	48hrs Freezing – 65% Humidity	5529.86	7252.26	8247.42
	Room Temperature – 24hrs Saturation	4077.55	5796.48	7872.76
	48hrs Freezing – 24hrs Saturation (A)	4519.31	6866.58	7844.13
	48hrs Freezing – 24hrs Saturation (B)	4055.58	6368.89	7392.17
	48hrs Freez. – 48hrs Sat. in 20% Salt-Water	3433.62	5362.32	6743.3
	Room Temp. – 48hrs Sat. in 20% Salt-Water	4172.47	5904.19	6559.81
	ADSORPTION50	0.08	0.05	0.02
	ADSORPTION98	0.25	0.17	0.06
	ABSORPTION	1.9	1.45	0.8
	FULL_ABSORP	1.9	1.4	0.85
	UNIT_WEIGHT	2.57	2.65	2.73
	DELTA_L	0.04	0.04	0.04
	ADS_98_RIGBY	0.23	0.13	0.05
	SUSPENSION	2.88	3.14	2.2
	STRENGTH	8.31	13.85	15.34
Young's Modulus Data	Room Temp. – Room Humidity (Initial Test)	1.60E+10	2.58E+10	3.40E+10
	Room Temp. – Room Humidity (Final Test)	1.56E+10	2.51E+10	3.49E+10
	Room Temperature – 98% Humidity	1.39E+10	2.40E+10	3.07E+10
	48hrs Freezing – 65% Humidity	1.45E+10	2.75E+10	3.67E+10
	Room Temperature – 24hrs Saturation	1.35E+10	2.21E+10	3.11E+10
	48hrs Freezing – 24hrs Saturation (A)	1.48E+10	2.36E+10	3.20E+10
	48hrs Freezing – 24hrs Saturation (B)	1.39E+10	2.17E+10	3.01E+10
	48hrs Freez. – 48hrs Sat. in 20% Salt-Water	1.46E+10	2.51E+10	3.19E+10
	Room Temp. – 48hrs Sat. in 20% Salt-Water	1.40E+10	2.19E+10	3.19E+10
	RDEN	2.64	2.66	2.79
	RADS	0.21	0.14	0.06
	RPORO	2.08	1.58	1.02
	RCAP32S	0.49	0.21	0.1
	RADSB	20.94	23.39	17.24
	DRYLOSS	0.15	0.23	0.08
	RVABGNV	22.1	23.72	14.21
	RCAP32B	26.74	15.85	19.48
	RSATBIF	83.26	80.66	70.46
	RBUV	55.16	50.89	51.35
	RABS	1.44	1.08	0.6
	RBUS	1.23	0.93	0.54
	RBUB	79.11	73.94	83.14

When samples are exposed to humidity, water molecules are adsorbed by rock pore surface and a layer of adsorbed water is formed. The thickness of this layer depends on humidity and also on the nature of the rock pore surface (Section B, Chapter IV). The difference in the amount of adsorbed water is due to the changes in surface areas, given that the humidity was constant during experiment and the samples consist of rocks with almost similar physical properties. Since the thickness of the adsorbed layer is assumed constant, this suggests that the surface area of Cluster 1 is 4 times the surface area of Cluster 3 and about 1.5 times the surface area of Cluster 2. It is also interesting to see that the thermal contraction coefficient due to sub zero temperatures is very similar among the three clusters. This shows that the thermal contraction is more function of the mineral content rather than the grain size, Young's Modulus, or strength.

Paired t-test was performed for the Stress and Young's Modulus variables within each cluster (Table 18). Similar results to paired t- test on Group Sigma were obtained.

G. Factor Analysis

Factor analysis is a data reduction technique in multivariate statistics. It reduces a large number of variables into a small number of factors. Each factor describes the relationship among sets of many interrelated variables (Williams 1986).

	Test	Cluster 1								Cluster 2								Cluster 3							
		RT_RH_INI	RT_RH_FIN	RT_96RH	FRZ_65RH	RT_SATURTD	FRZ_SAT_A	FRZ_SAT_B	FRZ_SALTSOL	RT_RH_INI	RT_RH_FIN	RT_96RH	FRZ_65RH	RT_SATURTD	FRZ_SAT_A	FRZ_SAT_B	FRZ_SALTSOL	RT_RH_IN	RT_RH_FIN	RT_96RH	FRZ_65RH	RT_SATURTD	FRZ_SAT_A	FRZ_SAT_B	FRZ_SALTSOL
Stress	Room Temp. – Room Humidity (Final Test)																								
	Room Temperature – 98% Humidity	+	+							+	+							+	+						
	48hrs Freezing – 65% Humidity			-								-								-					
	Room Temperature – 24hrs Saturation	+	+		+					+	+		+						+						
	48hrs Freezing – 24hrs Saturation (A)	+	+		+							-		-											
	48hrs Freezing – 24hrs Saturation (B)	+	+	+	+		+			+	+		+	+				+	+		+				
	48hrs Freez. – 48hrs Sat. in 20% Salt-Water	+	+	+	+	+	+	+		+	+	+	+		+	+		+	+		+	+			
	Room Temp. – 48hrs Sat. in 20% Salt-Wate	+	+		+				-	+	+		+		+		-	+	+		+	+	+	+	
Young's Modulus	Room Temp. – Room Humidity (Final Test)																								
	Room Temperature – 98% Humidity	+	+								+							+	+						
	48hrs Freezing – 65% Humidity		+							-		-								-					
	Room Temperature – 24hrs Saturation	+	+							+	+		+					+	+		+				
	48hrs Freezing – 24hrs Saturation (A)					-					+		+	-							+				
	48hrs Freezing – 24hrs Saturation (B)	+	+							+	+	+	+		+			+	+		+				
	48hrs Freez. – 48hrs Sat. in 20% Salt-Water		+											-		-					+				
	Room Temp. – 48hrs Sat. in 20% Salt-Wate	+	+							+	+	+	+				+				+				

(+) Column variable is significantly higher than row variable

(-) Column variable is significantly lower than row variable

Table 18. Paired t-test among all variables within each Cluster

Factor analysis was performed using principal components analysis method and varimax rotation analysis was selected as the rotation factor. The extraction parameter was set at a minimum factor value (latent root or eigenvalue) of one. Eigenvalue can also be presented in percentage. Each factor is represented by a component loading for a variable. A high positive component loading describes a high direct influence of variable on the representing factor and a high negative component loading describes a high inverse influence. The sum of squared correlation coefficients between a variable and all its representing factors (component loadings) is called communality number. A low communality number shows a weak correlation between a variable and existing factors.

Factor analysis was first performed on entire data set (Group Sigma). Based on the obtained results, DRYLOSS variable was omitted from the data set due to its low communality number. Variables RBUV, RVABGNV, RSATBIF and DELTA_L were also omitted from the data set due to their low eigenvalues. First run of Factor analysis produced seven factors with a total variance of 80.7%.

Factor analysis was then run on the remaining variables. This second run was set to produce four factors. Due to the high correlation of variables and factors, the total variance was improved to 83% in the second run. Result of second factor analysis is presented in Tables 19a and 19b.

Based on the results presented on Table 19b, variables can be divided into 4 groups by the highest eigenvalue among the four factors.

Factor 1, called the Strength and Elasticity Factor, contains the strength and elasticity parameters. It accounts for 22.4% of the total variance and includes all the Young's Modulus variables along with the strength variable. This factor has high

positive loading of Young's Modulus variables and somewhat lower positive loading on the strength variable. The reason for a lower positive loading for strength variable is due to the fact that strength directly represents a stress value, and the strength is tensional strength as obtained in the Brazilian test. On the other hand, Young's Modulus is the ratio of compressive stress to strain. The inclusion of the strength variable in this factor shows that the strength of rock is directly related to its modulus under all conditions of exposure. Among all Young's Modulus results there are three variables that possess the highest component loadings. They include: 48hrs Freezing – 24hrs Saturation (B) (FRZ_SAT_B), Room Temperature – Room Humidity (Initial Test) (RT_RH_INI), and 48hrs Freezing – 65% Humidity (FRZ_65RH). This shows the high direct influence of these variables on this factor. As mentioned in section D of Chapter VIII, the above mentioned variables represent the lowest measured (48hrs Freezing – 24hrs Saturation (B) (FRZ_SAT_B)) and highest measured (Room Temperature – Room Humidity (Initial Test) (RT_RH_INI), 48hrs Freezing – 65% Humidity (FRZ_65RH)) Young's Modulus under all conditions.

Factor 2, called Surface Area Factor, contains the variables that are controlled by the internal surface area characteristics of the rock, since it includes all the adsorption variables with a high negative loading. The negative loading on most of the variables suggests the inverse relationship of this factor to the strength factor. The negatively loaded variables also represent the non-freezable portion of the water in pores. However the factor also includes bulk water fraction (RBUB) with a high positive loading, which represents freezable water. Similar relationships have been encountered in factor analysis

performed by Ondrasik (1996), who named the factor as 'rock freezability' factor. Factor 2 with 18.4% of the total variance, shows the lowest variance among all factors.

Factor 3, dubbed the Stress Factor, makes up 20.4% of the total variance. This factor is dominated by stress variables, i.e., stress required to bring the rock sample to constant strain. As in the Strength Factor 1, all variables show a positive loading. The highest communality belongs to Room Temperature - 98% Humidity (RT_98RH) condition and 48hrs Freezing - 65% Humidity (FRZ_65RH) condition has the lowest communality among all variables. 48hrs Freezing - 65% Humidity (FRZ_65RH) condition and 48hrs Freezing - 48hrs Saturation in 20% Salt-Water (FRZ_SALTSOL) condition have the lowest loading among all variables.

Factor 4, called the Void Factor, contains variables that describe the void characteristics of the sample population and it accounts for 21.8% of the total variance. Porosity variables including vacuum absorption porosity (RPORO) and (FULL_ABSORP), absorption (ABSORPTION), Bulk water (RBUS), and absorbed water (RABS) show very high communality number and a high negative loading. The negative loading indicates that these variables inversely affect the strength and stress characteristics of the samples. Rate of water absorption (RCAP32S) is included in this group and has the lowest communality number. This suggests that although the rate of absorption is related to the porosity and pore size in a sample, it has less importance than absorption. Unit weight (UNIT_WEIGHT) and density (RDEN) both have a positive loading, which confirms that unit weight and density correlate positively with strength and stress variables.

Table 19a. Final statistics of Group Sigma factor analysis

Factor	Eigenvalue	Variance%	Cum. Var.%
1	7.609	22.4	22.4
2	6.263	18.4	40.8
3	6.921	20.4	61.2
4	7.395	21.8	83.0

Table 19b. Detailed statistics of Group Sigma factor analysis

	Variable	Factor 1	Factor 2	Factor 3	Factor 4	Communality
Young's Modulus&Strength	48hrs Freezing – 24hrs Saturation (B)	0.832	0.208	0.301	0.27	0.898989
	Room Temp. – Room Humidity (Initial Test)	0.822	0.125	0.316	0.265	0.86139
	48hrs Freezing – 65% Humidity	0.812	-0.013	0.314	0.336	0.884061
	Room Temperature – 98% Humidity	0.82	0.134	0.346	0.194	0.847708
	Room Temp. – Room Humidity (Final Test)	0.79	0.133	0.365	0.345	0.894039
	Room Temperature – 24hrs Saturation	0.723	0.322	0.234	0.45	0.883669
	48hrs Freezing – 24hrs Saturation (A)	0.721	0.183	0.233	0.368	0.743043
	48hrs Freez. – 48hrs Sat. in 20% Salt-Water	0.701	0.292	0.284	0.245	0.717346
	Room Temp. – 48hrs Sat. in 20% Salt-Water	0.663	0.399	0.216	0.318	0.74655
	STRENGTH	0.595	-0.528	0.244	0.124	0.707721
Surface Area	ADSORPTION98	-0.115	-0.957	-0.071	0.02	0.934515
	RADS	-0.113	-0.943	-0.217	-0.007	0.949156
	ADSORPTION50	-0.117	-0.927	-0.13	0.039	0.891439
	ADS_98_RIGBY	-0.125	-0.894	-0.077	0.079	0.827031
	RADSB	-0.031	-0.781	0.066	0.445	0.813303
	SUSPENSION	-0.179	-0.756	0.129	-0.088	0.627962
	RBUB	0.057	0.746	-0.104	-0.465	0.786806
Stress Data	Room Temperature – 24hrs Saturation	0.077	0.056	0.872	0.187	0.804418
	Room Temp. – Room Humidity (Final Test)	0.33	0.014	0.848	0.039	0.829721
	Room Temperature – 98% Humidity	0.385	-0.11	0.84	0.095	0.87495
	48hrs Freezing – 24hrs Saturation (A)	0.265	0.108	0.804	0.312	0.825649
	Room Temp. – Room Humidity (Initial Test)	0.363	-0.166	0.784	0.07	0.778881
	48hrs Freezing – 24hrs Saturation (B)	0.132	-0.166	0.759	0.369	0.757222
	Room Temp. – 48hrs Sat. in 20% Salt-Water	0.2	0.126	0.742	0.172	0.636024
	48hrs Freezing – 65% Humidity	0.114	0.059	0.738	0.112	0.573665
	48hrs Freez. – 48hrs Sat. in 20% Salt-Water	0.275	0.285	0.704	0.146	0.673782
Void	RPORO	-0.275	0.149	-0.2	-0.91	0.965926
	FULL_ABSORP	-0.312	0.087	-0.114	-0.904	0.935125
	ABSORPTION	-0.295	0.02	-0.208	-0.9	0.940689
	RBUS	-0.274	0.133	-0.287	-0.89	0.967234
	RABS	-0.293	-0.006	-0.31	-0.886	0.966981
	RCAP32S	-0.287	0.087	-0.293	-0.795	0.807812
	RDEN	0.608	-0.208	0.035	0.706	0.912589
	UNIT_WEIGHT	0.605	-0.153	0.027	0.726	0.917239

VIII. DISCUSSION

The environmental conditions of exposure have significant effects on the elastic and strength properties of rocks. This is seen in Tables 8 to 11, where F-test and Wilcoxon test show that for the combined carbonates, a significant difference exists between these properties at different exposures. These differences can be ascribed to the nature of water in the rock pores, and especially the relative proportion of adsorbed water. Salt solution increases the proportion of adsorbed water, so greater differences are seen where samples contain salt water in their pores. Adsorbed water was shown to be elastic (Dananaj, 2001), and its elasticity can be used to explain the differences observed. The data also show that limestones as a group are less affected by environmental conditions than dolomites – i.e., fewer significant differences exist among exposure conditions for limestones. The differences between limestone and dolomite are likely due to their different crystallinity and pore structure.

The correlation tests between stress and modulus results under various exposure conditions show a positive significant correlation in almost all combinations (Table 12). This is to be expected. However, the more interesting results are found in Appendix D.3, where physical properties are compared to stress and modulus properties. Significant correlation exists between unit weight and water adsorption at 50%RH and 98%RH, and the elastic properties. This corroborates the observations of the previous paragraph, and points to the importance of pore structure and adsorbed water. Positive correlations are seen between density and elastic properties, and negative correlation between adsorption and elastic properties. The denser the rock, less pore space, and lower the adsorbed water content.

When the physical and elastic properties of different rock types are compared in Appendices E.1 to E.6 by two sample t-test, it is seen that the rock types show significantly different behavior. The differences in their behavior can be ascribed to both the mineral content (where stress and elastic properties are concerned), and to the nature of their pore system and both the absolute amounts of contained pore water and the proportion of adsorbed versus absorbed water.

Paired t-test in Table 14 compares the effect of the environment on the elastic properties of rock, and is similar to the F-test and Wilcoxon test, and essentially corroborates their results, showing that the environmental conditions have a significant effect on the elastic properties of rocks.

Cluster analysis is essentially a classifying procedure, grouping rocks of similar properties into clusters. The procedure was requested to group the samples into three clusters. Tables 16 to 18 show that the elastic properties clearly define the clusters. The physical properties more or less fall into place as well, e.g., unit weight, adsorption, and strength data support the divisions.

The significance of the cluster divisions is seen in Table 20, which can be considered as the summary table of the research results. The group t-test results show that the elastic properties are almost uniformly mutually exclusive among the cluster, i.e., each cluster contains rock with distinctly different elastic properties. The physical property differences are not as clearly defined, and significant differences occur only between all three clusters in unit weight and adsorption at 98RH (Rigbey). Cluster 3 is characterized by the highest stress to reach a constant strain in all conditions. The rocks in this cluster are classified as good quality rocks. The rocks in Cluster 2 are less durable

than rocks in cluster 3 and can be classified as medium quality or fair rocks. Cluster 1 is classified as fairly weak and contains rocks of poor durability.

The elastic property differences between the clusters are shown in Figures 30 and 31. Both figures show not only the clear division between the clusters, but also the effect of the environmental exposure on the elastic properties. These effects can be summarized as follows: Room Temperature – Room Humidity (Initial Test) (RT_RH_INI) and (Final Test) (RT_RH_FIN) required the highest stress to reach a constant strain of 8×10^{-7}cm. It also has the highest Young's Modulus under these conditions. Due to the low humidity the thickness of adsorbed layer of water was at its minimum in Room Temperature – Room Humidity condition. As a result surface energy and friction coefficient reduction were at their minimum (Section II.B).

As the moisture level in the samples increases, the amount of stress required to reach a constant 8×10^{-7}cm strain decreases (Fig. 30). When samples are exposed to humidity and ionic solutions in sub zero temperature, the required stress is at its minimum. The ionic solutions decrease the amount of water freezing, and increase the amount of adsorbed water. The rock can be considered to be in super-saturated conditions with unfrozen, un-attached water that can be easily expelled under applied stress. A thicker layer of adsorbed water decreases the surface energy at grain boundaries, which results in rock strength weakening.

The 48hrs Freezing – 24hrs Saturation (B) condition (FRZ_SAT_B) has produced the lowest Young's Modulus among good and fair quality rocks. It has also produced one of the lowest Young's Modulus among the three clusters. This shows that exposing saturated samples to sub zero temperatures results in a weakest rock.

Table 20. Cluster Group Mean comparison by Group t-test

(** 99% significant difference of means, * 95% significant difference of means)

Factor	Variables	Cluster Group Mean			Cl.1 vs Cl.2	Cl.1 vs Cl.3	Cl.2 vs Cl.3	Standard Dev.		
		Cl. 1	Cl. 2	Cl. 3				Cl. 1	Cl. 2	Cl. 3
Stress Factor	RT_RH_INI	5233.08	7037.77	8547.22	**	**	**	1692.99	1810.39	2648.58
	RT_RH_FINAL	5312.26	7414.58	8910.87	**	**	**	2202.94	1442.32	2407.68
	RT_98RH	4239.87	6234.03	7220.31	**	**	*	1678.21	1532.82	2096.87
	FRZ_65RH	5529.86	7252.26	8247.42	**	**		1852.09	2276.13	2329
	RT_SATURATED	4077.55	5796.48	7872.76	**	**	**	2263.75	1725.36	2795.26
	FRZ_SAT_A	4519.31	6866.58	7844.13	**	**		2144.36	1442.88	2379.71
	FRZ_SAT_B	4055.58	6368.89	7392.17	**	**		1991.74	1636.19	2460.05
	FRZ_SALTSOL	3433.62	5362.32	6743.3	**	**	**	1684.91	1104.06	1758.3
	RT_SALTSOL	4172.47	5904.19	6559.81	**	**	*	1701.91	1096.38	1315.17
Void Factor	ABSORPTION	1.9	1.45	0.8		**	*	1.4	1.1	0.78
	FULL_ABSORP	1.9	1.4	0.85		**	*	1.59	1.01	0.79
	UNIT_WEIGHT	2.57	2.65	2.73	**	**	**	0.13	0.06	0.1
	RDEN	2.64	2.66	2.79			**	0.3	0.06	0.27
	RPORO	2.08	1.58	1.02		**		1.63	1.22	0.95
	RCAP32S	0.49	0.21	0.1		*		0.79	0.4	0.13
	RABS	1.44	1.08	0.6		**	**	1.13	0.88	0.56
	RBUS	1.23	0.93	0.54		**		1.14	0.9	0.57
Surface Area Factor	ADSORPTION50	0.08	0.05	0.02		**	**	0.07	0.05	0.01
	ADSORPTION98	0.25	0.17	0.06		**	**	0.22	0.15	0.05
	ADS_98_RIGBY	0.23	0.13	0.05	*	**	**	0.28	0.11	0.04
	SUSPENSION	2.88	3.14	2.2			*	1.47	1.56	1.07
	RADS	0.21	0.14	0.06		**	**	0.18	0.11	0.04
	RADSB	20.94	23.39	17.24				19.22	21.44	14.63
	RBUB	79.11	73.94	83.14				20.19	25.77	17.46
Young's Modulus Factor	Y_RT_RH_FINL	1.60E+10	2.58E+10	3.40E+10	**	**	**	2.59E+09	4.05E+09	6.27E+09
	Y_RT_RH_INI	1.56E+10	2.51E+10	3.49E+10	**	**	**	3.77E+09	4.46E+09	7.75E+09
	Y_RT_98RH	1.39E+10	2.40E+10	3.07E+10	**	**	**	2.92E+09	3.61E+09	4.36E+09
	Y_FRZ_65RH	1.45E+10	2.75E+10	3.67E+10	**	**	**	3.70E+09	6.11E+09	6.53E+09
	Y_RT_SATURTD	1.35E+10	2.21E+10	3.11E+10	**	**	**	2.29E+09	3.92E+09	4.10E+09
	Y_FRZ_SAT_A	1.48E+10	2.36E+10	3.20E+10	**	**	**	3.56E+09	3.52E+09	5.80E+09
	Y_FRZ_SAT_B	1.39E+10	2.17E+10	3.01E+10	**	**	**	3.02E+09	3.17E+09	4.45E+09
	Y_FRZ_SALTSO	1.46E+10	2.51E+10	3.19E+10	**	**	**	3.38E+09	5.44E+09	6.23E+09
	Y_RT_SALTSOL	1.40E+10	2.19E+10	3.19E+10	**	**	**	2.84E+09	4.07E+09	7.01E+09
	Strength	8.31	13.85	15.34	**	**		3.72	4.2	4.55

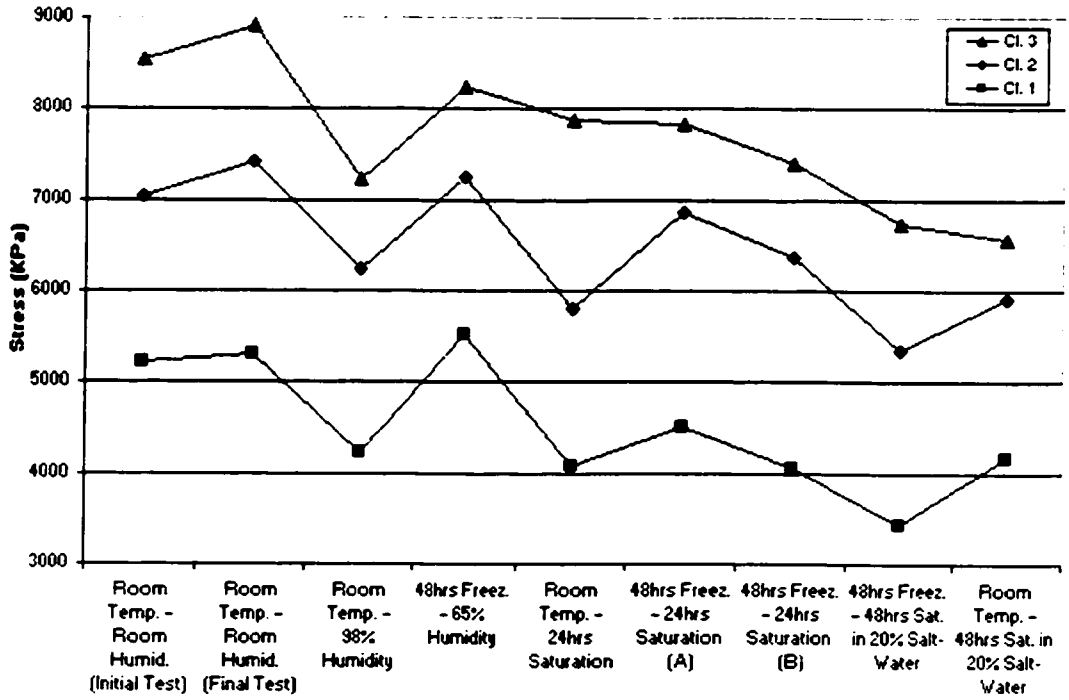

Figure 30. Graph of Stress to fixed Strain for Clusters 1, 2, and 3, from K-means Clustering.

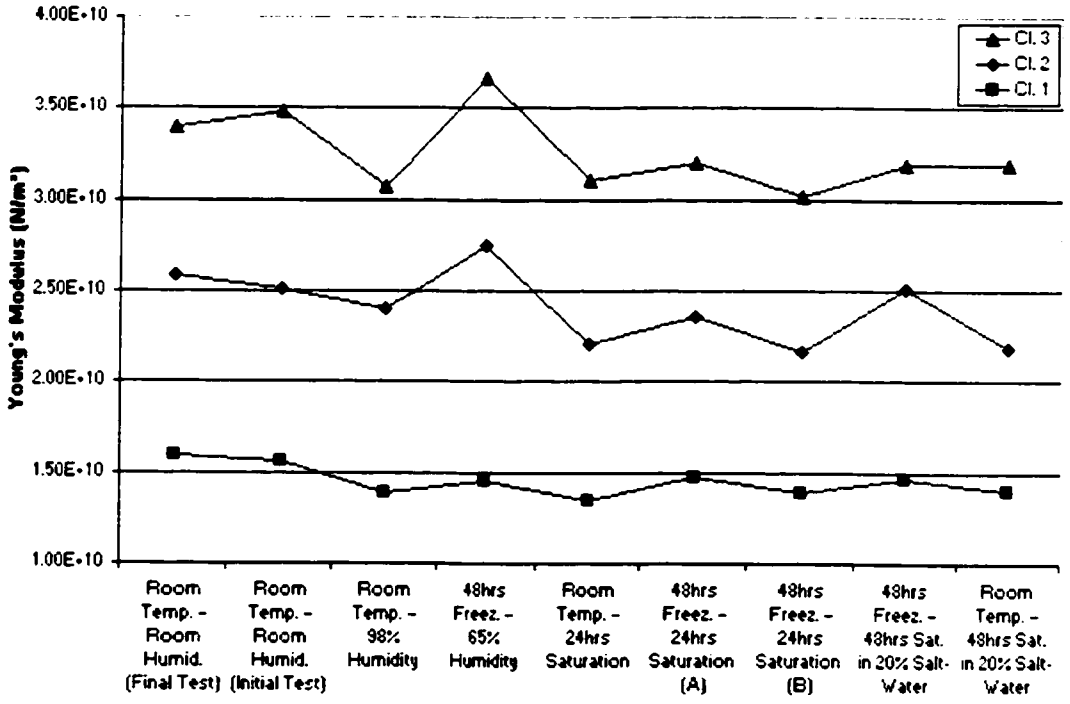

Figure 31. Graph of Young's Modulus for Clusters 1, 2, and 3, from K-means Clustering.

IX. CONCLUSIONS, APPLICATIONS AND RECOMMENDATIONS

A) CONCLUSIONS

The following can be concluded from this research:

1. The thickness of adsorbed layer of water reaches its maximum in presence of salt solution. F test revealed a significant difference in Stress and Young's Modulus obtained from 48 hours Freezing – 48 hours Saturation (20% Salt-Water) (Y_FRZ_SALTSOL) and Room Temperature – 48hrs Saturation (20% Salt-Water) (Y_RT_SALTSOL) conditions and the rest of variables.
2. Since adsorbed water is elastic, the increase of thickness in adsorbed layer of water will increase the elasticity of the rock system. As a result, the Strength and Young's Modulus of the rock is reduced.
3. A predictable, and highly significant to significant relationship was found between stress required to bring sample to constant strain and Young's Modulus.
4. There exists an inverse Correlation significant relationship between 48hrs Freezing – 48hrs Saturation (20% Salt-Water) (FRZ_SALTSOL) and adsorption in 98% humidity (RADS). Adsorption increases with increase of specific surface area and surface charge. Ionic solution increases the amount of adsorbed water, increasing the elasticity (decreasing Young's Modulus).

5. A highly significant to significant direct relationship exists between Young's Modulus results and unit weight. Higher unit weight (density), lower porosity, and therefore less adsorbed water.
6. Internal surface area and unit weight are the most important physical parameters of the rocks affecting elastic and durability properties of the rocks.
7. Elastic and strength properties of rocks are sensitive to changes in moisture content and temperature of their environment. Decrease of temperature to below zero, in absence of moisture causes contraction in rock and it increases the Young's Modulus of the rock. Increase of moisture in any environment increases the amount of adsorption in rock. Since adsorbed water layers act as an elastic material, they reduce the strength and Young's Modulus of the rock.
8. A high Young's Modulus and strength in good quality rocks is related to their lower surface area and higher unit weight. This results in less adsorption and absorption. Lower adsorption reduces the amount of available adsorbed water that can act as an elastic material.
9. The presence of cations in pore water decreases the rock strength and Young's Modulus. Cations are adsorbed to the negatively charged pore walls due to their positive charge. They cluster polar water molecules to themselves and increase the thickness of adsorbed water. As a result there is more elastic material available in the system, which reduces the strength and Young's Modulus.

10. Rock type exerts basic control on the elastic and physical properties, but environmental conditions impose an overriding effect on these parameters. Dolomites, as a group, are most affected.

b) Applications

One of the applications of this study is in tunneling and underground mining. This research has shown that rocks have their highest strength in dry condition. Most uniaxial compressive strength tests are carried out on dry rock specimens, whereas in nature, the rock is at least partially saturated. This can effect the applicability of rock strength results in design of structures. Performing insitu strength tests such as pressure meter test in boreholes and in wet condition can produce lower, but more representative rock strength results.

Elastic properties of rocks as determined by Young's Modulus are important considerations in foundation engineering for masonry dams, bridge abutments, and any structures that will place substantial load or stress on a rock foundation. Most moduli are determined on dry rocks under room temperature. This research shows that the modulus is environment-sensitive. The expected strains for given load will vary as the condition of the environment change, and those calculated for dry conditions will not apply to other conditions. Larger than expected strains based on wrong Modulus determination may result in the foundation and perhaps the structure failure.

This research is also applicable to strength of pillars in underground mines, and the stability of slopes in open pit mines, which may change as the environmental conditions change.

Data obtained in this research can be used in mining calculations of longwall faces, cuts, supports, room side stability, sudden falls and general instability. A better understanding of effective factors on Young's Modulus and strength of rock materials, will help to control failures and maintain their integrity (Mandzic, 1979).

Most of the time in open pit mining or in aggregate quarries the size of blasted material is very important. Fully saturated rocks transmit shock (P and S) waves much easier than the partially saturated rocks, and have lower strengths. Thus, over-breakage can result in blasting fully saturated rocks (Lienhart, 1994).

c) Recommendations

In order to achieve more accurate results it is suggested that the experimental procedure and the uniaxial stress frame be modified as follows:

1. Conduct the experiment with a tri-axial stress frame and then compare the results to the results obtained from uniaxial stress frame. Since the sample is confined in tri-axial test, the pore water will not drain out under saturated conditions, more closely simulating conditions in nature.
2. Use an automatic hydraulic pump instead of the manual hydraulic pump to achieve a constant loading rate for all the samples. Even slightly different loading rates change the Young's Modulus for the same rock (Section II.A).
3. Perform each stress test in the same environmental condition that the samples were exposed to (e.g., test frozen sample under freezing conditions rather than at room temperature). This can be accomplished by

building an environmental cell between the stress piston and the base to maintain the temperature, moisture and ionic condition of the. This will avoid any disturbance to the samples due to environment changes while being tested.

4. Use fresh samples instead of previously used samples for each test. Rocks are not completely elastic and conditions of the previous test may affect their response in the next test.

5. Choose a variety of rock types with a wider range of grain size from fine to coarse. This study was focused on mainly two rock types. Samples of other rock types were studied in small populations only.

6. Conduct a mercury porosimetry test on the samples to determine the pore size distribution and its relationship to Young's Modulus. This will determine the actual porosity of the samples, rather than inferred one from absorption and adsorption tests.

REFERENCES

Althaus, E., Friz-Topfer, A., Lempp, Ch., Natau, O., 1994, Effects of Water on Strength and Failure Mode of Coarse-Grained Granites at 300°C, Rock Mechanics and Rock Engineering, Vol. 27, No. 1, Springer-Verlag, New York, pp. 1-21.

Anderson, G. M., 1996, Thermodynamics of Natural Systems, University of Toronto, John Wiley & Sons, Inc, 382p.

ASTM Special Technical Publication No. 402, 1965, Testing techniques for rock mechanics, Philadelphia.

Bell, F. G., 1987, Ground Engineer's Reference Book, Butterworths, Cornwall, 59/20p.

Bellanger, M., Homand, F., Remy, J. M., 1993, Water Behavior in Limestones as a Function of pores Structure: Application to Frost resistance of Some Lorraine limestones, Volume 36 Nos. ½, Engineering Geology , An International Journal, Elsevier, pp. 99-108.

Boozer, G. D., Hiller, K., Serdengecti, S., 1962, Effects of Pore Fluids on the Deformation Behavior of Rocks Subjected to Triaxial Compression. Proc. of the 5th Symp. on Rock Mech., Pergamon, pp. 579-625.

Broch, E., 1979, Changes in Rock Strength Caused by Water, International Congress on Rock Mechanics, International Society for Rock Mechanics, Proceedings, Vol. 1, Montreux, pp. 71-75.

Broch, E., Franklin, J. A., 1972, The Point Load Strength Test, International Journal of Rock Mechanics and Mineral Sciences, Vol. 9, pp. 669-697.

Colback, P. S., Wiid, B. L., 1965, Influence of Moisture Content on the Compressive Strength of Rocks, Proc. 3rd Canadian Symposium, Rock Mechanics, Toronto, pp. 65-83.

Dananaj, I., 2001, Rock Stress Relaxation in Dry and Saturated States, Master Thesis, University of Windsor, Windsor, Ontario, Canada, 123p.

Dullien, F. A. L., 1979, Porous Media: Fluid Transport and Pore Structure, Academic Press, New York, N.Y, 395p.

Dunn, J. R., Hudec, P. P., 1965, The influence of clays on water and ice in rock pores, Physical Research Report, State of New York, Department of Public Works, Eng. Res. Ser. 65-5, pp. 138.

Franklin, J. A., Dusseault, M. B., 1989, Rock Engineering, McGraw-Hill, New York, 600p.

Fredrich, J. T., Evans, B., Wong, T. F., 1990, Effect of Grain Size on Brittle and Semibrittle Strength: Implications for Micromechanical Modeling of Failure in Compression, Journal of Geophysics Res, pp. 907-920.

Garrels, R. M., MacKenzie, 1971, Evolution of Sedimentary Rocks, New York, Norton, 397p.

Hatzor, Y. H., Palchik, V., 1998, A microstructure-based Failure Criterion for Aminadav dolomites, International Journal of Rock Mech. Min. Sci. Geomech, pp. 797-805.

Hilbert, L. B., Hwong, T. K., Cook, N. G. W., Nihei, K. T., Myer, L. R., 1994, Effects of Strain Amplitude on the Static and Dynamic Nonlinear Deformation of Berea Sandstone, Rock Mechanics Models and Measurements Challenges from Industry, Proceedings of the 1st North A,erican Rock Mechanics Symposium, University of Texas at Austin, A. A. Balkema, Rotterdam, pp. 497-504.

Horrigmoe, G., 1985, Effect of Pore Water and its Diffusion in Concrete, Mechanics of Geomaterials, John Wiley & Sons Ltd., Norwich, pp. 349-377.

Hudec, P. P., 1974, Rock Weathering on the Molecular Level, engineering case histories Number 11, Geological Society of America, Boulder, Colorado, pp. 47-51.

Hudec, P. P., 1980, Effect of Deicing Salts on Deterioration and Dimensional Changes of Carbonate Rocks, Durability of Building Materials and Components, ASTM STP 691, P. J. Sereda and G. G. Litvan, Eds., American Society for Testing and Materials, pp. 629-640.

Hudec, P. P., 1983, Aggregate test-Their Relationship and Significance: Durability of Building Materials, No. 1, Elsevier Scientific Publishing Company, Amsterdam, pp. 275-300.

Hudec, P. P., 1987, Deterioration of aggregates-the underlying causes, concrete durability, Katharine and Bryant Mather International conference, American concrete institute, SP-100, 2, pp. 1325-1342.

Hudec, P. P., 1989a, Durability of Rock as Function of Grain Size, Pore Size, and Rate of Capillary Absorption of Water, Journal of Materials in Civil Engineering, Vol. 1, No. 1, pp. 3-9.

Hudec, P. P., 1989b, Ionic Control in Deterioration of the Building Materials, Proceedings of the 6th International Symposium on Water-Rock Interaction , Malvern, A.A. Balkema, Rotterdam, Brookfield, pp. 305-308.

Hudec, P. P., 1991, Freezing or Osmosis as Deterioration Mechanism of Concrete and Aggregate? Low Temperature Effects on Concrete Proceedings, Second Canadian/Japan Workshop, August, 1-2, Ottawa, Ontario, pp. 1-8.

Hudec, P. P., 1993, Aggregate and Concrete Durability as Controlled by Water and Cation Adsorption and Osmosis, CANMET, Concrete Durability, Mexico, pp. 32-52.

Hudec, P. P., Sitar, N., 1975, Effect of Sorption on Carbonate Rock Expansion, Canadian Geotechnical Journal, Vol. 12, No. 2, pp. 179-186.

Jaeger, C., 1972, Rock Mechanics and Engineering, Cambridge University Press, London, 416p.

Jaeger, J. C., Cook, N. G. W., 1976, Fundamentals of Rock Mechanics, 3rd Edition, Chapman and Hall, London, 585p.

Jones, M. E., Willis, S., Kageson Leo, N., Mortimore, R. N., Leddra, M. J., 1994, The Influence of Geological Burial on the Deformation Characteristics of Bonded Carbonate Rocks, Rock Mechanics Models and Measurements Challenges from Industry, Proceedings of the 1st North A,erican Rock Mechanics Symposium, University of Texas at Austin, A. A. Balkema, Rotterdam, pp. 707-713.

Jumikis, A. R., 1983, Rock Mechanics, Series on Rock and Soil Mechanics, Vol. 7, 2nd Edition, Trans Tech Publications, Rockport, 613p.

Kwon, O., Kronenberg, A. K., 1994, Deformation of Wilcox shale: Undrained Strengths and Effects of Strain Rate, Rock Mechanics Models and Measurements Challenges from Industry, Proceedings of the 1st North A,erican Rock Mechanics Symposium, University of Texas at Austin, A. A. Balkema, Rotterdam, pp. 757-765.

Lide, D. R., Frederikse, H. P. R., 1998, CRC Handbook of Chemistry and Physics, CRC Press Inc., New York,

Lienhart, D. A., 1994, Durability Issues in the Production of Rock for Erosion Control, Rock Mechanics Models and Measurements Challenges from Industry, Proceedings of the 1st North A,erican Rock Mechanics Symposium, University of Texas at Austin, A. A. Balkema, Rotterdam, pp. 1083-1090.

Mandzic, E., 1979, Generalization of Factors Effecting the Uniaxial Strength of Rock Material, International Congress on Rock Mechanics, International Society for Rock Mechanics, Proceedings, Vol. 1, Montreux, pp. 397-408.

Marchand, J., Sellevold, E. J., Pigeon, M., 1994, The Deicer Salt Scaling Deterioration of Concrete – An Overview, International Conference, Concrete Durability, Nice, France, V.M. Malhotra, SP 145-1, pp.1-46.

Martin, R. J., Haupt, R. W., 1994, Static and Dynamic Elastic Moduli in Granite: The Effect of Strain amplitude, Rock Mechanics Models and Measurements Challenges from Industry, Proceedings of the 1st North A,erican Rock Mechanics Symposium, University of Texas at Austin, A. A. Balkema, Rotterdam, pp. 473-480.

Matsuka, N., 1989, Mechanisms of Rock Breakdown by Frost Action: An Experimental Approach, Volume 17, No. 2, Cold Regions Science and Technology, pp. 253-269.

Means, W. D., 1976, Stress and Strain: Basic Concepts of Continuum Mechanics for Geologists, Springer – Verlag, New York, 339p.

Motulsky, H., 1999, Analyzing Data with GraphPad Prism, A Companion to GraphPad Prism version 3, GraphPad Software, Inc, 379p.

Mowar, S., Zaman, M., Stearns, D. W., Roegiers, J. C., 1994, Pore Collapse Mechanisms In Cordoba Cream Limestone, Effect of Strain amplitude, Rock Mechanics Models and Measurements Challenges from Industry, Proceedings of the 1st North A,erican Rock Mechanics Symposium, University of Texas at Austin, A. A. Balkema, Rotterdam, pp. 767-773.

Ondrasik, M., 1996, Some Thermodynamics of Pore Water in Rock Deterioration, Master of Applied Sciences Thesis, University of Windsor, Windsor, Ontario, 158p.

Palchik, V., 1999, Influence of Porosity and Elastic Modulus on Uniaxial Compressive Strength in Soft Brittle Porous Sandstones, Rock Mechanics and Rock Engineering, Vol. 32, No. 4, Springer-Verlag, New York, pp. 303-309.

Powers, T. C., 1975, Freezing Effect in Concrete: Durability of Concrete, ACI SP 47, American Concrete Institute, Detroit, Michigan, pp. 1-11.

Price, N. J., 1960, The Compressive Strength of Coal Measure Rocks, Colleray Engineering, vol. 37, pp. 283-292.

Price, R. H., Boyd, P. J., Noel, J. S., Martin, R. J., 1994, Relationship between Static and Dynamic Rock Properties in Welded and nonwelded Tuff, Rock Mechanics Models and Measurements Challenges from Industry, Proceedings of the 1st North A,erican Rock Mechanics Symposium, University of Texas at Austin, A. A. Balkema, Rotterdam, pp. 505-512.

Rahn, P. H., 1996, Engineering Geology, an environmental approach, Prentice Hall, New Jersey, 657p.

Rao, K. S., Venkatappa Rao, G., Ramamurthy, T., 1987, Strength of Sandstones in Saturated and Partially Saturated Conditions, Geotechnical Engineering Journal of Southeast Asian Geotechnical Society, pp. 99-127.

Rigbey, S. J., 1980, The Effect of Sorbed Water on Expansivity and Durability of Rock Aggregates, Master of Applied Sciences Thesis, University of Windsor, Windsor, Ontario, 165p.

Rogers, C. O., Pang, S. S., Kumano, A., Goldsmith, W., 1986, Response of Dry- and Liquid-Filled Porous Rocks to Static and Dynamic Loading by Variously-Shaped Projectiles, Rock Mechanics and Rock Engineering, Vol. 19, No. 4, Springer-Verlag, New York, pp. 235-260.

Rudnicki, J. W., 1985, Effect of Pore Fluid Diffusion on Deformation and Failure of Rock, Mechanics of Geomaterials, John Wiley & Sons Ltd., Norwich, pp. 315-347.

Serdengecti, S., Boozer, G. D., 1961, The Effects of Strain Rate and Temperature on The Behavior of Rocks Subjected to Triaxial Compression, Proceedings of Fourth Symposium on Rock Mechanics, Penn. State University, pp. 83-97.

Swan, G., Cook, J., Bruce, S., Meehan, R., 1989, Strain Rate effects in Kimmeridge Bay Shale, International Journal of Rock Mechanics Mineral Sciences & Geochemistry, Vol. 26, pp. 135-149.

Systat, 1997, Systat 7.0, New Statistics, Software Instruction Manual, Systat, 303p.

Szechy, K., 1966, The Art of Tunnelling, Budapest: Akademiai Kiado, 1097p.

Thurston, P. C., Williams, H. R., Sutcliffe, R. H., Stott, G. M., 1992, Geology of Ontario, Ministry of Northern Development and Mines, Ontario, 1525p.

Tucker, M. E., 1991, Sedimentary Petrology, An Introduction to the Origin of the Sedimentary Rocks, Blackwell, Oxford, 260p.

Van Eeckhout, E. M., 1976, The Mechanism of Strength Reduction Due to Moisture in Coal Mine Shales, International Journal of Rock Mechanics and Mineral Sciences and Geomechanics, Abstract, Vol. 13, pp. 61-67.

Vutukuri, V. S., Lama, R. D., Saluja, S. S., 1974, Handbook on Mechanical Properties of Rocks, Series on Rock and Soil Mecanics, Vol. 1, Trans Tech Publications, Germany, 280p.

Williams, F., 1986, Reasoning with Statistics, How to Read Quantitative Research, 3rd edition, Holt, Rinehart and Winston, The Dryden Press, Saunders College Publishing, 214p.

Wong, R. H. C., Chau, K. T., Wang, P., 1996, Microcracking and Grain Size Effect in Yeun Long marbles, International Journal of Rock Mech. Min. Sci. Geomech, pp. 479-485.

Yale, D. P., Jamieson, W. H., 1994, Static and Dynamic Mechanical Properties of Carbonates, Rock Mechanics Models and Measurements Challenges from Industry, Proceedings of the 1st North A,erican Rock Mechanics Symposium, University of Texas at Austin, A. A. Balkema, Rotterdam, pp. 463-471.

Zimmerman, R. W., 2000, Coupling in Poroelasticity and Thermoelasticity, International Journal of Rock Mechanics and Mining Sciences, Vol. 37, pp. 79-87.

Appendices

Appendix A.1. Sample Location and Lithology (modified from Ondrasik 1996)

MacGregor Quarry					
County		**Township**	**Quarry**	**Lot & Location**	
Essex		Anderdon	1	Lot 10; 10 km northeast of Amherstburg	
No.	**Lithology**	**Formation**	**Member**	**Color**	**Matrix**
3	Limestone	Lucas	Anderdon	light grey	fine crystalline
4	Limeston	Lucas	Anderdon	buff and light grey	aphanitic to microcrystalline

Vinemount Quarry					
County		**Township**	**Quarry**	**Lot & Location**	
Wentworth		Saltfleet	2	Lot 5; 4 km south of Winona	
No.	**Lithology**	**Formation**	**Member**	**Color**	**Matrix**
5	Dolomite	Lockport	Decew	dark grey to brown	medium crystalline
8	Dolomite	Lockport	Eramosa	medium brown with dark grey streaks	aphanitic

Collins Bay Quarry					
County		**Township**	**Quarry**	**Lot & Location**	
Frontenac		Kingston	3	Lots 2,3; 2.5 km west of the highway 38 - highway 2 intersection	
No.	**Lithology**	**Formation**	**Member**	**Color**	**Matrix**
10	Limestone	Gull River	A	dark grey	microcrystalline

Wings (Maitland) Quarry					
County		**Township**	**Quarry**	**Lot & Location**	
Grenville		Augusta	5	Lot 24; 6km north of Maitland	
No.	**Lithology**	**Formation**	**Member**	**Color**	**Matrix**
15	Dolomite	Oxford	-	brown to dark grey	medium crystalline
16	Dolomite	Oxford	-	brown to dark grey	medium crystalline

Appendix A.1. Continued... Sample Location and Lithology

Ridgemount Quarry					
County		**Township**	**Quarry**	**Lot & Location**	
Welland		Bartie	6	Lot 8; 4km south of Stevensvill	
No.	**Lithology**	**Formation**	**Member**	**Color**	**Matrix**
17	Limestone	Bois Blanc	-	light grey to green	fine crystalline
18	Dolomite	Bertie	Arcon	medium brown to grey	fine crystalline to aphanitic
19	Dolomite	Bertie	Arcon	mottled light and medium grey	aphanitic

Dundas Quarry					
County		**Township**	**Quarry**	**Lot & Location**	
Wentworth		W.Flamborough	7	Lots 10, 11; north west of Hamilgton	
No.	**Lithology**	**Formation**	**Member**	**Color**	**Matrix**
20	Dolomite	Lockport	Eramosa	medium brown	fine crystalline to aphanitic
21	Dolomite	Guelph	-	light grey	fine crystalline to aphanitic
22	Dolomite	Guelph	-	light grey	fine crystalline to aphanitic
23	Dolomite	Lockport	Eramosa	light brown	fine crystalline aphanitic
24	Dolomite	Lockport	Eramosa	grey to dark brown	fine crystalline to aphanitic

Cayuga Quarry					
County		**Township**	**Quarry**	**Lot & Location**	
Haldimand		N. Cayuga	8	Lots 45,46; 5.5km west of the village Cayuga	
No.	**Lithology**	**Formation**	**Member**	**Color**	**Matrix**
26	Dolomite	Bertie	Arcon	light brown and light grey	aphanitic

Appendix A.1. Continued... Sample Location and Lithology

Waubaushene Quarry					
County		**Township**	**Quarry**	**Lot & Location**	
Simcoe		Tay	9	Lot 9; 7km north of the village Coldwater	
No.	**Lithology**	**Formation**	**Member**	**Color**	**Matrix**
28	Limestone	Gull River	Lower	medium brown to greyish green	aphanitic

Stoney Creek Quarry					
County		**Township**	**Quarry**	**Lot & Location**	
Wentworth		Saltfleet	10	Lots 27, 28; west of Highway 20, southern edge of Stoney Creek	
No.	**Lithology**	**Formation**	**Member**	**Color**	**Matrix**
32	Dolomite	Lockport	Eramosa	grey - brown	aphanitic
34	Dolomite	Lockport	Eramosa	medium brown	aphanitic

MacLeod Quarry					
County		**Township**	**Quarry**	**Lot & Location**	
Stormont		Cornwall	11	Lot 4; 5km north of Cornwall	
No.	**Lithology**	**Formation**	**Member**	**Color**	**Matrix**
37	Dolomite	Gull River	Lower	light grey	fine crystalline to aphanitic
37.1	Limestone	Gull River	Lower	light grey	fine crystalline to aphanitic

Appendix A.1. Continued... Sample Location and Lithology

J.Dennison (Napanee) Quarry					
County		**Township**	**Quarry**	**Lot & Location**	
Lennox and Addington		North Fredericksburgh	12	Lot 21; North side of Highway 2, eastern of Napanee	
No.	**Lithology**	**Formation**	**Member**	**Color**	**Matrix**
39	Limestone	Gull River	D	brownish grey	aphanitic

Boyce (South Gloucester) Quarry					
County		**Township**	**Quarry**	**Lot & Location**	
		Gloucester	14	Lot 25; 3km north of the hamlet of South Gloucester	
No.	**Lithology**	**Formation**	**Member**	**Color**	**Matrix**
41	Dolomite	Oxford	-	light grey	aphanitic
42	Dolomite	Oxford	-	dark grey	fine crystalline

Northwest Quarry					
County		**Township**	**Quarry**	**Lot & Location**	
Haldimand		Walpole	15	Lots 12, 13	
No.	**Lithology**	**Formation**	**Member**	**Color**	**Matrix**
45	Dolomite	Bertie	-	medium to dark grey	fine crystalline
46	Dolomite	Bertie	-	buff to light brown	aphanitic
50	Limestone	Bois Blanc	-	light to medium grey	fine crystalline
51	Limestone	Bois Blanc	-	light grey	fine grained
52	Dolomite	Bertie	-	buff to light brown	aphanitic
53	Dolomite	Bertie	-	medium brown	aphanitic

Appendix A.1. Continued... Sample Location and Lithology

Flamboro Quarry					
County		**Township**	**Quarry**	**Lot & Location**	
-		W.Flamboro	16	Lot 6; west side of Brock Road	
No.	**Lithology**	**Formation**	**Member**	**Color**	**Matrix**
54	Dolomite	Lockport	-	Medium brown	aphanitic
55	Dolomite	Lockport	Eramosa	light to medium brown	aphanitic
56	Dolomite	Guelph	-	light grey	aphanitic
57	Dolomite	Guelph	-	light grey to buff	aphanitic

Halton Quarry					
County		**Township**	**Quarry**	**Lot & Location**	
Halton		Nassagaweya	17	Lot 8; 6 km west of Milton	
No.	**Lithology**	**Formation**	**Member**	**Color**	**Matrix**
60	Dolomite	Amable	middle silurian	light grey	fine crystalline
61	Dolomite	Reynales	lower silurian	medium grey	aphanitic

Uhthoff Quarry					
County		**Township**	**Quarry**	**Lot & Location**	
Simcoe		Orillia	18	Lot 10	
No.	**Lithology**	**Formation**	**Member**	**Color**	**Matrix**
62	Limestone	Gull River	Middle Ordovician	dark brown	lithographic

Gamebridge Quarry					
County		**Township**	**Quarry**	**Lot & Location**	
Ontario		Mara	19	Lot 11; 1 km northwest of Gamebridge	
No.	**Lithology**	**Formation**	**Member**	**Color**	**Matrix**
65	Limestone	Bobcaygeon		medium grey to buff	medium grained

Appendix A.1. Continued... Sample Location and Lithology

Kingston Quarry					
County		**Township**	**Quarry**	**Lot & Location**	
Frontenac		Kingston	21	Lot 9; west of Highway 38 - Highway 401 interchange	
No.	**Lithology**	**Formation**	**Member**	**Color**	**Matrix**
68	Limestone	Gull River		light grey	Aphanitic
70	Limestone	Gull River		medium brownish grey	fine crystalline to aphanitic

Pittsburg Quarry					
County		**Township**	**Quarry**	**Lot & Location**	
Frontenac		Pittsburg	24	3.5 km north of Barriefield	
No.	**Lithology**	**Formation**	**Member**	**Color**	**Matrix**
74	Limestone	Gull River	Middle Ordovician	light brownish grey	fine crystalline
75	Limestone	Gull River	Middle Ordovician	medium brownish grey	aphanitic

MacLanchlan (Beamsville) Quarry					
County		**Township**	**Quarry**	**Lot & Location**	
Lincoln		Clinton	25	Lot 20; 6.4 km south of town	
No.	**Lithology**	**Formation**	**Member**	**Color**	**Matrix**
76	Dolomite	Lockport	Erasoma	medium brown	fine crystalline
78	Dolomite	Lockport	Eramosa	brownish grey	aphanitic
79	Dolomite	Lockport	Eramosa	brownish grey	aphanitic

Port Dover Quarry					
County		**Township**	**Quarry**	**Lot & Location**	
Norfolk		Woodhouse	26	Lot 13; 3.2 km northeast of town	
No.	**Lithology**	**Formation**	**Member**	**Color**	**Matrix**
80	Limestone	Dundee		light brown	aphanitic
81	Limestone	Dundee		light brown grey	aphanitic

Appendix A.1. Continued... Sample Location and Lithology

Brockville Quarry					
County		**Township**	**Quarry**	**Lot & Location**	
Leeds		Elizabethtown	27	Lot 4; Eastern outskirts of the city Brockville	
No.	**Lithology**	**Formation**	**Member**	**Color**	**Matrix**
83	Limestone	Middle Black River	-	medium grey	fine crystalline
84	Dolomite	March or Oxford	-	light grey	aphanitic
85	Limestone	Middle Black River	-	medium brownish grey	fine crystalline

Cornwall Quarry					
County		**Township**	**Quarry**	**Lot & Location**	
Stormont		Cornwall	28	Lot 25; 6 km northwest of Cornwall	
No.	**Lithology**	**Formation**	**Member**	**Color**	**Matrix**
87	Limestone	Gull River		dark grey	aphanitic

Port Colborne Quarry					
County		**Township**	**Quarry**	**Lot & Location**	
Welland		Humberstone	29	Lots 24, 24; 2 km northeast of PortColborne	
No.	**Lithology**	**Formation**	**Member**	**Color**	**Matrix**
88	Dolomite	Bertie	Akron	medium brownish	aphanitic
91	Dolomite	Bertie	Arkon	dark brown to grey	aphanitic
92	Dolomite	Bertie	Arkon	medium grey	aphanitic

Queenston Quarry					
County		**Township**	**Quarry**	**Lot & Location**	
Lincoln		Niagara	30	Lots 47,48,49; 3 km west of Queenston	
No.	**Lithology**	**Formation**	**Member**	**Color**	**Matrix**
93	Dolomite	Decew	-	medium grey	aphanitic
94	Limestone	Lockport	Gasport	medium grey	medium crystalline
95	Dolomite	Lockport	Gasport	light grey	medium crystalline
96	Limestone	Irondequoit	-	light grey	medium to fine crystalline
97	Limestone	Irondequoit	-	light to medium grey	medium to fine crystalline

Appendix A.1. Continued... Sample Location and Lithology

Madam Area Quarry					
County		Township	Quarry	Lot & Location	
			31	4.8 km southeast of town	
No.	Lithology	Formation	Member	Color	Matrix
98	Marble			light greenish grey	aphanitic
99	Marble			white	aphanitic
100	Marble			dark grey	aphanitic

Kingston Quarries					
County		Township	Quarry	Lot & Location	
Frontenac		Storrington	32	Lot 11	
No.	Lithology	Formation	Member	Color	Matrix
101	Sandstone	Potsdam		greyish - pink to red	coarse to medium grained
102	Sandstone	Potsdam		grey pink	coarse to medium grained

Rice and McHarg Quarry					
County		Township	Quarry	Lot & Location	
Halton		Esquesing	33	Lot 21; 1 km south of town	
No.	Lithology	Formation	Member	Color	Matrix
103	Sandstone	Medina	Whirlpool	light grey	fine grained

Cooksville Quarry					
County		Township	Quarry	Lot & Location	
Peel		Toronto	35	Lots 19, 20	
No.	Lithology	Formation	Member	Color	Matrix
108	Shale	Billings		medium grey	Limy, medium bedded

road cut, flesh blast					
County		Township	Quarry	Lot & Location	
Peterborough		Burleigh	38	Highway 36, 1km west of highway 28 near Burleigh Falls	
No.	Lithology	Formation	Member	Color	Matrix
114	Granite			pink and black	coarse grained

Appendix A.1. Continued... Sample Location and Lithology

Nephton Quarry					
County		**Township**	**Quarry**	**Lot & Location**	
Peterborough		Methuel	39		
No.	**Lithology**	**Formation**	**Member**	**Color**	**Matrix**
115	Nepheline Syenite			white with black dots	phaneritic
117	Syenite			white with black dots	phaneritic

Thorold Quarry					
County		**Township**	**Quarry**	**Lot & Location**	
			42	Lots 30, 31; 4 km northwest of the town Stamford	
No.	**Lithology**	**Formation**	**Member**	**Color**	**Matrix**
120	Dolomite	Decew		medium to dark grey	fine crystalline
121	Dolomite	Decew		medium to dark grey	fine crystalline
122	Dolomite	Lockport	Gasport	pink grey	fine to coarse crystalline

Cayuga Quarry					
County		**Township**	**Quarry**	**Lot & Location**	
		North Cayuga	43	Lots 44-47; 5.5 km west of the village of Cayuga	
No.	**Lithology**	**Formation**	**Member**	**Color**	**Matrix**
124	Sandstone	Oriskany		light cream to white	medium to coarse grained
125	Dolomite	Bertie		grey to brown	fine crystalline

Ridgemount Quarry					
County		**Township**	**Quarry**	**Lot & Location**	
-		Bertie	44	Lots 5-8; 4 km southeast of Stevensville	
No.	**Lithology**	**Formation**	**Member**	**Color**	**Matrix**
126	Limestone	Bois Blanc	-	light grey	fine crystalline
128	Dolomite	Bertie	Scajaquanda	dark brown to dark grey	sub to fine crystalline
129	Dolomite	Bertie	Falkirk	light to dark brown	very fine to fine crystalline

Appendix A.1. Continued... Sample Location and Lithology

Pelee Island Quarry					
County		**Township**	**Quarry**	**Lot & Location**	
Essex		Pelee Island	45	Lots 1, 2; 150 m north of the north shore	
No.	**Lithology**	**Formation**	**Member**	**Color**	**Matrix**
130	Limestone	Dundee		brown	fine to medium crystalline
131	Limestone	Dundee		light brown	medium crystalline

6	Dolomite	Lockport	Gasport	light brown to buff	medium crystalline

1	Limestone	Lucas	Anderdon	buff to brown	aphanitic, fossiliferous

40	Limestone	Gull River	D	brownish grey	aphanitic

58	Dolomite	Amable		medium grey	fine crystalline

75.1	Limestone	Gull River	Middle Ordovician	medium brownish grey	aphanitic

90	Dolomite	Bertie	Arkon	dark grey	aphanitic

123	Shale	Rochester		black to dark grey	sub to fine crystalline

127	Dolomite	Bertie	Williamsville	light to medium brown	sub to fine crystalline

road cut					
County		**Township**	**Quarry**	**Lot & Location**	
Hastings		Marmora	40	Highway 7, 1.6 km west of Marmora	
No.	**Lithology**	**Formation**	**Member**	**Color**	**Matrix**
118	Hornblende Diorite			greenish black	phaneritic

Appendix B.1. Stress Test Results

No.	RT_RH_IN	RT_RH_FIN	RT_98RH	FRZ_65RH	RT_SAT	FRZ_SAT_A	FRZ_SAT_B	FRZ_SLTSOL	RT_SLTSOL
3	5730	5636	4350	5098	4619	4000	4455	3039	5625
4	6473	5866	5569	6376	3692	5480	3935	3612	4132
5	7800	8964	6588	9335	6792	9028	8364	5242	5344
8	7589	11559	7054	9934	6000	6598	4857	6775	5739
10	10111	7297	8064	9137	8105	8186	7499	6569	6778
15	6328	5508	5606	7355	4849	7216	6022	7211	5638
16	7569	8254	5396	7315	7397	11330	9477	6651	6601
17	4690	5982	4049	4464	5324	4689		2976	3006
18	7963	8203	7234	9637	4665	6962	6533	4195	5170
19	7298	11145	8031		7851	12164	9959	6422	7956
20	8024	8531	7154	7623	8099	7384	4774	7609	5585
21	9380	8796	6565	3003	6804	7400	7023	6055	7628
22	7589	7332	8201	8824	5366	9116	7648	6676	7042
23	6817	5231	6269	6360	3723	6178	5029	6474	5429
24	9153	8050	8523	8103	11866	9756	7043	9331	5288
26	8567	8623	7747	9253	6799	6108	6878	7311	6385
28	5367	5237	3951	5263	4314	4695	5194	2951	4503
32	8275	7754	4976	5403	6528	6265	7374	5323	6002
34	9768	8983	8970	11889	5841	8591	5906	7166	5420
37	8642	7347	7504	2039	6419	6928	8065	6066	5114
37	4379	3964	2745	4523	2713	3596	2691	2284	4312
39	7985	7833	7125	8706	8946	7817	6046	6129	7643
41	6496	6206	6349	7221	5535	4675	5085	4285	6403
42	5627	5250	4490	5815	4023	5464	5202	4137	4772
45	4695	7038	3292	4607	3255	4737	3280	4803	4205
46	6281	10408	5391	2753	1724	4890	5675	6872	5679
50	6184	4875	5637	7746	6958	8363	4846	4190	5414
51	2976	2864	1807	2918	1579	2263	1512	1726	1648
52	10566	11346	7578	9660	8231	9704	9899	6798	
53	7668	9607	6584	12555	10050	9063	7339	6128	7498
54	7503	7632	7343	8176	6017	6559	6764	6258	7212
55	6154	6795	6182	7018	6424	6903	4932	5736	4309
56	10606	8860	7827	8993	5783	9190	5831	6252	7036
57	9924	12481	9459	11517	5985	8480	6113	5811	6400
60	5831	5893	5811	5603	3829	6835	5260	3350	5238
61	7801	8236	5806	8313	7795	8690	4824	5945	4079
62	8028	7183	6266	8545	5661	6146	7662	4154	4781
65	4331	3891	5076	5621	2735	3820	3337	3869	4498
68	4841	7697	7514	5918	8465	5542	9601	3904	7548
70	7639	7713	7181	8757	6258	7780	8562	6585	6631
74	14779	14791	9376		11495		13696	7715	9968
75	8186	10059	9233	9779	8890	7537	9205	6417	7733
76	6916	8441	6990	4970	4621	7229	6453	6566	6270
78	5395	6366	5809	6143	4670	4961	2478	3886	3773
79	3697		4136	4765	3993	4860			
80	5895	7103	5209	6083	4651	4890	5362	3759	4530
81	5112	7070	4382	8548	5337	5848	5302	3688	6841

Appendix B.1. Continued... Stress Test Results

No.	RT_RH_INI	RT_RH_FIN	RT_98RH	FRZ_65RH	RT_SAT	FRZ_SAT_A	FRZ_SAT_B	FRZ_SLTSOL	RT_SLTSOL
83	7845	9916	7541	11129	7296	9411	6397	6007	8050
84	5265	5661	3638	6118	3679	4218	4661	2443	2759
85	3130	3976	2369	4829	2323	4041	3192	1722	2169
87	6693	8003	9514	9343	12394	7964	9062	6543	5498
88	13513	9908	9102	9742	9104		9195	6467	7645
91	9879	7857	7455	9672	6220	8338	5484	5789	6537
92	9140	8646	7927	9963	7695	7832	5095	5640	5103
93	6250	4007	4098	5830	2935	3083	2382	1664	2341
94	4926	4709	5192	6075	2453	3231	2188	2047	3366
95	5809	7510	4475	6853	7181	7552	8022	6370	6914
96	5283	5126	3679	4921	3049	4257	5191	5773	4673
97	4721	3989	3709	5129	3540	4345	3714	4073	3499
98	13315		11137		15501	1423	12414	13024	8456
99	3991	5106	4701	4533	4248	5429	4858	4368	6154
100	2207	1722	1990	1953	1793	2072	2480	2179	3090
101	7278	10299	6803	8263	6407	7763	8725	6066	8456
102	7615	6044	6467	8599	6752	8522	7152	7677	6883
103	3713	4950	2506	4436	2489	2392	2505	4251	4959
108	6696	6470	6502	8519	7447	7204	8938	5587	6736
114	4855	5602	5039	6083	5088	5360	5241	6026	4705
115	4957	7609	4143	5480	5318	7516	6187	5376	5877
117	5115	4896	5263	6779	6380	4356	5147	3619	5876
121	6912	6951	6141	6303	5029	8257	5872	4982	6848
122	6687	6902	5252	5216	4194	8138	6330	4893	5511
124	9335	11200	8452	10235	11730	10657	8013	7110	7064
125	6126		930		7543		6527	7232	5644
126	4098	3511	2786	5110	4796	2534	2256	2418	4055
128	11589	9453	8859	9928	6081	8747	7446	3937	5609
129	8678	8497	6721	7496	7337	8080	6281	5735	6766
130	6841	6196	4350	5613	4732	5117	4108	3520	3566
131	4675	4750	3921	3591	2373	3497	3250	2720	3161

Appendix B.2. Physical Properties Results

No.	50% Ads	98% Ads	Abs%	Full-Abs%	Un.W.(gr/cm³)	% Delta L
3	0.012	0.026	1.714	1.854	2.546	0.044
4	0.146	0.533	0.988	1.006	2.754	0.048
5	0.031	0.102	2.647	2.189	2.596	0.028
8	0.045	0.154	0.491	0.467	2.789	0.051
10	0.083	0.361	0.476	0.490	2.669	0.030
15	0.019	0.063	0.325	0.288	2.760	0.029
16	0.010	0.032	0.225	0.198	2.770	0.021
17	0.150	0.407	1.515	1.444	2.564	0.040
18	0.093	0.312	0.981	0.964	2.749	0.064
19	0.043	0.168	1.148	0.969	2.707	0.045
20	0.009	0.019	1.208	1.121	2.680	0.057
21	0.034	0.107	0.691	0.649	2.727	0.048
22	0.018	0.064	0.836	1.073	2.697	0.051
23	0.015	0.030	1.800	2.164	2.654	0.024
24	0.010	0.028	0.377	0.378	2.773	0.036
26	0.053	0.173	3.132	2.478	2.589	0.033
28	0.170	0.500	0.921	0.973	2.638	0.030
32	0.018	0.047	0.702	0.511	2.741	0.025
34	0.037	0.130	1.343	0.994	2.694	0.114
37	0.300	0.659	0.801	0.812	2.715	0.036
37	0.144	0.318	0.522	0.654	2.685	0.021
39	0.046	0.137	0.211	0.228	2.684	0.041
41	0.030	0.133	2.798	2.250	2.603	0.028
42	0.041	0.151	0.833	0.690	2.781	0.047
45	0.033	0.118	4.310	3.400	2.523	0.023
46	0.040	0.129	3.838	3.081	2.543	0.036
50	0.030	0.100	0.809	0.711	2.615	0.046
51	0.088	0.263	2.795	2.729	2.486	0.048
52	0.012	0.029	2.010	1.612	2.631	0.060
53	0.018	0.055	3.311	2.493	2.573	0.027
54	0.005	0.013	0.799	0.976	2.718	0.046
55	0.008	0.016	1.861	2.072	2.623	0.026
56	0.012	0.033	0.082	1.289	2.708	0.024
57	0.012	0.041	0.515	0.351	2.773	0.041
60	0.029	0.071	1.381	2.257	2.605	0.036
61	0.024	0.071	0.421	1.005	2.749	0.045
62	0.042	0.140	0.280	0.280	2.674	0.028
65	0.049	0.138	0.378	0.481	2.677	0.030
68	0.045	0.162	0.264	0.264	2.686	0.045
70	0.020	0.081	0.218	0.215	2.692	0.034
74	0.048	0.159	0.242	0.235	2.731	0.045
75	0.030	0.368	2.378	2.630	2.611	0.042
76	0.003	0.012	1.828	3.275	2.574	0.024
78	0.076	0.228	1.355	1.095	2.737	0.040
79	0.011	0.030	1.632	2.115	2.668	0.033
80	0.016	0.052	0.775	0.659	2.656	0.033
81	0.039	0.175	0.560	0.529	2.665	0.039

Appendix B.2. Continued... Physical Properties Results

No.	50% Ads	98% Ads	Abs%	Full-Abs%	Un. W.(gr/cm³)	% Delta L
83	0.051	0.170	0.260	0.280	2.693	0.035
84	0.099	0.389	2.027	1.806	2.652	0.034
85	0.091	0.328	1.751	0.979	2.667	0.100
87	0.013	0.052	0.140	0.154	2.688	0.029
88	0.045	0.145	0.490	0.470	2.779	0.032
91	0.053	0.153	1.918	1.735	2.726	0.030
92	0.025	0.076	1.590	1.229	2.709	0.053
93	0.216	0.705	2.495	2.196	2.624	0.039
94	0.193	0.603	1.916	1.665	2.678	0.026
95	0.015	0.044	1.732	3.540	2.553	0.034
96	0.050	0.167	1.500	1.591	2.637	0.043
97	0.035	0.103	0.883	0.764	2.628	0.012
98	0.012	0.051	0.166	0.171	3.073	0.034
99	0.002	0.005	0.172	0.162	2.795	0.046
100	0.005	0.009	0.243	0.245	2.674	0.076
101	0.014	0.033	0.934	0.701	2.533	0.058
102	0.017	0.047	2.973	3.774	2.385	0.063
103	0.091	0.261	5.462	6.411	2.233	0.038
108	0.135	0.489	0.853	0.840	2.647	0.048
114	0.026	0.043	0.322	0.273	2.603	0.032
115	0.006	0.010	0.129	0.111	2.608	0.044
117	0.007	0.012	0.129	0.110	2.607	0.065
121	0.100	0.340	2.194	1.735	2.622	0.039
122	0.051	0.145	1.197	1.097	2.725	0.057
124	0.012	0.022	1.952	2.468	2.447	0.027
125	0.015	0.064	1.100	0.828	2.724	0.051
126	0.117	0.394	2.168	2.067	2.560	0.046
128	0.113	0.403	1.288	1.247	2.708	0.051
129	0.018	0.059	3.280	2.624	2.566	0.052
130	0.015	0.038	2.048	1.582	2.587	0.016
131	0.018	0.044	5.362	5.403	2.397	0.014

Appendix B.3. Young's Modulus Results

No.	Y-RT_RH_FINAL	Y-RT_RH_INI	Y-RT_98RH	Y-FRZ_100RH	Y-RT_SATURATED
3	1.60E+10	1.71E+10	1.46E+10	1.34E+10	1.50E+10
4	1.94E+10	2.10E+10	1.54E+10	2.32E+10	1.38E+10
5	2.90E+10	2.60E+10	2.52E+10	3.22E+10	2.54E+10
8	3.89E+10	3.58E+10	2.23E+10	3.92E+10	2.61E+10
10	2.97E+10	3.30E+10	2.57E+10	2.90E+10	2.19E+10
15	3.53E+10	2.99E+10	2.39E+10	3.15E+10	3.31E+10
16	3.19E+10	2.80E+10	2.61E+10	3.14E+10	2.95E+10
17	1.67E+10	1.94E+10	1.81E+10	1.87E+10	1.64E+10
18	3.10E+10	2.71E+10	2.67E+10	4.11E+10	2.20E+10
19	3.08E+10	4.14E+10	3.68E+10	4.79E+10	3.28E+10
20	3.49E+10	3.34E+10	2.93E+10	3.11E+10	2.96E+10
21	3.62E+10	4.15E+10	3.67E+10	4.09E+10	2.99E+10
22	3.24E+10	2.97E+10	2.70E+10	3.36E+10	3.00E+10
23	1.65E+10	2.42E+10	2.33E+10	4.25E+10	1.61E+10
24	3.67E+10	3.51E+10	3.03E+10	3.71E+10	2.64E+10
26	2.49E+10	2.45E+10	2.53E+10	2.77E+10	2.36E+10
28	1.77E+10	1.57E+10	1.43E+10	2.05E+10	1.26E+10
32	1.90E+10	2.28E+10	3.42E+10	4.13E+10	1.51E+10
34	3.01E+10	2.91E+10	2.57E+10	2.96E+10	2.46E+10
37	2.70E+10	2.43E+10	2.23E+10	2.69E+10	1.92E+10
37	9.67E+09	1.33E+10	1.22E+10	1.26E+10	1.16E+10
39	2.99E+10	2.70E+10	2.69E+10	2.71E+10	2.37E+10
41	2.08E+10	2.20E+10	2.61E+10	2.25E+10	1.70E+10
42	2.35E+10	2.17E+10	2.14E+10	2.25E+10	2.16E+10
45	2.43E+10	2.85E+10	2.44E+10	2.17E+10	1.43E+10
46	3.14E+10	2.94E+10	2.75E+10	3.10E+10	2.25E+10
50	3.23E+10	3.22E+10	2.51E+10	2.81E+10	2.58E+10
51	1.23E+10	1.04E+10	1.02E+10	1.09E+10	1.11E+10
52	2.66E+10	2.15E+10	3.78E+10	4.11E+10	2.80E+10
53	3.06E+10	3.14E+10	2.72E+10	4.02E+10	2.82E+10
54	2.92E+10	3.70E+10	3.12E+10	3.76E+10	2.99E+10
55	2.66E+10	2.81E+10	2.70E+10	3.15E+10	2.77E+10
56	3.35E+10	3.02E+10	3.11E+10	3.58E+10	2.52E+10
57	3.42E+10	4.16E+10	3.41E+10	3.55E+10	4.05E+10
60	2.65E+10	2.35E+10	2.23E+10	2.34E+10	2.34E+10
61	2.56E+10	3.04E+10	2.94E+10	2.70E+10	2.97E+10
62	2.73E+10	2.52E+10	2.36E+10	2.95E+10	2.31E+10
65	1.56E+10	1.45E+10	1.56E+10	1.40E+10	1.30E+10
68	2.24E+10	2.17E+10	2.01E+10	1.78E+10	2.38E+10
70	2.43E+10	2.81E+10	2.58E+10	3.11E+10	2.57E+10
74	4.02E+10	3.85E+10	3.17E+10	3.50E+10	3.27E+10
75	3.33E+10	2.66E+10	2.70E+10	2.52E+10	2.72E+10
76	2.90E+10	2.90E+10	3.18E+10	2.81E+10	2.56E+10
78	2.41E+10	1.96E+10	2.34E+10	2.29E+10	2.24E+10
79	2.09E+10	2.03E+10	2.51E+10	1.89E+10	1.42E+10
80	1.83E+10	1.97E+10	1.89E+10	1.71E+10	1.40E+10
81	2.35E+10	2.27E+10	2.18E+10	2.63E+10	1.49E+10

Appendix B.3. Continued... Young's Modulus Results

No.	Y-RT_RH_FINAL	Y-RT_RH_INI	Y-RT_98RH	Y-FRZ_100RH	Y-RT_SATURATED
83	3.05E+10	3.37E+10	2.63E+10	3.04E+10	2.56E+10
84	1.61E+10	1.48E+10	1.36E+10	1.59E+10	1.52E+10
85	1.78E+10	2.16E+10	1.43E+10	1.40E+10	1.38E+10
87	4.28E+10	3.27E+10	3.07E+10	3.07E+10	3.48E+10
88	3.95E+10	4.17E+10	3.59E+10	3.51E+10	2.99E+10
91	2.53E+10	3.25E+10	2.54E+10	3.40E+10	2.29E+10
92	3.17E+10	3.05E+10	2.78E+10	4.08E+10	2.96E+10
93	1.44E+10	1.56E+10	1.26E+10	1.29E+10	1.09E+10
94	1.68E+10	1.57E+10	1.25E+10	1.64E+10	1.20E+10
95	2.65E+10	2.35E+10	2.45E+10	2.42E+10	2.62E+10
96	2.23E+10	1.94E+10	1.89E+10	2.00E+10	1.96E+10
97	1.85E+10	1.59E+10	1.89E+10	1.48E+10	1.72E+10
98	5.33E+10	5.14E+10	3.62E+10	5.00E+10	4.04E+10
99	2.99E+10	3.09E+10	2.93E+10	2.96E+10	3.49E+10
100	1.66E+10	7.49E+09	7.90E+09	7.56E+09	1.02E+10
101	1.75E+10	1.85E+10	1.49E+10	1.48E+10	1.41E+10
102	1.51E+10	1.29E+10	1.14E+10	1.30E+10	1.14E+10
103	1.14E+10	1.00E+10	9.93E+09	9.32E+09	1.05E+10
108	2.06E+10	2.10E+10	2.30E+10	2.40E+10	1.88E+10
114	2.22E+10	2.19E+10	2.26E+10	2.44E+10	2.31E+10
115	2.78E+10	2.29E+10	1.86E+10	2.47E+10	2.39E+10
117	2.46E+10	2.63E+10	2.49E+10	3.40E+10	3.38E+10
121	2.35E+10	2.11E+10	1.96E+10	2.24E+10	2.46E+10
122	2.34E+10	1.56E+10	1.24E+10	2.30E+10	2.86E+10
124	1.79E+10	1.57E+10	1.66E+10	1.46E+10	1.54E+10
125	3.40E+10	5.41E+10	3.41E+10	5.08E+10	3.34E+10
126	1.45E+10	1.41E+10	1.23E+10	1.14E+10	1.66E+10
128	2.94E+10	3.21E+10	2.59E+10	3.39E+10	2.20E+10
129	2.82E+10	2.11E+10	2.24E+10	2.26E+10	2.06E+10
130	1.95E+10	2.08E+10	1.61E+10	1.82E+10	1.74E+10
131	1.37E+10	1.25E+10	1.20E+10	1.15E+10	1.13E+10

Appendix B.3. Continued... Young's Modulus Results

No.	Y-FRZ_SAT_A	Y-FRZ_SAT_B	Y-FRZ_SALTSOL	Y-RT_SALTSOL
3	1.18E+10	1.24E+10	1.30E+10	1.39E+10
4	1.81E+10	1.71E+10	1.43E+10	1.70E+10
5	2.52E+10	2.47E+10	2.61E+10	2.03E+10
8	3.24E+10	2.42E+10	2.94E+10	2.48E+10
10	2.40E+10	2.36E+10	2.29E+10	2.25E+10
15	2.26E+10	2.89E+10	3.65E+10	3.39E+10
16	3.63E+10	3.06E+10	3.72E+10	3.62E+10
17	1.97E+10	1.97E+10	1.53E+10	1.61E+10
18	2.33E+10	2.33E+10	2.16E+10	1.71E+10
19	3.61E+10	3.45E+10	2.83E+10	3.17E+10
20	2.68E+10	3.01E+10	3.53E+10	3.35E+10
21	3.44E+10	3.11E+10	3.36E+10	2.10E+10
22	3.49E+10	3.03E+10	3.31E+10	3.12E+10
23	2.42E+10	1.57E+10	2.15E+10	2.20E+10
24	2.39E+10	2.11E+10	3.03E+10	3.97E+10
26	2.39E+10	2.19E+10	3.77E+10	2.43E+10
28	1.57E+10	1.41E+10	1.36E+10	1.17E+10
32	1.52E+10	1.57E+10	1.35E+10	3.44E+10
34	2.28E+10	2.58E+10	2.89E+10	2.63E+10
37	2.25E+10	2.05E+10	2.25E+10	1.39E+10
37	1.29E+10	1.14E+10	8.70E+09	1.19E+10
39	2.47E+10	1.95E+10	2.55E+10	2.62E+10
41	2.05E+10	1.71E+10	2.36E+10	2.10E+10
42	2.03E+10	2.01E+10	3.12E+10	2.15E+10
45	1.72E+10	1.96E+10	2.60E+10	1.69E+10
46	2.73E+10	2.13E+10	2.97E+10	2.12E+10
50	2.82E+10	2.57E+10	1.96E+10	2.42E+10
51	1.04E+10	1.05E+10	1.11E+10	1.07E+10
52	3.79E+10	2.57E+10	2.15E+10	3.31E+10
53	2.62E+10	2.52E+10	2.58E+10	2.68E+10
54	2.53E+10	2.93E+10	5.08E+10	2.73E+10
55	2.64E+10	2.50E+10	3.52E+10	1.80E+10
56	2.38E+10	2.84E+10	2.26E+10	3.42E+10
57	2.65E+10	3.46E+10	2.99E+10	5.45E+10
60	3.11E+10	2.03E+10	2.55E+10	2.21E+10
61	3.36E+10	3.23E+10	3.45E+10	2.31E+10
62	2.21E+10	2.49E+10	2.08E+10	2.40E+10
65	1.14E+10	1.07E+10	1.59E+10	1.24E+10
68	2.37E+10	1.77E+10	1.82E+10	1.70E+10
70	2.59E+10	1.67E+10	2.99E+10	2.04E+10
74	3.23E+10	3.28E+10	3.27E+10	3.25E+10
75	1.54E+10	2.24E+10	3.51E+10	2.00E+10
76	2.88E+10	3.20E+10	2.98E+10	3.50E+10
78	2.36E+10	2.26E+10	2.48E+10	2.00E+10
79	1.90E+10	2.40E+10	2.02E+10	3.19E+10
80	1.94E+10	1.42E+10	1.30E+10	1.87E+10
81	2.24E+10	1.51E+10	1.82E+10	1.83E+10

Appendix B.3. Continued... Young's Modulus Results

No.	Y-FRZ_SAT_A	Y-FRZ_SAT_B	Y-FRZ_SALTSOL	Y-RT_SALTSOL
83	2.48E+10	2.55E+10	2.31E+10	2.65E+10
84	1.28E+10	1.43E+10	1.47E+10	1.44E+10
85	1.45E+10	2.11E+10	1.15E+10	1.05E+10
87	3.37E+10	3.12E+10	2.79E+10	2.69E+10
88	3.84E+10	2.96E+10	3.15E+10	3.17E+10
91	2.47E+10	2.32E+10	2.19E+10	1.75E+10
92	3.60E+10	3.43E+10	3.00E+10	2.56E+10
93	1.22E+10	1.14E+10	1.21E+10	1.17E+10
94	1.49E+10	1.23E+10	1.45E+10	1.31E+10
95	2.68E+10	2.38E+10	3.45E+10	2.47E+10
96	2.03E+10	2.07E+10	2.67E+10	1.97E+10
97	1.58E+10	1.57E+10	2.02E+10	1.58E+10
98	3.71E+10	4.31E+10	4.02E+10	4.13E+10
99	3.02E+10	2.52E+10	2.54E+10	3.15E+10
100	1.11E+10	1.04E+10	1.54E+10	1.47E+10
101	1.36E+10	1.32E+10	2.13E+10	1.97E+10
102	1.31E+10	1.38E+10	1.33E+10	1.22E+10
103	1.03E+10	1.00E+10	1.14E+10	1.07E+10
108	2.30E+10	2.24E+10	2.21E+10	2.07E+10
114	2.55E+10	2.08E+10	1.80E+10	2.13E+10
115	2.66E+10	2.34E+10	2.51E+10	2.30E+10
117	3.21E+10	2.91E+10	3.05E+10	3.00E+10
121	2.67E+10	2.31E+10	2.52E+10	2.21E+10
122	2.38E+10	2.67E+10	2.80E+10	2.09E+10
124	1.67E+10	1.53E+10	2.04E+10	1.42E+10
125	4.60E+10	2.95E+10	3.72E+10	2.78E+10
126	2.30E+10	1.32E+10	1.46E+10	1.18E+10
128	2.88E+10	2.44E+10	2.34E+10	2.21E+10
129	2.30E+10	1.97E+10	2.59E+10	2.25E+10
130	2.00E+10	1.77E+10	2.02E+10	1.94E+10
131	1.28E+10	1.29E+10	1.25E+10	1.43E+10

Appendix A.1. Basic statistic summary of the test results

Test	N of cases	Minimum	Maximum	Mean	Standard Dev.	Units
RT_RH_INI	78	2206.6	14779.0	6997.0	2391.8	KPa
RT_RH_FINAL	75	1722.4	14791.0	7244.9	2374.5	KPa
RT_98RH	78	930.0	11137.3	5988.0	2075.7	KPa
FRZ_65RH	74	1953.1	12555.0	7019.0	2382.3	KPa
RT_SATURATED	78	1579.0	15500.7	5945.9	2628.7	KPa
FRZ_SAT_A	75	1422.7	12164.0	6470.0	2299.5	KPa
FRZ_SAT_B	76	1512.0	13696.0	6069.8	2362.2	KPa
FRZ_SALTSOL	77	1664.0	13023.8	5248.8	1935.8	KPa
RT_SALTSOL	76	1648.0	9968.0	5615.5	1628.2	KPa
ADSORPTION50	78	0.002	0.300	0.050	0.055	% of dry w
ADSORPTION98	78	0.005	0.705	0.161	0.165	% of dry w
ABSORPTION	78	0.082	5.462	1.377	1.174	% of dry w
FULL_ABSORP	78	0.110	6.411	1.370	1.195	% of dry w
UNIT_WEIGHT	78	2.233	3.073	2.654	0.110	g/cm^3
DELTA_L	78	0.012	0.114	0.041	0.017	% of L
Y_RT_RH_FINL	78	9.7E-09	5.3E+10	2.6E+10	8.1E+09	N/m^2
Y_RT_RH_INI	78	7.5E-09	5.4E+10	2.5E+10	9.1E+09	N/m^2
Y_RT_98RH	78	7.9E-09	3.8E+10	2.3E+10	7.3E+09	N/m^2
Y_FRZ_65RH	78	7.6E-09	5.1E+10	2.7E+10	1.0E+10	N/m^2
Y_RT_SATURTD	78	1.0E-10	4.1E+10	2.2E+10	7.5E+09	N/m^2
Y_FRZ_SAT_A	78	1.0E-10	4.6E+10	2.4E+10	7.8E+09	N/m^2
Y_FRZ_SAT_B	78	1.0E-10	4.3E+10	2.2E+10	7.1E+09	N/m^2
Y_FRZ_SALTSO	78	8.7E-09	5.1E+10	2.4E+10	8.4E+09	N/m^2
Y_RT_SALTSOL	78	1.1E-10	5.5E+10	2.2E+10	8.3E+09	N/m^2

Appendix B.1 Correlation coefficients between Stress and Young's Modulus results, and the entire data set
78 cases and 50 variables processed and saved.
Pearson correlation matrix
(** 99% significant difference of means, * 95% significant difference of means)

	RT_RH_INI	RT_RH_FINAL	RT_98RH	FRZ_100RH	RT_SATURATED	FRZ_SAT_A	FRZ_SAT_B	FRZ_SALTSOL	RT_SALTSOL
ADSORPTION50	-0.062	-0.254	-0.143	-0.239	-0.261	-0.300	-0.207	-0.393	-0.350
ADSORPTION98	-0.053	-0.228	-0.113	-0.140	-0.239	-0.300	-0.182	-0.419	-0.318
ABSORPTION	-0.166	-0.083	-0.272	-0.186	-0.285	-0.301	-0.311	-0.152	-0.218
FULL_ABSORP	-0.150	-0.086	-0.243	-0.193	-0.251	-0.238	-0.253	-0.079	-0.141
UNIT_WEIGHT	0.306	0.184	0.339	0.215	0.164	0.290	0.189	0.137	0.075
DELTA 1.	-0.029	-0.036	0.020	0.090	-0.076	-0.017	-0.069	-0.062	-0.036
ADS_98_RIGBY	-0.170	-0.302	-0.132	-0.113	-0.240	-0.266	-0.190	-0.342	-0.264
SUSPENSION	0.069	-0.042	0.106	0.081	0.162	-0.078	0.142	-0.165	0.009
Y_RT_RH_FINL	0.562**	0.631**	0.667**	0.473*	0.560**	0.657**	0.502**	0.629**	0.480*
Y_RT_RH_INI	0.631**	0.646**	0.661**	0.503**	0.498**	0.618**	0.434	0.591**	0.490**
Y_RT_98RH	0.608**	0.607**	0.643**	0.423	0.525**	0.586**	0.500**	0.614**	0.526**
Y_FRZ_100RH	0.636**	0.574**	0.610**	0.488*	0.436	0.593**	0.457	0.576**	0.462*
Y_RT_SATURTD	0.424	0.508**	0.573**	0.435	0.501**	0.591**	0.462*	0.539**	0.462*
Y_FRZ_SAT_A	0.416	0.460*	0.495**	0.338	0.444	0.586**	0.416	0.474*	0.418
Y_FRZ_SAT_B	0.508**	0.527**	0.556**	0.428	0.436	0.634**	0.419	0.524**	0.382
Y_FRZ_SALTSO	0.414	0.495**	0.499**	0.337	0.406	0.525**	0.446	0.651**	0.461*
Y_RT_SALTSOL	0.479*	0.516**	0.518**	0.418	0.412	0.562**	0.391	0.568**	0.445
RDEN	0.285	0.194	0.335	0.202	0.158	0.271	0.207	0.125	0.065
RADS	-0.109	-0.260	-0.208	-0.218	-0.331	-0.337	-0.255	-0.463*	-0.423
RPORO	-0.149	-0.076	-0.269	-0.202	-0.267	-0.237	-0.288	-0.084	-0.153
RCAP32S	-0.305	-0.215	-0.380	-0.289	-0.302	-0.381	-0.365	-0.194	-0.226
RADSB	0.057	-0.027	0.147	0.026	0.105	-0.008	0.199	-0.122	0.017
DRYLOSS	-0.053	-0.065	-0.028	-0.006	-0.076	-0.125	-0.072	-0.112	0.002
RVABGNV	-0.032	-0.009	-0.135	-0.031	-0.057	-0.054	-0.160	-0.052	0.099
RCAP32B	-0.363	-0.259	-0.381	-0.282	-0.177	-0.297	-0.283	-0.126	-0.116
RSATBIF	-0.145	-0.156	-0.270	-0.098	-0.308	-0.293	-0.257	-0.388	-0.262
RBUV	-0.157	-0.103	-0.232	-0.052	-0.250	-0.209	-0.287	-0.137	-0.311
RABS	-0.163	-0.097	-0.297	-0.220	-0.333	-0.310	-0.344	-0.169	-0.258
RBUS	-0.160	-0.062	-0.281	-0.199	-0.294	-0.268	-0.317	-0.105	-0.202
RBUB	-0.081	0.009	-0.151	-0.040	-0.114	-0.014	-0.210	0.102	-0.058

Appendix B.1. Continued... (Correlation coefficients between Stress, and Young's Modulus results, and the entire data set)

	Y_RT_RH_FIN	Y_RT_RH_INI	Y_RT_98RH	Y_FRZ_100RH	Y_RT_STRTD	Y_FRZ_SAT_A	Y_FRZ_SAT_B	Y_FRZ_SALTSO	Y_RT_SALTSOL
ADSORPTION50	-0.300	-0.285	-0.364	-0.249	-0.399	-0.282	-0.315	-0.390	-0.467*
ADSORPTION98	-0.281	-0.270	-0.355	-0.259	-0.394	-0.314	-0.315	-0.376	-0.470*
ABSORPTION	-0.382	-0.354	-0.328	-0.338	-0.415	-0.383	-0.348	-0.210	-0.396
FULL_ABSORP	-0.378	-0.368	-0.306	-0.345	-0.386	-0.348	-0.313	-0.181	-0.351
UNIT_WEIGHT	0.522**	0.539**	0.489*	0.559**	0.497**	0.460*	0.480*	0.370	0.468*
DELTA_L	0.039	0.001	-0.127	-0.052	0.036	-0.000	0.102	0.006	-0.068
ADS_98_RIGBY	-0.304	-0.284	-0.307	-0.290	-0.330	-0.324	-0.317	-0.341	-0.375
RDEN	0.532**	0.531**	0.476*	0.546**	0.488*	0.438	0.460*	0.376	0.451
RADS	-0.316	-0.294	-0.381	-0.275	-0.420	-0.329	-0.314	-0.395	-0.476*
RPORO	-0.371	-0.337	-0.286	-0.319	-0.377	-0.313	-0.294	-0.167	-0.320
RCAP32S	-0.432	-0.403	-0.385	-0.423	-0.395	-0.389	-0.374	-0.299	-0.318
RADSB	0.087	0.060	-0.027	-0.003	-0.031	-0.008	-0.031	-0.167	-0.152
DRYLOSS	-0.126	-0.060	0.011	-0.096	-0.144	-0.118	-0.089	-0.058	-0.073
RVABGNV	-0.087	-0.051	-0.021	-0.056	-0.058	-0.081	-0.113	-0.015	0.042
RCAP32B	-0.348	-0.290	-0.265	-0.304	-0.141	-0.159	-0.185	-0.081	-0.109
RSATBIF	-0.235	-0.170	-0.277	-0.137	-0.309	-0.252	-0.291	-0.333	-0.273
RBUV	-0.173	-0.191	-0.168	-0.095	-0.186	-0.196	-0.186	-0.111	-0.122
RABS	-0.386	-0.346	-0.328	-0.324	-0.437	-0.382	-0.351	-0.239	-0.383
RBUS	-0.347	-0.311	-0.277	-0.290	-0.378	-0.335	-0.310	-0.184	-0.314
RBUB	-0.081	-0.074	0.031	0.001	0.046	0.020	0.033	0.157	0.168

Appendix B.2. Number of cases included into the correlation test

	RT_RH_INI	RT_RH_FINAL	RT_98RH	FRZ_100RH	RT_SATURATED	FRZ_SAT_A	FRZ_SAT_B	FRZ_SALTSOL	RT_SALTSOL
ADSORPTION50	78	75	78	74	78	75	76	77	76
ADSORPTION98	78	75	78	74	78	75	76	77	76
ABSORPTION	78	75	78	74	78	75	76	77	76
FULL_ABSORP	78	75	78	74	78	75	76	77	76
UNIT_WEIGHT	78	75	78	74	78	75	76	77	76
DELTA_L	78	75	78	74	78	75	76	77	76
ADS_98_RIGBY	77	74	77	73	77	74	75	76	75
SUSPENSION	77	74	77	73	77	74	75	76	75
Y_RT_RH_FINL	78	75	78	74	78	75	76	77	76
Y_RT_RH_INI	78	75	78	74	78	75	76	77	76
Y_RT_98RH	78	75	78	74	78	75	76	77	76
Y_FRZ_100RH	78	75	78	74	78	75	76	77	76
Y_RT_SATURTD	78	75	78	74	78	75	76	77	76
Y_FRZ_SAT_A	78	75	78	74	78	75	76	77	76
Y_FRZ_SAT_B	78	75	78	74	78	75	76	77	76
Y_FRZ_SALTSO	78	75	78	74	78	75	76	77	76
Y_RT_SALTSOL	78	75	78	74	78	75	76	77	76
RDEN	78	75	78	74	78	75	76	77	76
RADS	78	75	78	74	78	75	76	77	76
RPORO	78	75	78	74	78	75	76	77	76
RCAP32S	78	75	78	74	78	75	76	77	76
RADSB	78	75	78	74	78	75	76	77	76
DRYLOSS	78	75	78	74	78	75	76	77	76
RVABGNV	78	75	78	74	78	75	76	77	76
RCAP32B	78	75	78	74	78	75	76	77	76
RSATBIF	78	75	78	74	78	75	76	77	76
RBUV	78	75	78	74	78	75	76	77	76
RABS	78	75	78	74	78	75	76	77	76
RBUS	78	75	78	74	78	75	76	77	76
RBUB	78	75	78	74	78	75	76	77	76

Appendix B.2. Continued... (Number of cases included into the correlation test)

	Y_RT_RH_FINL	Y_RT_RH_INI	Y_RT_98RH	Y_FRZ_100RH	Y_RT_SATURTD	Y_FRZ_SAT_A	Y_FRZ_SAT_B	Y_FRZ_SALTSO	Y_RT_S
ADSORPTION50	78	78	78	78	78	78	78	78	
ADSORPTION98	78	78	78	78	78	78	78	78	
ABSORPTION	78	78	78	78	78	78	78	78	
FULL_ABSORP	78	78	78	78	78	78	78	78	
UNIT_WEIGHT	78	78	78	78	78	78	78	78	
DELTA_L	78	78	78	78	78	78	78	78	
ADS_98_RIGBY	77	77	77	77	77	77	77	77	
RDEN	78	78	78	78	78	78	78	78	
RADS	78	78	78	78	78	78	78	78	
RPORO	78	78	78	78	78	78	78	78	
RCAP32S	78	78	78	78	78	78	78	78	
RADSB	78	78	78	78	78	78	78	78	
DRYLOSS	78	78	78	78	78	78	78	78	
RVABGNV	78	78	78	78	78	78	78	78	
RCAP32B	78	78	78	78	78	78	78	78	
RSATBIF	78	78	78	78	78	78	78	78	
RBUV	78	78	78	78	78	78	78	78	
RABS	78	78	78	78	78	78	78	78	
RBUS	78	78	78	78	78	78	78	78	
RBUB	78	78	78	78	78	78	78	78	

Appendix D.3. Highly significant to significant correlations between stress results and other variables

Variables			Positive (+) or Negative (−) Relationship	Significance of R
RT_RH_INI	vs	Y-RT_RH_FINAL	+	1%
RT_RH_INI	vs	Y-RT_RH_INI	+	1%
RT_RH_INI	vs	Y-RT_98RH	+	1%
RT_RH_INI	vs	Y-FRZ_65RH	+	1%
RT_RH_INI	vs	Y-FRZ_SAT_B	+	1%
RT_RH_INI	vs	Y-RT_SALTSOL	+	5%
RT_RH_FINAL	vs	Y-RT_RH_FINAL	+	1%
RT_RH_FINAL	vs	Y-RT_RH_INI	+	1%
RT_RH_FINAL	vs	Y-RT_98RH	+	1%
RT_RH_FINAL	vs	Y-FRZ_65RH	+	1%
RT_RH_FINAL	vs	Y-RT_SATURATED	+	1%
RT_RH_FINAL	vs	Y-FRZ_SAT_A	+	5%
RT_RH_FINAL	vs	Y-FRZ_SAT_B	+	1%
RT_RH_FINAL	vs	Y-FRZ_SALTSOL	+	1%
RT_RH_FINAL	vs	Y-RT_SALTSOL	+	1%
RT_98RH	vs	Y-RT_RH_FINAL	+	1%
RT_98RH	vs	Y-RT_RH_INI	+	1%
RT_98RH	vs	Y-RT_98RH	+	1%
RT_98RH	vs	Y-FRZ_65RH	+	1%
RT_98RH	vs	Y-RT_SATURATED	+	1%
RT_98RH	vs	Y-FRZ_SAT_A	+	1%
RT_98RH	vs	Y-FRZ_SAT_B	+	1%
RT_98RH	vs	Y-FRZ_SALTSOL	+	1%
RT_98RH	vs	Y-RT_SALTSOL	+	1%

Appendix D.3. Continued... (Highly significant to significant correlations between stress results and other variables)

Variables			Positive (+) or Negative (–) Relationship	Significance of R
FRZ_65RH	vs	Y-RT_RH_FINAL	+	5%
FRZ_65RH	vs	Y-RT_RH_INI	+	1%
FRZ_65RH	vs	Y-FRZ_65RH	+	5%
RT_SATURATED	vs	Y-RT_RH_FINAL	+	1%
RT_SATURATED	vs	Y-RT_RH_INI	+	1%
RT_SATURATED	vs	Y-RT_98RH	+	1%
RT_SATURATED	vs	Y-RT_SATURATED	+	1%
FRZ_SAT_A	vs	Y-RT_RH_FINAL	+	1%
FRZ_SAT_A	vs	Y-RT_RH_INI	+	1%
FRZ_SAT_A	vs	Y-RT_98RH	+	1%
FRZ_SAT_A	vs	Y-FRZ_65RH	+	1%
FRZ_SAT_A	vs	Y-RT_SATURATED	+	1%
FRZ_SAT_A	vs	Y-FRZ_SAT_A	+	1%
FRZ_SAT_A	vs	Y-FRZ_SAT_B	+	1%
FRZ_SAT_A	vs	Y-FRZ_SALTSOL	+	1%
FRZ_SAT_A	vs	Y-RT_SALTSOL	+	1%
FRZ_SAT_B	vs	Y-RT_RH_FINAL	+	1%
FRZ_SAT_B	vs	Y-RT_98RH	+	1%
FRZ_SAT_B	vs	Y-RT_SATURATED	+	5%
FRZ_SALTSOL	vs	Y-RT_RH_FINAL	+	1%
FRZ_SALTSOL	vs	Y-RT_RH_INI	+	1%
FRZ_SALTSOL	vs	Y-RT_98RH	+	1%
FRZ_SALTSOL	vs	Y-FRZ_65RH	+	1%
FRZ_SALTSOL	vs	Y-RT_SATURATED	+	1%
FRZ_SALTSOL	vs	Y-FRZ_SAT_A	+	5%
FRZ_SALTSOL	vs	Y-FRZ_SAT_B	+	1%
FRZ_SALTSOL	vs	Y-FRZ_SALTSOL	+	1%
FRZ_SALTSOL	vs	Y-RT_SALTSOL	+	1%
FRZ_SALTSOL	vs	RADS	+	5%
RT_SALTSOL	vs	Y-RT_RH_FINAL	+	5%
RT_SALTSOL	vs	Y-RT_RH_INI	+	1%
RT_SALTSOL	vs	Y-RT_98RH	+	1%
RT_SALTSOL	vs	Y-FRZ_65RH	+	5%
RT_SALTSOL	vs	Y-RT_SATURATED	+	5%
RT_SALTSOL	vs	Y-FRZ_SALTSOL	+	5%

Appendix E.1. Two sample t-test grouped by rock type (dolomite and limestone)

Test	Rock Type	N.	Mean	St. Dev.	t	df	Prob.
Stress to fixed strain at Room Temp. – Room Humidity (Initial Test)	Dolomite	43	7559.884	2016.690	2.216	65	0.030
	Limestone	24	6317.208	2501.704			
Stress to fixed strain at Room Temp. – Room Humidity (Final Test)	Dolomite	41	7875.707	1991.285	2.361	63	0.021
	Limestone	24	6523.500	2588.653			
Stress to fixed strain at 48hrs Freezing – 24hrs Saturation (A)	Dolomite	41	7178.927	2072.914	3.013	62	0.004
	Limestone	23	5574.870	1989.730			
Stress to fixed strain at 48hrs Freez. – 48hrs Sat. in 20% Salt-Water	Dolomite	42	5590.881	1624.608	2.968	64	0.004
	Limestone	24	4335.792	1701.558			
UNIT_WEIGHT	Dolomite	43	2.679	0.074	2.347	65	0.022
	Limestone	24	2.634	0.080			
ACID_INSOLUB	Dolomite	42	12.199	10.078	-2.009	64	0.049
	Limestone	24	18.706	16.278			
ADS_98_RIGBY	Dolomite	42	0.106	0.101	-2.427	64	0.018
	Limestone	24	0.211	0.248			
SUSPENSION	Dolomite	42	2.552	1.127	-2.801	64	0.007
	Limestone	24	3.463	1.490			
ABSORP20_SAT	Dolomite	37	1.190	0.743	2.859	56	0.006
	Limestone	21	0.632	0.657			
VAC_SAT	Dolomite	37	1.862	1.090	4.131	56	0.000
	Limestone	21	0.739	0.793			
PLUS4_SAT	Dolomite	37	1.087	0.673	2.836	56	0.006
	Limestone	21	0.574	0.642			
ULT_STRNGT	Dolomite	24	14.529	3.330	3.335	33	0.002
	Limestone	11	10.155	4.162			

Test	Rock Type	N.	Mean	St. Dev.	t	df	Prob.
Young's Modulus at Room Temp. – Room Hum. (Final Test)	Dolomite	43	2.744E+10	6.726E+09	2.230	65	0.029
	Limestone	24	2.327E+10	8.309E+09			
Young's Modulus at Room Temp. – Room Hum. (Initial Test)	Dolomite	43	2.787E+10	8.473E+09	2.522	65	0.014
	Limestone	24	2.264E+10	7.504E+09			
Young's Modulus at Room Temperature – 98% Humidity	Dolomite	43	2.590E+10	6.617E+09	3.477	65	0.001
	Limestone	24	2.018E+10	6.150E+09			
Young's Modulus after 48hrs Freezing – 65% Humidity	Dolomite	43	3.066E+10	9.183E+09	4.143	65	0.000
	Limestone	24	2.158E+10	7.423E+09			
Young's Modulus at Room Temperature – 24hrs Saturation	Dolomite	43	2.422E+10	6.650E+09	2.713	65	0.009
	Limestone	24	1.962E+10	6.681E+09			
Young's Modulus after 48hrs Freezing – 24hrs Saturation (A)	Dolomite	43	2.602E+10	7.471E+09	3.113	65	0.003
	Limestone	24	2.041E+10	6.290E+09			
Young's Modulus after 48hrs Freezing – 24hrs Saturation (B)	Dolomite	43	2.417E+10	6.210E+09	3.327	65	0.001
	Limestone	24	1.896E+10	6.053E+09			
Young's Mod. after 48hrs Freez.–48hrs Sat.(20% Salt-Water)	Dolomite	43	2.731E+10	7.994E+09	3.856	65	0.000
	Limestone	24	1.982E+10	6.901E+09			
Young's Mod. at Room Temp –48hrs Sat.(20%Salt-Water)	Dolomite	43	2.518E+10	8.479E+09	3.287	65	0.002
	Limestone	24	1.877E+10	5.842E+09			
RADSB	Dolomite	43	16.368	16.585	-3.377	65	0.001
	Limestone	24	31.974	20.673			
MQBUBU	Dolomite	40	191.497	256.593	-2.103	61	0.040
	Limestone	23	366.120	403.037			
RBUB	Dolomite	43	84.239	17.050	3.819	65	0.000
	Limestone	24	64.049	26.194			

Appendix E.2. Two sample t-test grouped by rock type (crystalline and detrital)

Test	Rock Type	N.	Mean	St. Dev.	t	df	Prob.
Stress to fixed strain at 48hrs Freezing – 65% Humidity	Crystalline	5	4965.610	1875.087	-2.390	8	0.044
	Detrital	5	8010.357	2144.405			
ABSORPTION	Crystalline	6	0.193	0.075	-2.919	9	0.017
	Detrital	5	2.435	1.900			
FULL_ABSORP	Crystalline	6	0.178	0.068	-2.787	9	0.021
	Detrital	5	2.839	2.363			
UNIT_WEIGHT	Crystalline	6	2.726	0.185	2.651	9	0.026
	Detrital	5	2.449	0.156			
ABSORP20_SAT	Crystalline	6	0.139	0.057	-2.851	8	0.021
	Detrital	4	1.937	1.593			
VAC_SAT	Crystalline	6	0.183	0.089	-3.006	8	0.017
	Detrital	4	3.100	2.452			
NEG4_98H	Crystalline	6	0.010	0.010	-2.670	8	0.028
	Detrital	4	0.111	0.095			
PLUS4_98H	Crystalline	6	0.015	0.008	-2.458	8	0.039
	Detrital	4	0.147	0.135			
PLUS4_SAT	Crystalline	6	0.118	0.051	-3.005	8	0.017
	Detrital	4	1.704	1.333			
MGSO4	Crystalline	6	3.367	3.213	-3.675	8	0.006
	Detrital	4	67.250	43.776			
LOS_FRZ_THW1	Crystalline	6	1.541	0.783	-2.906	8	0.020
	Detrital	4	6.200	3.928			

Test	Rock Type	N.	Mean	St. Dev.	t	df	Prob.
LOS_FRZ_THW2	Crystalline	6	1.157	0.454	-7.509	8	0.000
	Detrital	4	22.727	7.243			
Young's Modulus at Room Temperature – 24hrs Saturation	Crystalline	6	2.773E+10	1.089E+10	2.681	9	0.025
	Detrital	5	1.406E+10	3.331E+09			
Young's Modulus after 48hrs Freezing – 24hrs Saturation (A)	Crystalline	6	2.710E+00	8.871E+09	2.636	9	0.027
	Detrital	5	1.535E+10	4.872E+09			
Young's Mod. at Room Temp.–48hrs Sat.(20%Salt-Water)	Crystalline	6	2.696E+10	9.335E+09	2.501	9	0.034
	Detrital	5	1.550E+10	4.449E+09			
RDEN	Crystalline	6	2.737	0.186	2.647	9	0.027
	Detrital	5	2.459	0.156			
RPORO	Crystalline	6	0.182	0.072	-2.970	9	0.016
	Detrital	5	2.950	2.307			
RFRTH	Crystalline	6	1.350	0.477	-6.710	8	0.000
	Detrital	4	14.465	4.906			
MQABAB	Crystalline	6	927.805	610.954	2.414	8	0.042
	Detrital	4	171.500	79.215			
RVANGNS	Crystalline	6	0.033	0.019	-3.137	8	0.014
	Detrital	5	0.165	0.103			
RABS	Crystalline	6	0.120	0.064	-2.795	9	0.021
	Detrital	5	1.806	1.492			
RBUS	Crystalline	6	0.102	0.059	-2.573	9	0.030
	Detrital	5	1.684	1.522			

Appendix E.3. Two sample t-test grouped by rock type (limestone and crystalline)

Test	Rock Type	N.	Mean	St. Dev.	t	df	Prob.
ADSORPTION50	Limestone	24	0.059	0.046	-2.556	28	0.016
	Crystalline	6	0.010	0.009			
ADSORPTION98	Limestone	24	0.204	0.152	-2.902	28	0.007
	Crystalline	6	0.022	0.020			
ABSORPTION	Limestone	24	1.193	1.187	-2.035	28	0.051
	Crystalline	6	0.193	0.075			
FULL_ABSORP	Limestone	24	1.148	1.186	-1.975	28	0.058
	Crystalline	6	0.178	0.068			
SUSPENSION	Limestone	24	3.463	1.490	-3.461	28	0.002
	Crystalline	6	1.317	0.337			
ABSORP35_60H	Limestone	21	0.040	0.033	-2.029	25	0.053
	Crystalline	6	0.012	0.014			
ABSORP35_80H	Limestone	21	0.081	0.060	-2.466	25	0.021
	Crystalline	6	0.019	0.023			
ABSORP35_95H	Limestone	21	0.119	0.083	-2.311	25	0.029
	Crystalline	6	0.038	0.033			
ABSORP20_98H	Limestone	21	0.104	0.079	-2.435	25	0.022
	Crystalline	6	0.024	0.020			
NEG4_98H	Limestone	21	0.063	0.061	-2.087	25	0.047
	Crystalline	6	0.010	0.010			
PLUS4_98H	Limestone	21	0.076	0.068	-2.142	25	0.042
	Crystalline	6	0.015	0.008			
PLUS20_98H	Limestone	21	0.117	0.112	-2.166	25	0.040
	Crystalline	6	0.016	0.015			
LOS_FRZ_THW2	Limestone	21	23.310	18.582	-2.879	25	0.008
	Crystalline	6	1.157	0.454			
Young's Modulus at Room Temperature – 24hrs Saturation	Limestone	24	1.962E+10	6.681E+09	2.336	28	0.027
	Crystalline	6	2.773E+10	1.089E+10			
Young's Modulus after 48hrs Freezing – 24hrs Saturation (A)	Limestone	24	2.041E+10	6.290E+09	2.149	28	0.040
	Crystalline	6	2.710E+10	8.871E+09			
Young's Mod. at Room Temp.–48hrs Sat.(20%Salt-Water)	Limestone	24	1.877E+10	5.842E+09	2.715	28	0.011
	Crystalline	6	2.696E+10	9.335E+09			
RADS	Limestone	24	0.155	0.118	-2.743	28	0.011
	Crystalline	6	0.020	0.015			
RFRTH	Limestone	21	15.184	13.183	-2.534	25	0.018
	Crystalline	6	1.350	0.477			
MQABS	Limestone	24	1.166	0.956	-1.478	26	0.151
	Crystalline	4	0.448	0.131			
MQABAB	Limestone	24	510.272	379.235	2.128	28	0.042
	Crystalline	6	927.805	610.954			
RCAP32B	Limestone	24	15.793	15.617	2.412	28	0.023
	Crystalline	6	38.184	34.574			

Appendix E.4. Two sample t-test grouped by rock type (limestone and detrital)

Test	Rock Type	N.	Mean	St. Dev.	t	df	Prob.
Stress to fixed strain at 48hrs Freez. – 48hrs Sat. in 20% Salt-Water	Limestone	24	4335.792	1701.558	-2.138	26	0.042
	Detrital	4	6276.000	1505.886			
ABSORPTION	Limestone	24	1.193	1.187	-2.338	26	0.027
	Detrital	4	2.830	1.942			
FULL_ABSORP	Limestone	24	1.148	1.186	-2.934	26	0.007
	Detrital	4	3.338	2.405			
UNIT_WEIGHT	Limestone	24	2.634	0.080	5.021	26	0.000
	Detrital	4	2.400	0.127			
ABSORP20_SAT	Limestone	21	0.632	0.657	-2.978	22	0.007
	Detrital	3	2.178	1.860			
VAC_SAT	Limestone	21	0.739	0.793	-4.420	22	0.000
	Detrital	3	3.712	2.602			
PLUS4_SAT	Limestone	21	0.574	0.642	-3.056	22	0.006
	Detrital	3	1.998	1.466			
MGSO4	Limestone	21	9.776	17.687	-7.359	22	0.000
	Detrital	3	88.467	13.177			
Young's Modulus at Room Temp. – Room Hum. (Initial Test)	Limestone	24	2.264E+10	7.504E+09	2.164	26	0.040
	Detrital	4	1.426E+10	3.641E+09			
Young's Modulus at Room Temperature – 98% Humidity	Limestone	24	2.018E+10	6.150E+09	2.201	26	0.037
	Detrital	4	1.319E+10	3.075E+09			
Young's Modulus after 48hrs Freezing – 65% Humidity	Limestone	24	2.158E+10	7.423E+09	2.275	26	0.031
	Detrital	4	1.294E+10	2.547E+09			
Young's Modulus after 48hrs Freezing – 24hrs Saturation (A)	Limestone	24	2.041E+10	6.290E+09	2.163	26	0.040
	Detrital	4	1.342E+10	2.639E+09			
RDEN	Limestone	24	2.648	0.084	4.881	26	0.000
	Detrital	4	2.411	0.129			
RPORO	Limestone	24	1.208	1.268	-2.965	26	0.006
	Detrital	4	3.485	2.278			
RCAP32S	Limestone	24	0.233	0.481	-2.410	26	0.023
	Detrital	4	1.090	1.409			
RADSB	Limestone	24	31.974	20.673	2.698	26	0.012
	Detrital	4	3.620	2.393			
RCAP32B	Limestone	24	15.793	15.617	-3.550	26	0.001
	Detrital	4	51.401	33.457			
RSATBIF	Limestone	24	83.173	17.703	2.657	26	0.013
	Detrital	4	58.145	15.297			
RABS	Limestone	24	0.847	0.912	-2.243	26	0.034
	Detrital	4	2.072	1.580			
RBUS	Limestone	24	0.674	0.927	-2.469	26	0.020
	Detrital	4	2.025	1.521			
RBUB	Limestone	24	64.049	26.194	-2.541	26	0.017
	Detrital	4	97.858	0.927			

Appendix E.5. Two sample t-test grouped by rock type (dolomite and crystalline)

Test	Rock Type	N.	Mean	St. Dev.	t	df	Prob.
Stress to fixed strain at Room Temp. – Room Humidity (Final Test)	Dolomite	41	7875.707	1991.285	-3.044	44	0.004
	Crystalline	5	4987.159	2117.378			
Stress to fixed strain at 48hrs Freezing – 65% Humidity	Dolomite	41	7363.439	2453.575	-2.103	44	0.041
	Crystalline	5	4965.610	1875.087			
Stress to fixed strain at 48hrs Freezing – 24hrs Saturation (A)	Dolomite	41	7178.927	2072.914	-3.076	45	0.004
	Crystalline	6	4359.326	2278.727			
ABSORPTION	Dolomite	43	1.522	1.019	-3.163	47	0.003
	Crystalline	6	0.193	0.075			
FULL_ABSORP	Dolomite	43	1.489	0.902	-3.527	47	0.001
	Crystalline	6	0.178	0.068			
ACID_INSOLUB	Dolomite	42	12.199	10.078	3.798	43	0.000
	Crystalline	3	39.981	33.757			
ADS_98_RIGBY	Dolomite	42	0.106	0.101	-2.161	46	0.036
	Crystalline	6	0.016	0.021			
SUSPENSION	Dolomite	42	2.552	1.127	-2.646	46	0.011
	Crystalline	6	1.317	0.337			
ABSORP20_SAT	Dolomite	37	1.190	0.743	-3.428	41	0.001
	Crystalline	6	0.139	0.057			
VAC_SAT	Dolomite	37	1.862	1.090	-3.731	41	0.001
	Crystalline	6	0.183	0.089			
PLUS4_SAT	Dolomite	37	1.087	0.673	-3.489	41	0.001
	Crystalline	6	0.118	0.051			
LOS_FRZ_THW2	Dolomite	37	16.306	14.397	-2.551	41	0.015
	Crystalline	6	1.157	0.454			
RADS	Dolomite	43	0.143	0.144	-2.067	47	0.044
	Crystalline	6	0.020	0.015			
RPORO	Dolomite	43	1.770	1.094	-3.524	47	0.001
	Crystalline	6	0.182	0.072			
RFRTH	Dolomite	37	10.090	8.285	-2.557	41	0.014
	Crystalline	6	1.350	0.477			
MQBUS	Dolomite	40	1.116	0.623	-2.379	42	0.022
	Crystalline	4	0.367	0.400			
MQBUBU	Dolomite	40	191.497	256.593	3.195	44	0.003
	Crystalline	6	642.075	632.162			
MQABS	Dolomite	42	1.241	0.702	-2.236	44	0.030
	Crystalline	4	0.448	0.131			
MQABAB	Dolomite	42	363.678	279.262	3.896	46	0.000
	Crystalline	6	927.805	610.954			
RVABGNS	Dolomite	42	0.262	0.195	-2.841	46	0.007
	Crystalline	6	0.033	0.019			
RCAP32B	Dolomite	43	17.001	15.674	2.611	47	0.012
	Crystalline	6	38.184	34.574			
RABS	Dolomite	43	1.174	0.815	-3.139	47	0.003
	Crystalline	6	0.120	0.064			
RBUS	Dolomite	43	1.037	0.810	-2.800	47	0.007
	Crystalline	6	0.102	0.059			

Appendix E.6. Two sample t-test grouped by rock type (dolomite and detrital)

Test	Rock Type	N.	Mean	St. Dev.	t	df	Prob.
ABSORPTION	Dolomite	43	1.522	1.019	-2.266	45	0.028
	Detrital	4	2.830	1.942			
FULL_ABSORP	Dolomite	43	1.489	0.902	-3.306	45	0.002
	Detrital	4	3.338	2.405			
UNIT_WEIGHT	Dolomite	43	2.679	0.074	6.788	45	0.000
	Detrital	4	2.400	0.127			
VAC_SAT	Dolomite	37	1.862	1.090	-2.531	38	0.016
	Detrital	3	3.712	2.602			
PLUS4_SAT	Dolomite	37	1.087	0.673	-2.061	38	0.046
	Detrital	3	1.998	1.466			
MGSO4	Dolomite	37	9.827	16.021	-8.247	38	0.000
	Detrital	3	88.467	13.177			
ULT_STRNGT	Dolomite	24	14.529	3.330	3.974	25	0.001
	Detrital	3	6.700	1.353			
Young's Modulus at Room Temp. – Room Hum. (Final Test)	Dolomite	43	2.744E+10	6.726E+09	3.491	45	0.001
	Detrital	4	1.549E+10	2.987E+09			
Young's Modulus at Room Temp. – Room Hum. (Initial Test)	Dolomite	43	2.787E+10	8.473E+09	3.159	45	0.003
	Detrital	4	1.426E+10	3.641E+09			
Young's Modulus at Room Temperature – 98% Humidity	Dolomite	43	2.590E+10	6.617E+09	3.773	45	0.000
	Detrital	4	1.319E+10	3.075E+09			
Young's Modulus after 48hrs Freezing – 65% Humidity	Dolomite	43	3.066E+10	9.183E+09	3.812	45	0.000
	Detrital	4	1.294E+10	2.547E+09			
Young's Modulus at Room Temperature – 24hrs Saturation	Dolomite	43	2.422E+10	6.650E+09	3.366	45	0.002
	Detrital	4	1.287E+10	2.307E+09			
Young's Modulus after 48hrs Freezing – 24hrs Saturation (A)	Dolomite	43	2.602E+10	7.471E+09	3.325	45	0.002
	Detrital	4	1.342E+10	2.639E+09			
Young's Modulus after 48hrs Freezing – 24hrs Saturation (B)	Dolomite	43	2.417E+10	6.210E+09	3.516	45	0.001
	Detrital	4	1.309E+10	2.238E+09			
Young's Mod. after 48hrs Freez.–48hrs Sat.(20% Salt-Water)	Dolomite	43	2.731E+10	7.994E+09	2.623	45	0.012
	Detrital	4	1.658E+10	4.998E+09			
Young's Mod. at Room Temp.–48hrs Sat.(20%Salt-Water)	Dolomite	43	2.518E+10	8.479E+09	2.542	45	0.015
	Detrital	4	1.421E+10	3.915E+09			
RDEN	Dolomite	43	2.740	0.265	2.444	45	0.019
	Detrital	4	2.411	0.129			
RPORO	Dolomite	43	1.770	1.094	-2.713	45	0.009
	Detrital	4	3.485	2.278			
RCAP32S	Dolomite	43	0.226	0.360	-3.282	45	0.002
	Detrital	4	1.090	1.409			
RCAP32B	Dolomite	43	17.001	15.674	-3.775	45	0.000
	Detrital	4	51.401	33.457			
RBUS	Dolomite	43	1.037	0.810	-2.159	45	0.036
	Detrital	4	2.025	1.521			

Appendix F.1. Paired t-test of Group Sigma (all samples) stress results

Test	N.	Mean	Mean Diff.	Std.Dev.Diff.	t	df	Prob.
Room Temp. – Room Humidity (Initial Test) Room Temperature – 98% Humidity	78	6997.0 5988.0	1009.0	1360.5	6.550	77	0.000
Room Temp. – Room Humidity (Final Test) Room Temperature – 98% Humidity	75	7244.9 6011.4	1233.5	1482.7	7.204	74	0.000
Room Temperature – 98% Humidity 48hrs Freezing – 65% Humidity	74	5913.3 7019.0	-1105.6	1592.6	-5.972	73	0.000
Room Temp. – Room Humidity (Initial Test) Room Temperature – 24hrs Saturation	78	6997.0 5945.9	1051.1	1965.8	4.722	77	0.000
Room Temp. – Room Humidity (Final Test) Room Temperature – 24hrs Saturation	75	7244.9 5823.3	1421.6	1957.3	6.290	74	0.000
48hrs Freezing – 65% Humidity Room Temperature – 24hrs Saturation	74	7019.0 5694.5	1324.5	1952.6	5.835	73	0.000
Room Temp. – Room Humidity (Final Test) 48hrs Freezing – 24hrs Saturation (A)	73	7105.0 6561.2	543.8	1545.9	3.006	72	0.004
Room Temperature – 98% Humidity 48hrs Freezing – 24hrs Saturation (A)	75	5968.7 6470.0	-501.3	1876.7	-2.313	74	0.023
48hrs Freezing – 65% Humidity 48hrs Freezing – 24hrs Saturation (A)	73	6981.7 6461.2	520.5	1774.4	2.506	72	0.014
Room Temperature – 24hrs Saturation 48hrs Freezing – 24hrs Saturation (A)	75	5808.5 6470.0	-661.5	2376.9	-2.410	74	0.018
Room Temp. – Room Humidity (Initial Test) 48hrs Freezing – 24hrs Saturation (B)	76	7070.8 6069.8	1001.0	1803.6	4.838	75	0.000
Room Temp. – Room Humidity (Final Test) 48hrs Freezing – 24hrs Saturation (B)	74	7262.0 5977.9	1284.1	1680.9	6.571	73	0.000
48hrs Freezing – 65% Humidity 48hrs Freezing – 24hrs Saturation (B)	72	7085.8 5815.4	1270.4	2213.5	4.870	71	0.000
48hrs Freezing – 24hrs Saturation (A) 48hrs Freezing – 24hrs Saturation (B)	73	6516.5 5916.3	600.2	2009.7	2.552	72	0.013
Room Temp. – Room Humidity (Initial Test) 48hrs Freez. – 48hrs Sat. in 20% Salt-Water	77	7039.8 5248.8	1791.0	1779.1	8.834	76	0.000
Room Temp. – Room Humidity (Final Test) 48hrs Freez. – 48hrs Sat. in 20% Salt-Water	75	7244.9 5118.7	2126.2	1719.3	10.710	74	0.000
Room Temperature – 98% Humidity 48hrs Freez. – 48hrs Sat. in 20% Salt-Water	77	6012.0 5248.8	763.2	1629.9	4.109	76	0.000
48hrs Freezing – 65% Humidity 48hrs Freez. – 48hrs Sat. in 20% Salt-Water	73	7049.9 5065.3	1984.6	2097.2	8.085	72	0.000
Room Temperature – 24hrs Saturation 48hrs Freez. – 48hrs Sat. in 20% Salt-Water	77	5971.3 5248.8	722.5	1786.1	3.550	76	0.001
48hrs Freezing – 24hrs Saturation (A) 48hrs Freez. – 48hrs Sat. in 20% Salt-Water	74	6491.8 5172.2	1319.6	2127.4	5.336	73	0.000
48hrs Freezing – 24hrs Saturation (B) 48hrs Freez. – 48hrs Sat. in 20% Salt-Water	76	6069.8 5278.7	791.1	1712.6	4.027	75	0.000
Room Temp. – Room Humidity (Initial Test) Room Temp. – 48hrs Sat. in 20% Salt-Water	76	6993.4 5615.5	1378.0	1803.3	6.662	75	0.000
Room Temp. – Room Humidity (Final Test) Room Temp. – 48hrs Sat. in 20% Salt-Water	74	7189.5 5576.7	1612.8	1626.3	8.531	73	0.000
Room Temperature – 98% Humidity Room Temp. – 48hrs Sat. in 20% Salt-Water	76	5991.4 5615.5	375.9	1526.0	2.098	75	0.039
48hrs Freezing – 65% Humidity Room Temp. – 48hrs Sat. in 20% Salt-Water	72	7013.6 5482.7	1531.0	2021.9	6.425	71	0.000
48hrs Freezing – 24hrs Saturation (A) Room Temp. – 48hrs Sat. in 20% Salt-Water	73	6447.8 5527.7	920.1	1853.9	4.240	72	0.000
48hrs Freezing – 24hrs Saturation (B) Room Temp. – 48hrs Sat. in 20% Salt-Water	75	6018.7 5650.3	368.5	1415.1	2.255	74	0.027
48hrs Freez. – 48hrs Sat. in 20% Salt-Water Room Temp. – 48hrs Sat. in 20% Salt-Water	76	5228.4 5615.5	-387.0	1452.9	-2.322	75	0.023

Appendix F.2. Paired t-test of Group Sigma (all samples) Young's Modulus results

Test	N.	Mean	Mean Diff.	Std.Dev.Diff.	t	df	Prob.
Room Temp. – Room Humidity (Final Test) Room Temperature – 98% Humidity	78	2.558E+10 2.325E+10	2.334E+09	5.023E+09	4.105	77	0.000
Room Temp. – Room Humidity (Initial Test) Room Temperature – 98% Humidity	78	2.539E+10 2.325E+10	2.148E+09	4.776E+09	3.971	77	0.000
Room Temp. – Room Humidity (Initial Test) 48hrs Freezing – 65% Humidity	78	2.539E+10 2.669E+10	-1.300E+09	5.201E+09	-2.207	77	0.030
Room Temperature – 98% Humidity 48hrs Freezing – 65% Humidity	78	2.325E+10 2.669E+10	-3.448E+09	5.190E+09	-5.867	77	0.000
Room Temp. – Room Humidity (Final Test) Room Temperature – 24hrs Saturation	78	2.558E+10 2.242E+10	3.156E+09	4.223E+09	6.600	77	0.000
Room Temp. – Room Humidity (Initial Test) Room Temperature – 24hrs Saturation	78	2.539E+10 2.242E+10	2.969E+09	5.269E+09	4.976	77	0.000
48hrs Freezing – 65% Humidity Room Temperature – 24hrs Saturation	78	2.669E+10 2.242E+10	4.269E+09	6.598E+09	5.715	77	0.000
Room Temp. – Room Humidity (Final Test) 48hrs Freezing – 24hrs Saturation (A)	78	2.558E+10 2.370E+10	1.884E+09	5.454E+09	3.051	77	0.003
Room Temp. – Room Humidity (Initial Test) 48hrs Freezing – 24hrs Saturation (A)	78	2.539E+10 2.370E+10	1.697E+09	5.561E+09	2.695	77	0.009
48hrs Freezing – 65% Humidity 48hrs Freezing – 24hrs Saturation (A)	78	2.669E+10 2.370E+10	2.997E+09	6.194E+09	4.274	77	0.000
Room Temperature – 24hrs Saturation 48hrs Freezing – 24hrs Saturation (A)	78	2.242E+10 2.370E+10	-1.272E+09	4.396E+09	-2.555	77	0.013
Room Temp. – Room Humidity (Final Test) 48hrs Freezing – 24hrs Saturation (B)	78	2.558E+10 2.207E+10	3.513E+09	4.241E+09	7.316	77	0.000
Room Temp. – Room Humidity (Initial Test) 48hrs Freezing – 24hrs Saturation (B)	78	2.539E+10 2.207E+10	3.326E+09	5.145E+09	5.710	77	0.000
Room Temperature – 98% Humidity 48hrs Freezing – 24hrs Saturation (B)	78	2.325E+10 2.207E+10	1.179E+09	4.597E+09	2.265	77	0.026
48hrs Freezing – 65% Humidity 48hrs Freezing – 24hrs Saturation (B)	78	2.669E+10 2.207E+10	4.626E+09	6.572E+09	6.217	77	0.000
48hrs Freezing – 24hrs Saturation (A) 48hrs Freezing – 24hrs Saturation (B)	78	2.370E+10 2.207E+10	1.629E+09	4.439E+09	3.242	77	0.002
Room Temp. – Room Humidity (Final Test) 48hrs Freez. – 48hrs Sat. in 20% Salt-Water	78	2.558E+10 2.427E+10	1.309E+09	5.805E+09	1.991	77	0.050
48hrs Freezing – 65% Humidity 48hrs Freez. – 48hrs Sat. in 20% Salt-Water	78	2.669E+10 2.427E+10	2.422E+09	7.917E+09	2.702	77	0.008
Room Temperature – 24hrs Saturation 48hrs Freez. – 48hrs Sat. in 20% Salt-Water	78	2.242E+10 2.427E+10	-1.847E+09	5.013E+09	-3.255	77	0.002
48hrs Freezing – 24hrs Saturation (B) 48hrs Freez. – 48hrs Sat. in 20% Salt-Water	78	2.207E+10 2.427E+10	-2.205E+09	5.410E+09	-3.599	77	0.001
Room Temp. – Room Humidity (Final Test) Room Temp. – 48hrs Sat. in 20% Salt-Water	78	2.558E+10 2.273E+10	2.854E+09	6.092E+09	4.138	77	0.000
Room Temp. – Room Humidity (Initial Test) Room Temp. – 48hrs Sat. in 20% Salt-Water	78	2.539E+10 2.273E+10	2.667E+09	6.781E+09	3.474	77	0.001
48hrs Freezing – 65% Humidity Room Temp. – 48hrs Sat. in 20% Salt-Water	78	2.669E+10 2.273E+10	3.967E+09	7.394E+09	4.739	77	0.000

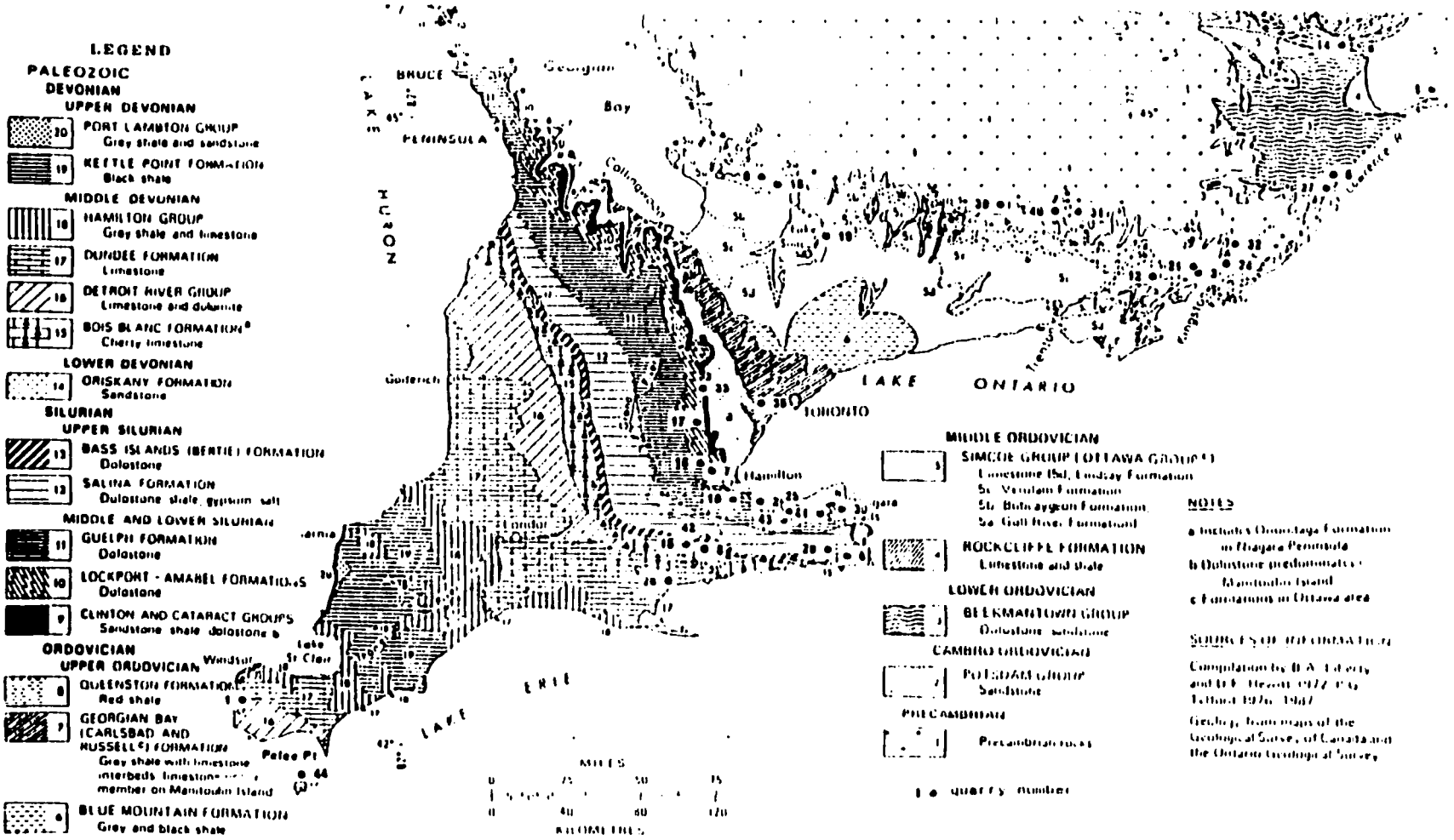

Appendix G.1. Southern Ontario map showing bedrock geology and sample location (Ondrasik, 1996 after Booth et al. 1989a)

VITA AUCTORIS

Pedram P. Molk Ara
374 Taylor Mills Drive South
Richmond Hill, Ontario L4C 2T1
Phone: (416)417-6866
E-mail: pedrammolkara@yahoo.ca

Working Experience

Engineering Geologist at AMEC Earth & Environmental Ltd. (Formerly AGRA)
1998-Present

Geologist/Engineering Geologist/Hydrogeologist at R. S. Consulting Engineers
1994-1996

Education

Master of Sciences, Geology (Engineering Geology) **1997-2002**
University of Windsor, Canada

Bachelor of Sciences, Geology (Hydrogeology) **1989-1993**
Shiraz University, Iran